ANL-6266

Argonne National Laboratory

INSTABILITY STUDIES WITH EBR-I, MARK III

by

R. R. Smith, J. F. Boland, F. D. McGinnis,
M. Novick and F. W. Thalgott

DISCLAIMER

LEGAL NOTICE

This report was prepared as an account of Government sponsored work. Neither the United States, nor the Commission, nor any person acting on behalf of the Commission:

A. Makes any warranty or representation, expressed or implied, with respect to the accuracy, completeness, or usefulness of the information contained in this report, or that the use of any information, apparatus, method, or process disclosed in this report may not infringe privately owned rights; or

B. Assumes any liabilities with respect to the use of, or for damages resulting from the use of any information, apparatus, method, or process disclosed in this report.

As used in the above, "person acting on behalf of the Commission" includes any employee or contractor of the Commission, or employee of such contractor, to the extent that such employee or contractor of the Commission, or employee of such contractor prepares, disseminates, or provides access to, any information pursuant to his employment or contract with the Commission, or his employment with such contractor.

Price $2.00 . *Available from the Office of Technical Services, Department of Commerce, Washington 25, D.C.*

ANL-6266
Reactor Technology
(TID-4500, 16th Ed.)
AEC Research and
Development Report

ARGONNE NATIONAL LABORATORY
9700 South Cass Avenue
Argonne, Illinois

INSTABILITY STUDIES WITH EBR-I, MARK III

by

R. R. Smith, J. F. Boland, F. D. McGinnis,
M. Novick and F. W. Thalgott

Idaho Division

December 1960

Operated by The University of Chicago
under
Contract W-31-109-eng-38

TABLE OF CONTENTS

TABLE OF CONTENTS

LIST OF FIGURES

LIST OF FIGURES

LIST OF FIGURES

INSTABILITY STUDIES WITH EBR-I, MARK III

by

R. R. Smith, J. F. Boland, F. D. McGinnis,
M. Novick and F. W. Thalgott

I. INTRODUCTION

From the viewpoint of design objectives, the operation of EBR-I has been highly successful: it established the validity of the breeding concept, it demonstrated that liquid metal-coolant systems could be operated on a practical basis, and it established the fact that useful power could be extracted from an extremely small and highly concentrated core.[1-5] From another point of view, that of reactor safety, the operational characteristics of EBR-I constituted a source of considerable concern. While steady-state operation at full power and full flow was smooth and posed no serious problems, it was nevertheless recognized that power oscillations could be initiated through modest departures from normal operating procedures. An even more disturbing feature consisted of a prompt positive power coefficient of reactivity which became obvious whenever the coolant flow was varied.[6]

Such features coupled with the ever-present possibilities of instrument malfunction and human error constitute a potentially hazardous situation for power-producing reactors. Since the physical origin of these effects was not at all understood, the need for fundamental investigation was evident.

The first attempt to study the dynamic behavior of the reactor was initiated in May 1955.[7] The results of these studies, in which the transfer function of the reactor was measured under various conditions of power and flow, demonstrated that the reactor could be brought into a resonant condition at certain frequencies. Unfortunately, these measurements were crude, and attempts to interpret the results in terms of physical feedback processes were unsuccessful.

In November 1955, a second, more comprehensive series of tests was initiated. Again the same oscillatory phenomena were observed. A transient experiment carried out with the main coolant flow stopped demonstrated conclusively the existence of the suspected positive coefficient and led to an unintentional partial meltdown of the core.[8,9]

As the result of this incident, concern was expressed for the safe operation of future fast power breeder reactors. Accordingly, a large amount of effort by many investigators was devoted to the analysis of the

instability and meltdown results. For the most part, earlier thinking was guided by the following well-established items of information. Under normal steady-state operating conditions the net power coefficient was negative. Reactivity had to be added at constant flow and constant temperature to initiate and sustain a power increase. However, it seemed clear then, as it does now, that the time behavior of the overall power coefficient was dominated by two components: one positive and prompt, and the other negative, but much larger in magnitude and much more slowly acting. Direct evidence of their presence was provided by the results of flow-change tests. Immediately following a reduction in flow, the power would increase, pass through a maximum, and would eventually decrease to some lower equilibrium value. After flow increase, the converse behavior was noted. Evidently the sudden increase in fuel and coolant temperature following a flow reduction was sensed by the reactor through the prompt positive component as an addition of reactivity, later cancelled and overridden by the more slowly acting, but larger, negative component.

From the oscillator results, it was known that the resonance peak shifted to lower frequencies as the flow rate was reduced. This behavior suggested that the process responsible for the negative component must have been associated in some way with the physical transport time of the coolant through the reactor. The results of the excursion experiment substantiated the validity of this concept, since at greatly decreased flows the normally overriding negative component diminished considerably in importance and caused the resultant power coefficient to be positive.

With these facts and concepts in mind, a large effort was devoted to the interpretation of the dynamic behavior of the reactor in terms of various feedback models which, in principle, should have accounted for the existence of the prompt positive and delayed negative power coefficient components.

Mela and Dana[10] observed that changes in the dimensions of the top and bottom plates effected through temperature were too small to explain the experimental results and suggested that some amplification mechanism, such as a flow maldistribution in the radial blanket, was needed. Following a different approach, Siegel and Hurwitz[11] suggested the possibility of resonance conditions arising from the combination of individual power coefficient components, each with its own characteristic time dependence. As an extension of these concepts, Thalgott[12] in 1955 was able to show that a feedback model based on prompt positive and delayed negative power coefficient components was in reasonable agreement with experimental observations.

In a similar direction Kinchin formulated a mathematical feedback model based on a positive component arising from an inward bowing of fuel rods and a delayed negative component resulting from a delayed expansion

of the tube sheet (the perforated shield plate located immediately above the Mark I and Mark II cores).[13] By assigning credible values for time constants and power coefficients associated with the effects of fuel, coolant and tube sheet expansion, and for rod bowing, Kinchin was able to reproduce in a qualitative manner the general structure of the EBR-I resonances.

Using an analytic rather than a synthetic approach, Bethe,[14] in his elaboration of the Kinchin concepts, arrived at a value for the effective transport lag associated with the delayed negative component (10 sec) and a partition of the net power coefficient into positive and negative components (X_{pos} = +1.45 x 10^{-6} $\Delta k/k/kw$ and X_{neg} = -6.9 x 10^{-6} $\Delta k/k/kw$). Although Bethe attributed the source of the prompt positive component to an inward bowing of fuel rods, as did Kinchin, he was unable to identify the delayed negative component with any specific structural member.

Rod bowing as the source of the prompt positive component received almost universal acceptance by workers in the field of fast reactor safety. A mechanism based on a large positive Doppler effect did receive considerable attention, but was later rejected in view of the results of Doppler measurements conducted on a Mark-II simulation in ZPR-III.[15]

The origin of the delayed negative component was, however, a matter of considerable speculation. Even before the 1955 oscillator studies, Lichtenberger proposed a mechanism based on the preheating of core inlet coolant by a transfer of heat across the flow divider from core outlet to blanket inlet.[6] Such a mechanism was at that time regarded favorably, since the physical transit time for coolant flowing from blanket to core was qualitatively consistent with the concept of a transport time lag. Detailed mechanisms based on strong blanket feedback effects were postulated by Mann[16] and by Wilson and Moore.[17] The results of oscillating temperature measurements carried out on the coolant as it leaves the blanket have for all practical purposes discounted the importance of preheating mechanisms. Recent measurements, which will be discussed in detail, indicate that mechanisms based on delayed structural expansion are more consistent with the experimental facts.

Thus, while the results of previous instability studies clearly indicated the existence of prompt positive and delayed negative power coefficient components, it was still not possible at that time to identify conclusively the origin of these components with physical heat-sensitive feedback processes. Nevertheless, existing circumstantial evidence was so strong that it was almost universally accepted that these unidentified processes were mechanical in origin and could be eliminated through rather elementary changes in design.

To prove there was nothing intrinsically unsafe in the operation of a fast reactor, the damaged Mark II core was removed and was replaced with a core specifically designed and sufficiently versatile to study in detail feedbacks arising from fuel, coolant, structure and rod deformation.(18) As the result of a comprehensive program, centered mainly around transfer function and power coefficient measurements, certain positive and important conclusions have been reached pertinent to the operation and construction of fast reactors.

II. PROGRAM

The general objective of the program was to demonstrate conclusively and unambiguously that those features responsible for the instability of Mark I and Mark II could be eliminated by changes in mechanical design, or what amounts to essentially the same, that there is nothing intrinsic in a fast reactor which would cause it to be unsafe. More specific objectives consisted of the following:

(1) To demonstrate that the reactor could be operated stably with a wide margin of safety at designed values of power, temperature, and flow.

(2) To complete a thorough series of transfer function measurements under a wide variety of power, flow and temperature conditions. These were supplemented whenever necessary by power coefficient measurements, flow-reduction tests, and steady-state and transient temperature measurements taken at sensitive locations throughout the core, blanket and structure.

(3) To study the possibility of delayed reactivity feedback effects originating in the radial breeding blanket, particularly for series flow.

(4) To establish experimentally the existence of rod bowing in a radial flux gradient and to show that rod bowing, if present, can be eliminated by a system of stabilizing ribs.

(5) Finally, as a less immediate phase of the program to correlate and to explain, if possible, all experimentally observed results in terms of mathematical models having immediate and practical physical significance. Such an accomplishment would contribute to the art of predicting the performance of various fast reactor concepts from knowledge of available physical and nuclear data.

III. DESIGN OF MARK III

Since a detailed description of the Mark III design has been given by Rice et al. [18] only those features pertinent to an understanding of the Mark III test results will be described.

A. Fuel and Blanket Rods

A cutaway view of a typical Mark III fuel rod is given in Fig. 1. The fuel material consists of an alloy, 98 w/o uranium and two w/o zirconium, with the uranium enriched in U^{235} to 93 percent. Cladding consists of 0.020 in. of Zircaloy-2 metallurgically bonded to the fuel through a coextrusion process. (In both Mark I and Mark II the fuel consisted of slugs spaced concentrically in a stainless steel can. An annulus of NaK served as a heat transfer bond.)

One of the more important features of the Mark III loading consists of a system of stabilizing ribs in the form of three 0.054-in. zirconium wires equispaced and spot welded to the cladding at 1/4-in. intervals. The diameters of the wires were reduced to a uniform 0.046 in. through machining operations. A fuel rod consists of three slugs welded end to end, a central fuel piece $8\frac{1}{2}$ in. long, and lower and upper blanket slugs of 98 w/o natural uranium and two w/o zirconium alloy, $3\frac{9}{16}$ in. and $7\frac{3}{4}$ in. long, respectively. The bottom of the rod consists of a Zircaloy-2 triangular-shaped tip for locating and orientation in the rod sheets. The maximum capacity of the core is a total of 252 rods containing 60 kg of enriched uranium. (Actual cold wet critical mass is 47.5 kg.)

A blanket rod consists of a single $19\frac{13}{16}$ in. long section of natural uranium-zirconium alloy. As to cladding, diameter, and stabilizing ribs, fuel and blanket rods may be considered identical.

B. Fuel Assemblies

A typical fuel or blanket rod assembly, shown in Fig. 2, consists of an hexagonally shaped tube, of $2\frac{7}{8}$-in. outside diameter across the flats, with a wall thickness of 0.040 in. At the bottom of the tube is a nozzle which fairs the hexagonal shape to that of a cylinder. Resting on the nozzle is a rod sheet perforated with circular and triangular holes. The triangular holes receive the rod tips which, in turn, locate and orient the rods. The round holes permit the NaK coolant to pass through the tube sheet into the interstices between rods..

The set of holes approximately three feet above the lower support plate permit NaK to flow from the fuel assemblies into an outlet plenum chamber. The upper set of holes is for overflow.

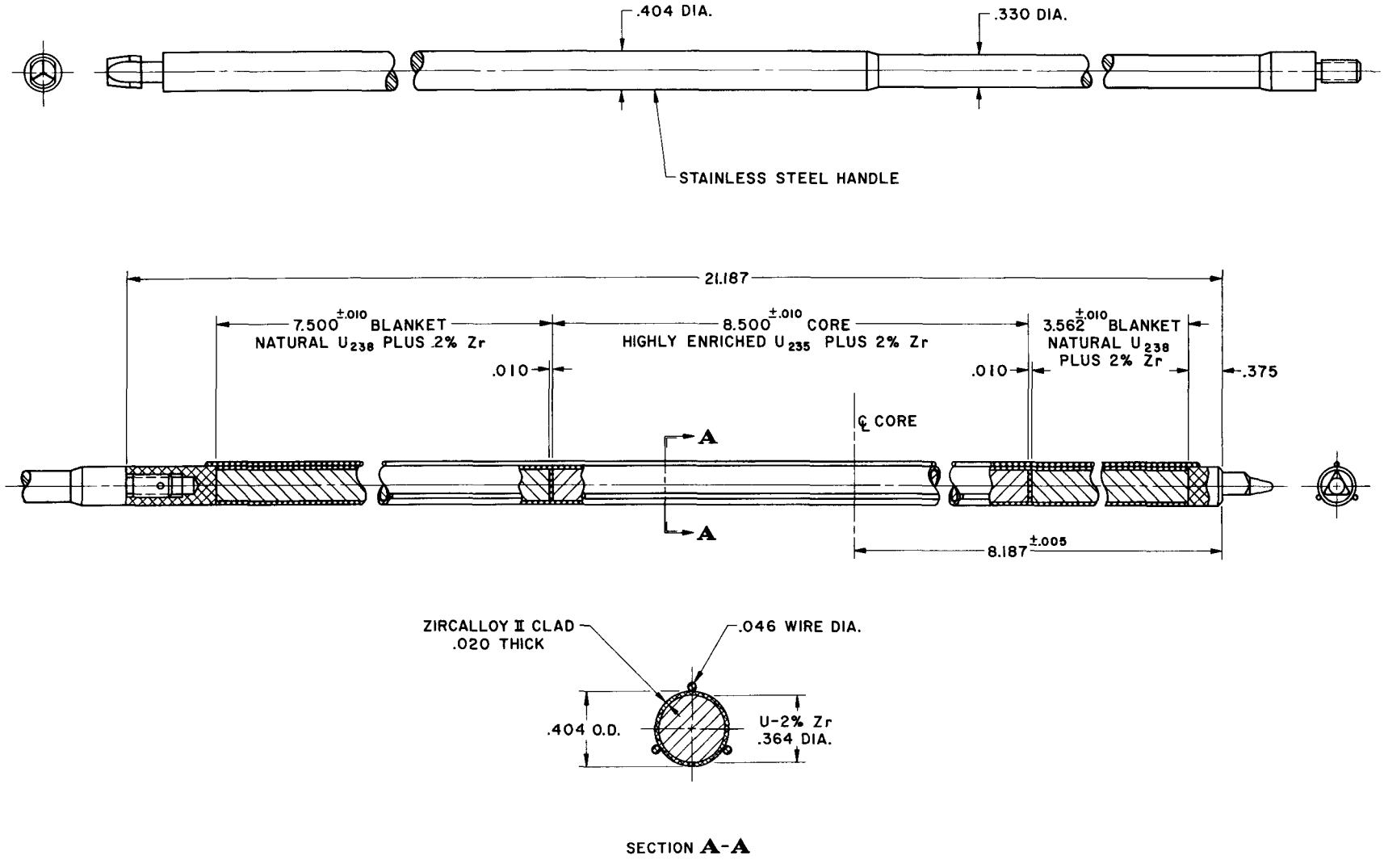

Fig. 1. Fuel Rod, EBR-I, Mark III

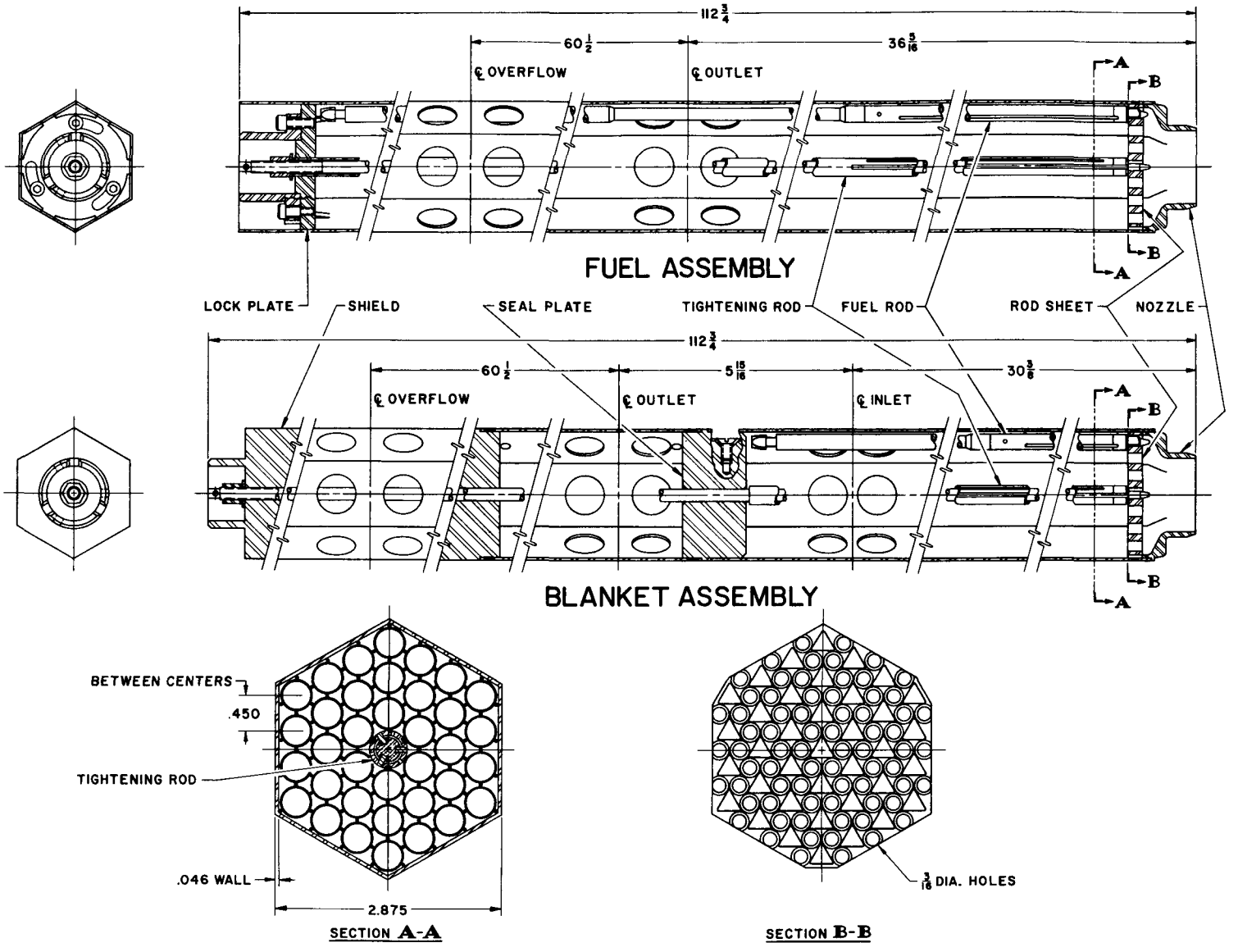

Fig. 2. Fuel and Blanket Assemblies, EBR-I, Mark III

The blanket assemblies differ from fuel assemblies in the following respects. Whereas fuel assemblies are designed to accept long-handled fuel and blanket rods, the blanket assemblies are designed to accept short-handled blanket rods only. Furthermore, blanket assemblies contain a set of holes located immediately below the seal plate to admit coolant in series flow. While these holes serve as an inlet in series flow, they serve as an outlet under parallel flow conditions. A seal plate in each blanket assembly separates inlet and outlet plenum chambers and serves to prevent short circuit flow.

C. Rod Arrangements

A single fuel or blanket assembly contains 37 rod positions, 36 normally occupied with fuel or blanket rods and the 37th occupied by a centrally located expandable tightening rod which forces the rods outward against the hex walls. A tightening rod, shown in Fig. 3, consists essentially of an outer split-tube which is expanded by means of a series of Woodruff key-type wedges riding in slots in the center shaft. The expansion is actuated by means of a nut on the central rod at the top of the assembly. With the tightening rod in the expanded condition, radial movement of the fuel and blanket rods is limited.

D. Assembly Arrangement

A cross-sectional view through the core at the vertical center line is given in Fig. 4. The inner seven assemblies are filled, for the most part, with fuel rods. Normally 47 of the 252 possible positions are occupied with long-handled blanket rods, since the nominal loading at full power consists of 205 fuel rods. To maintain an approximately cylindrical core, extra blanket rods are located at the outer edges of fuel assemblies. The outer ring of twelve assemblies is filled completely with short-handled blanket rods.

Located at the core centerline on each of the six flats at the outer periphery of the assemblies are double-wedge clamps used to force the outer assemblies inward against the center assembly. A second set of six shoe-type clamps mounted along the inner edge of the seal plate limits the bypass leakage rate and serves to lock fuel and blanket assemblies into a rigid array. Also shown in Fig. 4 are the twelve downcomers through which the coolant passes in parallel flow, the six tie rods holding the lower structure rigid, the Sb-Be source, and oscillator rod and thimble. A small fraction of the total number of thermocouple locations is also shown.

E. Inner Tank Assembly

A cutaway view of the inner tank assembly is given in Fig. 5. At the bottom of the structure is the tube sheet which receives, supports, and locates the nozzles of the rod assemblies. Immediately above the inlet

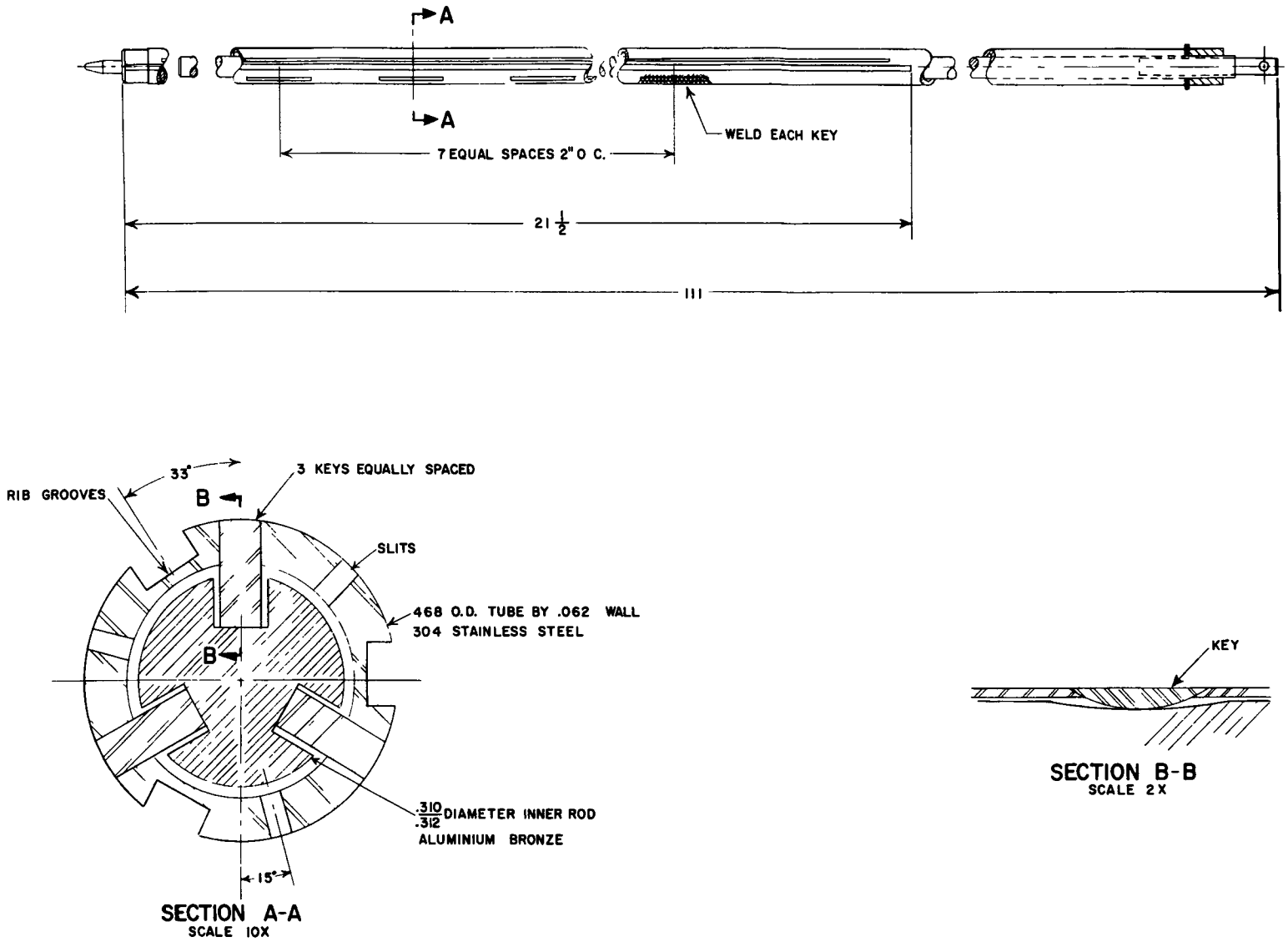

Fig. 3. Fuel-tightening Rod, EBR-I, Mark III

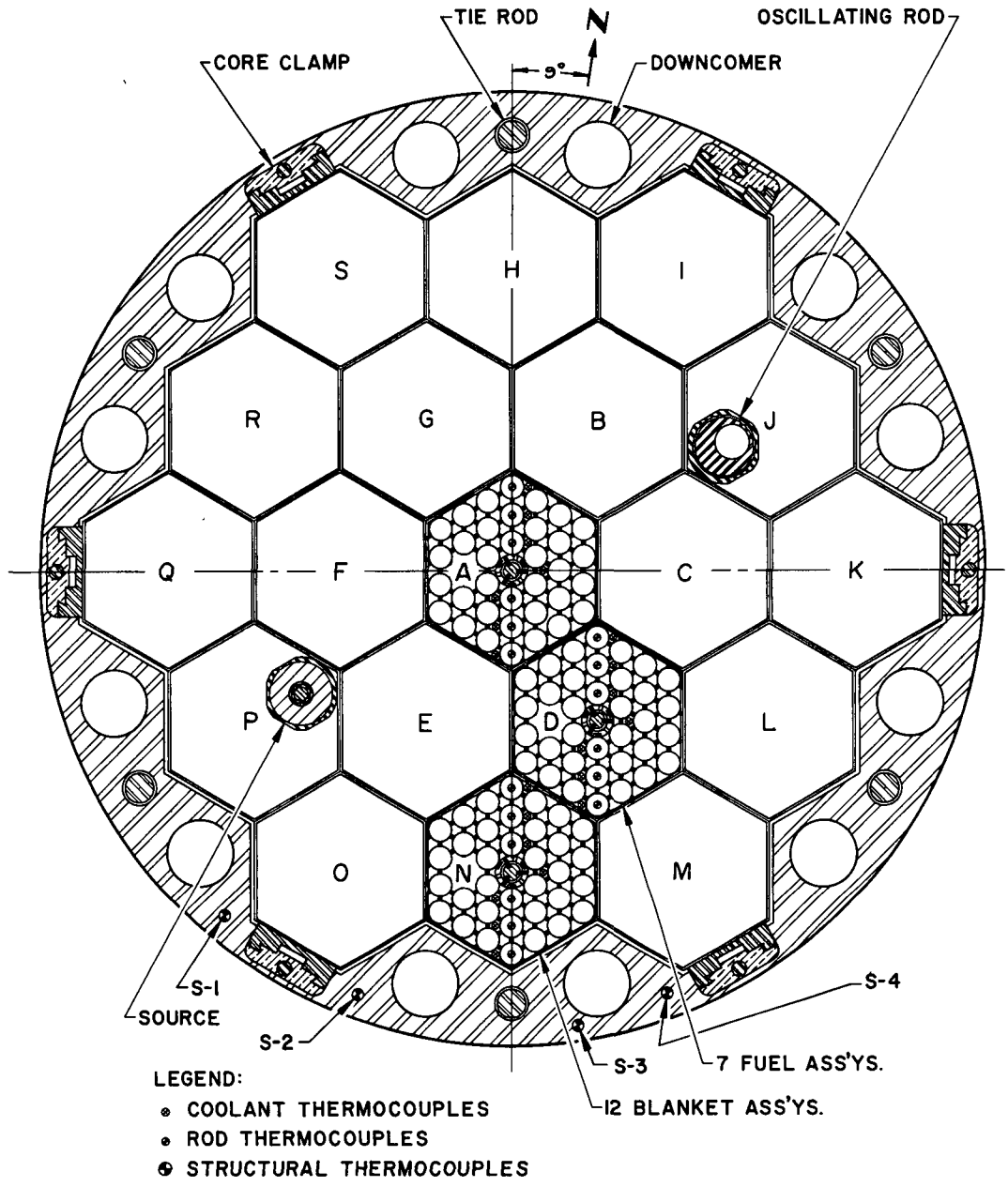

Fig. 4. Cross Section through Centerline of Core in EBR-I, Mark III

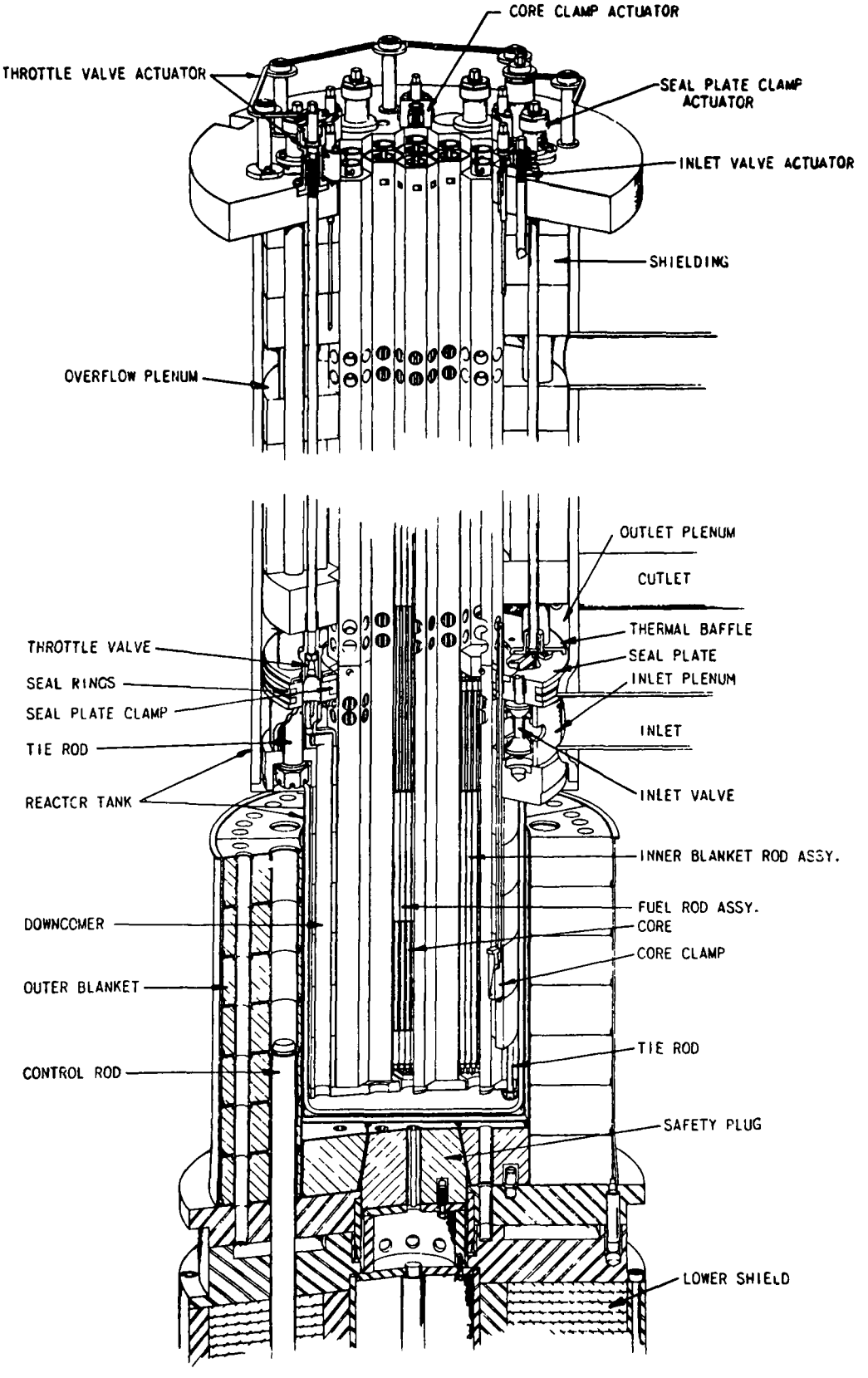

Fig. 5. Inner Tank Assembly of EBR-I, Mark III

plenum is the seal plate which, through a system of two expandable Inconel seal rings, restricts the bypass leakage occurring between the tank and the outer edge of the seal plate. The bypass leakage occurring between the inner edge of the seal plate and the blanket assemblies is restricted by the seal plate shoes.

Under series flow conditions, the inlet coolant enters the annular inlet plenum located immediately below the seal plate and flows into the outer ring of twelve blanket assemblies. At the bottom of the blanket assemblies the flow is reversed 180°, flows upward through the seven fuel assemblies, through the outlet holes at the top, and then radially outward through the perforated portion of the blanket assemblies into the outlet plenum.

Under parallel flow conditions, the coolant flows into a lower annular plenum located immediately above the mounting plate. Here the coolant is distributed to the twelve downcomers through which it flows to the lower plenum. Upward flow through fuel and blanket assemblies is partitioned by means of a series of throttle valves.

The actual flow through the core, both in series and parallel flow, is less than the flow indicated through the metering of the primary inlet. Of a nominal metered flow of 290 gpm, approximately 16 percent (47 gpm) is bypassed as leakage and for seal plate cooling in series flow. The remaining 84 percent passes through the blanket and core. For a metered flow of 278 gpm in parallel flow, approximately the same fraction, 84 percent, passes through the core; the remaining 16 percent passes through the blanket. Coolant from the blanket outlet cools the seal plate.

IV. THEORY

Of the three methods, transient, excursion, and oscillator, used to study the response of a reactor to arbitrary additions of reactivity, the oscillator method provides the most accurate and useful information. Accordingly, this method was used almost exclusively in the Mark III instability studies.

In this method the driving function consists of a sinusoidal variation of reactivity, which may be introduced as a function of frequency. The response or kinetic behavior of the reactor is completely described by the amplitude and phase relation of the sinusoidal variation in power or neutron flux. In the absence of feedback effects, the response of the reactor may also be expressed in terms of the neutron lifetime and the delayed neutron characteristics. The development of the necessary mathematics is well understood and has been treated in detail elsewhere.[19] The final expression for the transfer function of the reactor is given by

$$\frac{\Delta n}{n} \Big/ \frac{\Delta k}{k} = G_{iw} = \frac{1}{iw\left[\ell + \sum_i \frac{\beta_i}{iw + \lambda_i}\right]}, \qquad (1)$$

where $\Delta n/n$ is the fractional change in power caused by the sinusoidal addition of reactivity $\Delta k/k$, w is the oscillation frequency, β_i and λ_i are the respective abundances and decay constants for the various delayed neutron emitting groups, and ℓ is the effective prompt neutron lifetime. In a fast reactor the effects of fast fission in U^{238} must be considered in the above expression, since the fraction of delayed neutrons resulting from fast fission of U^{238} differs from that of U^{235}. In 1957 Okrent[20] modified the latest Keepin[21] delayed neutron data to include fast fission effects for the EBR-I spectrum. His results are given in Table I.

Table I

DELAYED NEUTRON EFFECTS FOR EBR-I SPECTRUM

Group	α_i	β_i	$\lambda_i(\text{sec}^{-1})$	$T_{\frac{1}{2}}(\text{sec})$
1	0.03425	0.000234	0.0127	54.51
2	0.2016	0.001377	0.0318	21.84
3	0.1841	0.001257	0.1153	6.0
4	0.40415	0.002760	0.311	2.23
5	0.14255	0.000974	1.40	0.496
6	0.03335	0.000228	3.87	0.179

Through the substitution of a value of 4×10^{-8} sec for the effective prompt neutron lifetime and values for β_i and λ_i into Equation 1, it is possible to evaluate the zero power transfer function G_0 as a function of oscillation frequency. The results of an evaluation of G_0 as a function of frequency are given in Fig. 6.

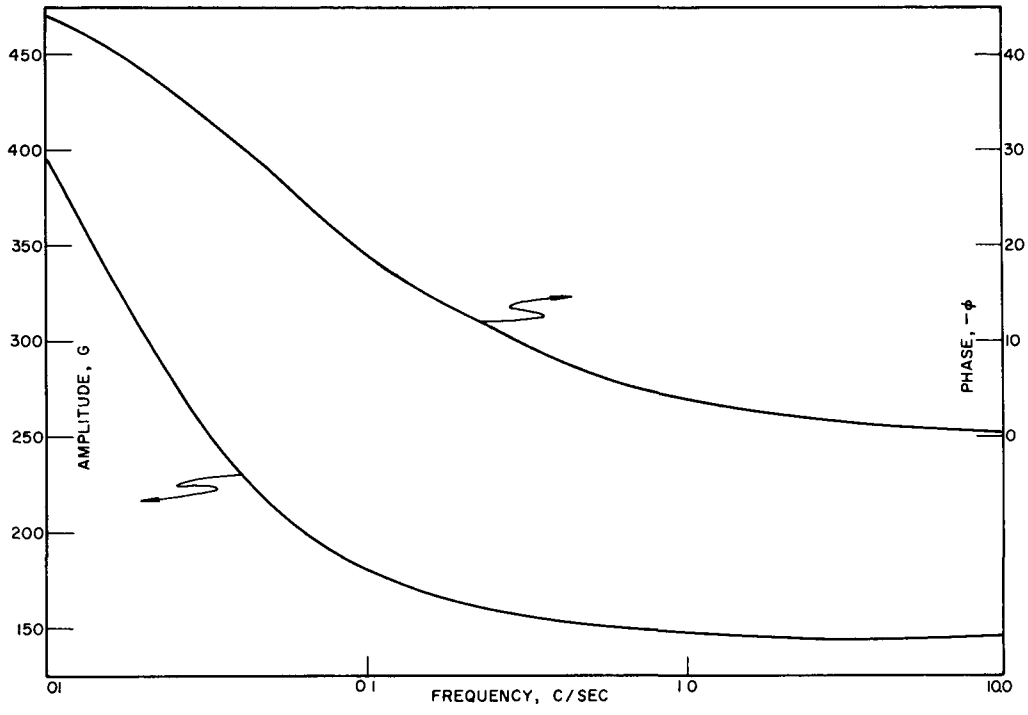

Fig. 6. Calculated Zero Power Transfer Function for EBR-I, Mark III

As the oscillation frequency approaches zero, the amplitude of the transfer function approaches infinity, since at zero frequency (and zero power) any reactivity addition leads to an exponential increase in power. For higher frequencies the amplitude drops rapidly, approximates a value of $1/\beta$ for frequencies of the order of 10 cps, and eventually goes to zero at extremely high frequencies. Since the prompt neutron lifetime for a fast spectrum is extremely short, the final break frequency is of the order of 10^5 cps, in contrast with a break frequency of 10-100 cps for a thermal spectrum. This difference, incidentally, is the only significant difference distinguishing the transient responses of fast and thermal reactors.

The phase relationship is also given in Fig. 6. At zero frequency the imaginary component of the transfer function vanishes and the phase lag goes to -90°. In the vicinity of 10-100 cps, where the delayed neutrons lose their effectiveness on the flux perturbations, the phase lag approaches zero. Here the response of the reactor is dictated by prompt neutrons.

For infinitely high frequencies, i.e., of the order of 10^6 cps, the reactor can no longer follow the impressed reactivity additions and the phase lag again approximates -90°. For a typical thermal spectrum the phase lag reaches a minimum in the vicinity of 10 cps and attains a value of -90° in the vicinity of 10^3 cps.

In theory and in practice the response of the reactor follows a predictable frequency-dependent form for the special case in which heat generation is negligible. For power levels at which sensible heating occurs, the effects of feedback modify the reactor response. Temperature increases in a given component are accompanied by density decreases which, in turn, are usually sensed by the reactor as reactivity losses. Since heating and expansion effects are time dependent, the reactivity fed back to the reactor is also time dependent, and the total reactivity sensed by the reactor is defined by the vector sum of the feedback and impressed reactivities. The immediate result of sensible heating, therefore, is a modification of the input reactivity wave which affects the phase and the amplitude of the measured transfer function. For a given set of operating conditions the departure of the measured transfer function from the zero power (calculated) transfer function constitutes an effective measurement of the reactivity feedback.

The feedback is defined, quite simply, by the following expression:

$$-H = \frac{1}{G} - \frac{1}{G_0}, \tag{2}$$

where $1/G$ and $1/G_0$ are the reciprocals of the measured and zero power transfer functions, respectively. Each of these terms has an amplitude and associated phase and is adequately described by a complex number.

In its simplest form the feedback may be described in terms of the power, a feedback power coefficient of reactivity, and an associated time constant. Using Bethe's[14] terminology, one possible representation is

$$-H = \frac{PX}{(1 + iwT_1)}, \tag{3}$$

where P, X, w, and T_1 are the power, power coefficient of reactivity, the oscillation frequency, and the time constant, respectively. The effect of the feedback described by Equation 3 on the transfer function is illustrated in Fig. 7. The inverse zero power gain always lies in the I quadrant, since the phase lag of the zero power transfer function is restricted to the region from 0 to -90°. The effect of the feedback on the measured transfer function is illustrated by the vector diagram. For all frequencies, $1/G$ will be larger than $1/G_0$. Therefore, the measured gain will always be less than the respective zero power gain.

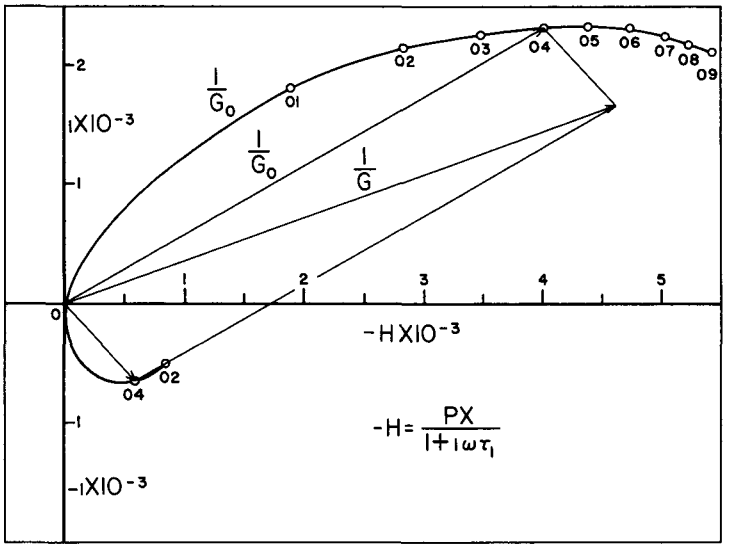

Fig. 7. The Effect of a Single-pole Feedback on Transfer Function

A more complicated feedback process described by two time constants is given by the following expression:

$$-H = \frac{PX}{(1 + iwT_1)(1 + iwT_2)}. \tag{4}$$

The effects of the additional time-dependent process on the measured gain are illustrated in Fig. 8.

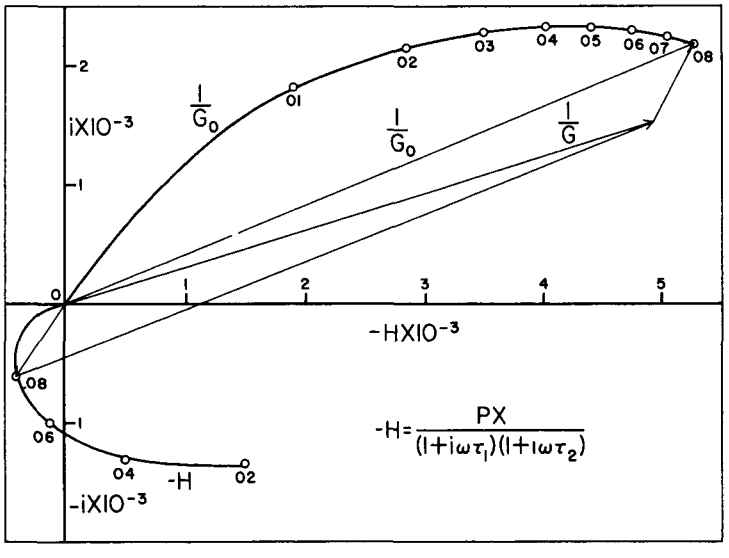

Fig. 8. The Effect of a Double-pole Feedback on Transfer Function

The feedback now enters the III quadrant and approaches zero at high frequencies with a phase lag of 180°. At frequencies where the feedback lies in the III quadrant, vector addition of the feedback and inverse zero gain components leads to a $1/G$ resultant which is smaller than $1/G_0$. The actual gain under these conditions is higher than the corresponding zero power gain. Assuming a linear feedback model, such as that illustrated by Equation 4, increase of the power will increase the magnitude of the feedback without changing the phase. At some combination of power and frequency, the phases and amplitudes of -H and $1/G_0$ will reach cancellation, and resonance will result. However, as will be shown for Mark III, the power level at which cancellation will occur is absurdly high.

The introduction of a third time constant into the denominator of Equation 4 causes the feedback to enter the II quadrant. In a somewhat different manner the inclusion of a transport lag dependence described by an e^{-iwT} term in the numerator of Equation 3 or 4 effectively increases the phase of the feedback without affecting the amplitude and can lead to an increase in gain for certain frequencies.

The feedback from a positive power coefficient of reactivity described by a single time constant lies entirely in the II quadrant. Depending on time-constant values, the coupling of a positive feedback with a negative feedback may be manifested by strong feedback phase increases which cause instability to be more likely. The presence of a positive power coefficient component effectively lowers the power level at which resonance will occur.

Expressions similar to Equations 3 and 4 constitute the mathematical basis for predicting safe operating limits. The principal assumptions upon which this application is based is that the power coefficient X and the associated time constants are unaffected by changes in power. In principle, the feedback is measured at some low arbitrary level of power. For a linear system any increase in power will produce a proportionate increase in -H. The response of the reactor at the higher power level may then be established through Equation 2.

The fact that the actual feedback may be considerably more complex than that described by Equations 3 or 4 is without influence on the validity of this concept - with the provision that linear behavior holds. Regardless of how complex the actual mathematical model may be, -H is always measured as the net result of all feedback terms. For Mark III the application of this technique seems to be limited by nonlinearities which appear in the feedback as the power is increased.

In principle, the feedback separated from transfer function measments may be interpreted in terms of individual feedback processes, each of which is characterized by a power coefficient and one or more time constants. The sign magnitude and time dependence of each term constitute a reliable basis for identification of each term with specific physical changes in the fuel, coolant and structure.

V. INSTRUMENTATION

A. Null-balance Equipment

Since the feedback for a reactor operating under stable conditions is the result of a subtraction between two numbers of almost equal magnitude, particularly at high frequencies, it is essential that measurements of amplitude and phase be made with the utmost accuracy. Two methods of measurement were considered: the electromechanical Fourier technique perfected by Brownigg et al. at Harwell,[22] and a null-balance method adapted for reactor kinetics experiments by Frost and Schemel at KAPL.[23] The null-balance technique requires a comparatively small amount of electronic equipment and is free from errors initiated through small drifts in power. Accordingly, this method, modified in a minor way, was used exclusively in the Mark III instability studies. The results of preliminary experiments conducted on a Mark III simulation in ZPR-III demonstrated the reliability of the method.[24]

The oscillator rod drive assembly consists of a 0.5-horsepower, controllable-speed drive motor connected through suitable reduction gears to the oscillator rod drive shaft which, in turn, extends downward through a packing gland in the reactor top and is supported by a bearing on the reactor core support structure. The oscillator rod is suspended from the drive shaft and is positioned by sleeve-type guide bearings located along and at the bottom of a surrounding protective tube. The drive unit, Fig. 9, is capable of driving the oscillator rod over a frequency range from 0.001 to 20 cps.

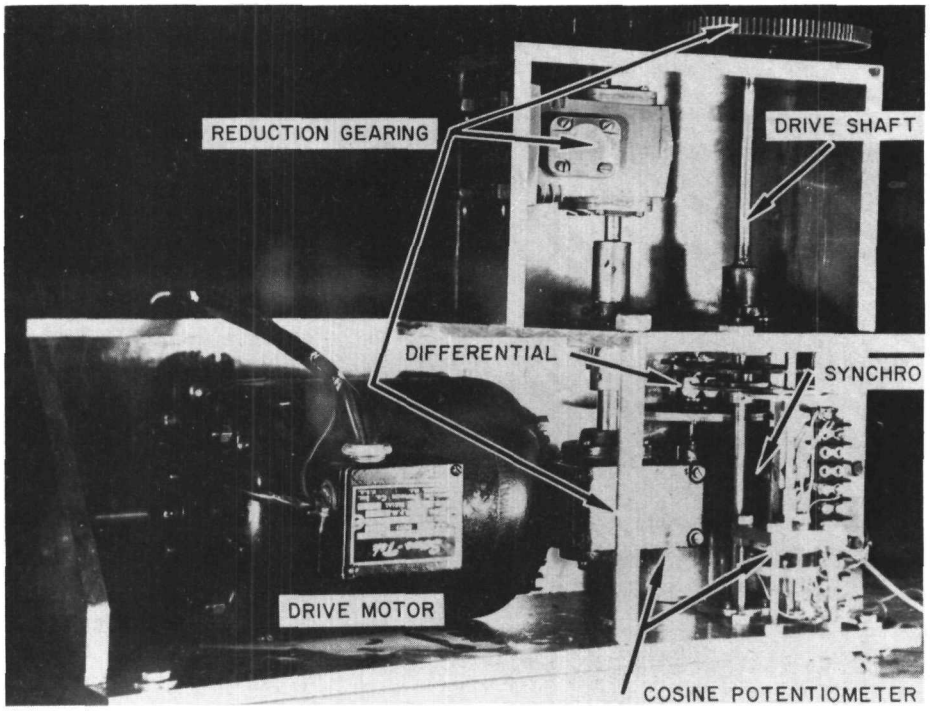

Fig. 9. Oscillator Rod Drive Unit

The cosine potentiometers used in the measuring circuits are gear driven directly from the oscillator drive shaft. One cosine potentiometer is synchronized with the oscillator rod to furnish a voltage signal corresponding to the position of the oscillator rod to a multichannel direct-recording oscillograph. A second potentiometer is used in the wave analyzer circuit for transfer function measurements. The synchromotor and differential are used in the wave analyzer circuit for changing the position of the slider on the cosine potentiometer with respect to the oscillator rod position.

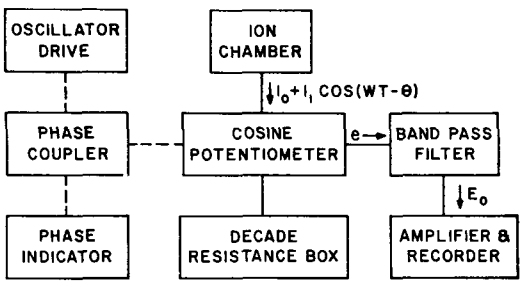

Fig. 10. Block Diagram of Wave Analyzer

A block diagram of the wave analyzer used for the transfer function measurements is given in Fig. 10. It consists essentially of an ion chamber, cosine potentiometer, decade resistance box, phase coupler, band-pass filter and null detector. The current from the ion chamber passes through the cosine potentiometer and the decade box in series. The voltage signal appearing at the wiper of the cosine potentiometer is filtered by the band-pass filter, amplified, and recorded. The following equation describes the voltage at the filter input:

$$E = I_0R_0 - I_0R_S\cos(w\tau-\phi) + I_1R_0\cos(w\tau-\theta)$$

$$- I_1R_S\cos(w\tau-\phi)\cos(w\tau-\theta), \qquad (5)$$

where

I_0 is the DC component of the ion chamber current

I_1 is the AC component of the ion chamber current

R_0 is the resistance of the decade resistance box

R_S is the resistance of the cosine potentiometer

ϕ is the phase angle between the oscillator rod and the wiper on the cosine potentiometer

θ is the phase angle between the ion chamber current and the oscillator rod.

The filter blocks the DC component of the input voltage and attenuates components that are higher and lower in frequency than the fundamental. The filter has an attenuation characteristic of 24 decibels per octave. The I_1R_S term in Equation 5 will be small with respect to the

I_0R_S and I_1R_0 terms if the power oscillation is small and therefore may be neglected as a first approximation. Both R_0 and ϕ are adjusted to make E_0 very nearly equal to zero, and Equation 5 then reduces to

$$I_1R_0 \cos(w\tau - \theta) \cong I_0R_S \cos(w\tau - \phi). \tag{6}$$

For this equality to be true, ϕ must equal θ, and I_0R_S must equal I_1R_0. It follows, therefore, that

$$\frac{I_1}{I_0} = \frac{R_S}{R_0} = \frac{\Delta p}{p}, \tag{7}$$

if the ion chamber is proportional to the reactor power p.

The magnitude of the transfer function is then equal to $R_Sk/R_0\Delta k$, and the phase angle of the transfer function is equal to ϕ. As used in the above expressions I_1, Δp, and $\Delta k/k$ are peak-to-peak values.

The following procedure is followed to determine the values of R_0 and ϕ required to satisfy Equation 7:

1. The phase coupler is set to some phase angle ϕ determined from transfer function calculations.

2. Recordings of the filter output voltage are obtained for several settings of the decade resistance box on both sides of an apparent null.

3. With the decade resistance box set at the apparent null setting, recordings of the filter output voltage are obtained for several settings of the phase coupler on both sides of an apparent phase null setting.

4. The voltages recorded in steps 2 and 3 are plotted as functions of resistance and phase angle, respectively, and the null values are obtained at the intersection of the best straight lines drawn through a series of points on each side of the null. Figure 11 gives a typical plot of filter output voltage as a function of phase coupler position.

5. Steps 1 and 2 are normally repeated using the null phase angle obtained in step 4 if this differs by more than three degrees from the value used in step 1. This becomes necessary since a large error in phase angle will result in broad null and consequently larger errors in the amplitude measurements.

Thermocouples were installed in fuel rods, blanket rods, coolant channels, and sensitive portions of the reactor structure to provide both static and dynamic information about temperature. The thermocouples consisted of iron-constantan junctions contained in stainless steel sheaths, with the junctions welded to the sheaths to obtain faster responses. Three sizes were used: $\frac{1}{8}$ in. for plenum measurements, $\frac{1}{16}$ in. for structure and plenum

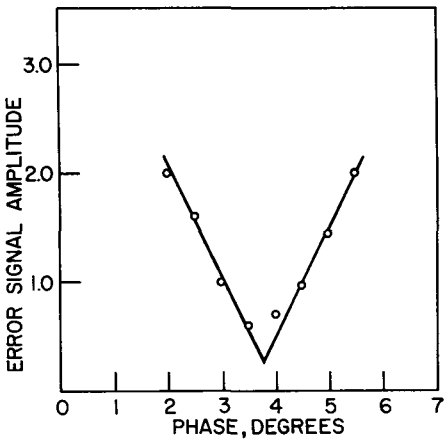

Fig. 11. Typical Null-balance Plot

measurements, and $\frac{1}{25}$ in. for coolant channel, fuel and blanket measurements. The sizes refer to the outside diameter of the stainless steel sheaths. The 63% time constants of these thermocouples in boiling water were approximately 0.5, 0.15 and 0.035 sec, respectively. Each thermocouple was calibrated at the boiling point of water and the freezing points of tin and zinc. Such calibrations are accurate to approximately ±1°C.

The thermocouple extension leads were led from the reactor tank through gas-tight connections and were terminated in a plug board which provided ease of connection to a six-channel recording oscillograph. The oscillograph assembly contains amplifiers and input couplers with bucking voltage supplies. With this arrangement, temperature changes as small as ±0.5°C could be sensed.

B. Oscillator Rod

The device used for producing a sinusoidal variation of reactivity consists of a $\frac{5}{8}$-in. B_4C (enriched in B^{10})-filled hole, 12 in. long, located eccentrically in a one-inch-diameter mild steel rod. The effect of rotation is one of alternately inserting and withdrawing the B_4C column relative to the core. Such design was shown from static calibration tests in ZPR-III to give a satisfactory sinusoidal variation of reactivity. A measure of the departure from a true sine wave may be inferred from Fig. 12, which gives the input reactivity wave as a function of angular position.

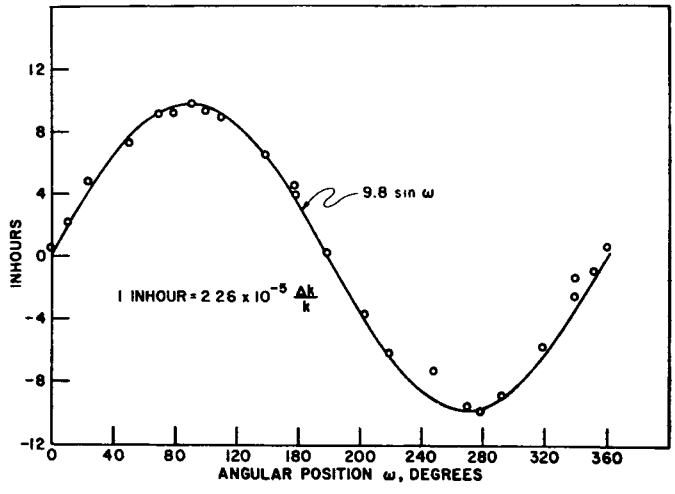

Fig. 12. Wave Shape of Reactivity Input (Boron-loaded Oscillator Rod)

The oscillator rod was located in a $1\frac{1}{16}$-in. thimble which, in turn, was located in the radial breeding blanket approximately $2\frac{1}{2}$ in. from the edge of the fuel-blanket interface (see Fig. 4).

Expansion effects arising from gamma and alpha heating in the B_4C limited operation to power levels below 900 kw. Above this level warping was sufficient to cause seizure in the thimble. Accordingly, the original rod, having a worth of 19.0 ih and a thimble clearance of $\frac{1}{32}$ in., was replaced by one of somewhat smaller diameter, having a worth of 13.6 ih and a thimble clearance of $\frac{1}{16}$ in.

The detector used in the measurements consisted of a cadmium-covered, boron-coated, parallel-plate ion chamber located in the graphite region diametrically across the core from the oscillator rod. The linearity of the chamber was periodically checked and found satisfactory by calibration against reactor power.

VI. RESULTS

A. Measurements

To establish the reliability of the method and equipment, transfer function measurements were carried out with the reactor operating at essentially zero power. The results for both phase and amplitude are given in Fig. 13.

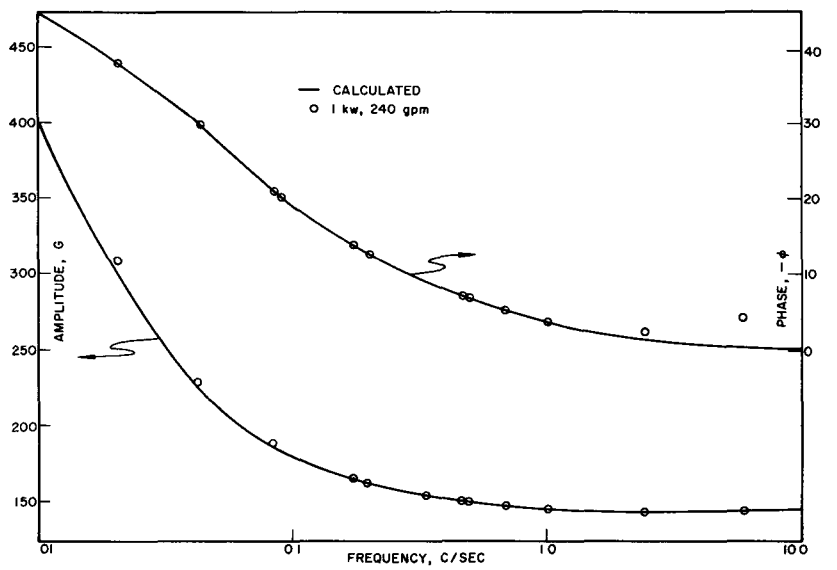

Fig. 13. Measured Zero Power Transfer Function

With the exception of phase lags for frequencies greater than two cps, all experimental phase values fall on or close to the curve calculated for zero power. Experiments in which the phase lag was measured as a function of detector distance demonstrated that the phase lag for frequencies exceeding two cps increased when the detector was moved outward from the core. Other experiments showed that covering the detector with 0.030 in. of cadmium foil decreased the high-frequency phase lag. Accordingly, the discrepancies have been associated with the time required for neutrons originating in the core to reach the detector. These discrepancies, however, are inconsequential. Experience has shown that the phase discrepancy for a given frequency is independent of power and can be eliminated by a constant correction factor. Furthermore, the region of discrepancy is of little practical interest since feedback effects at these frequencies are essentially nonexistent.

The amplitude of the transfer function is given by

$$G = \frac{\Delta n/n}{\Delta k/k}, \tag{8}$$

where $\Delta k/k$ is the sinusoidal driving function and $\Delta n/n$ is the resulting fractional change in neutron flux or power. The magnitude of G may be established, at any given frequency, from a knowledge of $\Delta k/k$, which remains constant, and $\Delta n/n$, which is established through the resistance settings at null balance. The input reactivity given by the peak-to-peak value of the oscillator rod worth may be found directly by measuring the difference in reactivity noted with the oscillator rod in its maximum and minimum worth positions through period measurements. However, the errors associated with determining $\Delta k/k$ in this manner are somewhat larger than the reproducibility of the null measurements. Furthermore it has been found from experience that the worth of the oscillator rod varied as much as 2-3 percent, depending on the power and inlet temperature. To avoid these difficulties and to eliminate errors associated with independent measurements of $\Delta k/k$, all amplitude measurements were normalized to the calculated zero power curve for frequencies greater than 2.0 cps. Essentially, the normalization amounts to an indirect determination of the effective rod worth $\Delta k/k$ from the expression

$$G_0 = \frac{R_s k}{R_0 \Delta k}, \tag{9}$$

where G_0 is the calculated zero power value of the amplitude at a given high frequency, and R_S and R_0 are the resistance values of the sine potentiometer and decade box, respectively. The successful application of this method relies on the validity of the assumption that feedback effects at high frequencies, i.e., greater than 2.0 cps, are negligible. In view of experimental results under a wide variety of operating conditions, this assumption was shown to be valid.

The measured value of G at the lower frequencies where feedback effects are important may then be found from the expression

$$G = M/R_0, \tag{10}$$

where M is an average value of the product G_0R_0 evaluated at the higher frequencies.

B. Results at Low Power and Reduced Flow

As a convenience the discussion of experimental results has been separated into the following distinct phases: (a) conclusions regarding the stability of Mark III, (b) interpretation of data in terms of empirical models, and (c) correlation of Mark III with Mark II results. Since a complete record of all experimental results obtained in this series of tests is available in the form of progress reports[25] only, those results immediately pertinent to an understanding of the Mark II and Mark III behaviors will be cited.

The results of three sets of transfer function measurements, each at substantially different flow rates for approximately 500 kw and for series and parallel flow, are summarized in feedback form in Fig. 14 and 15, respectively. Values for the feedback were found from Equation 2, where $1/G$ and $1/G_0$ are the inverse measured and zero power gains, respectively.

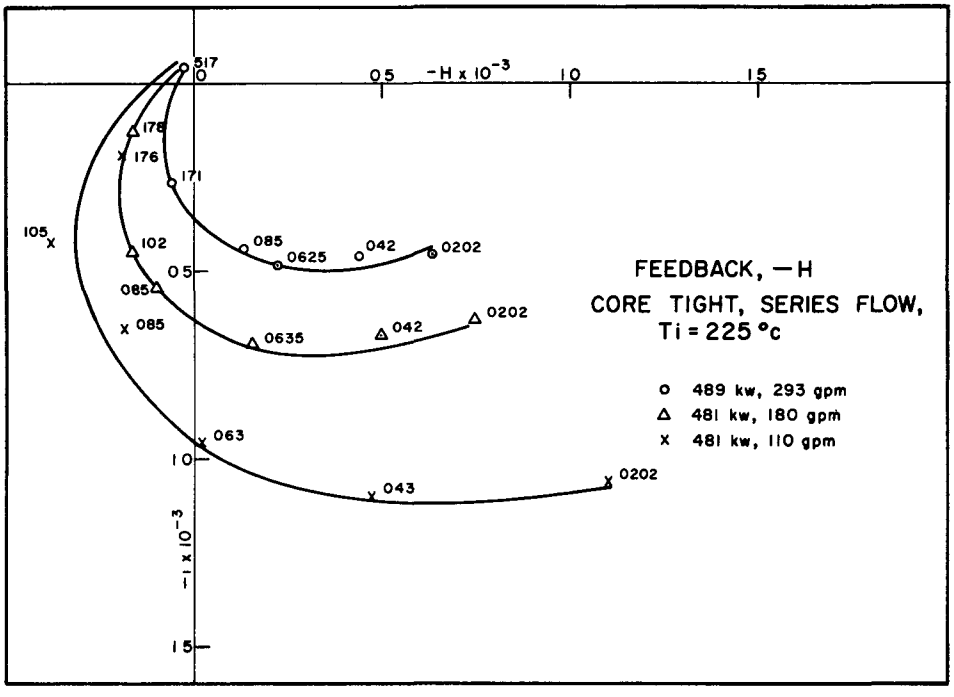

Fig. 14. Reduced Flow Feedbacks, Series Flow

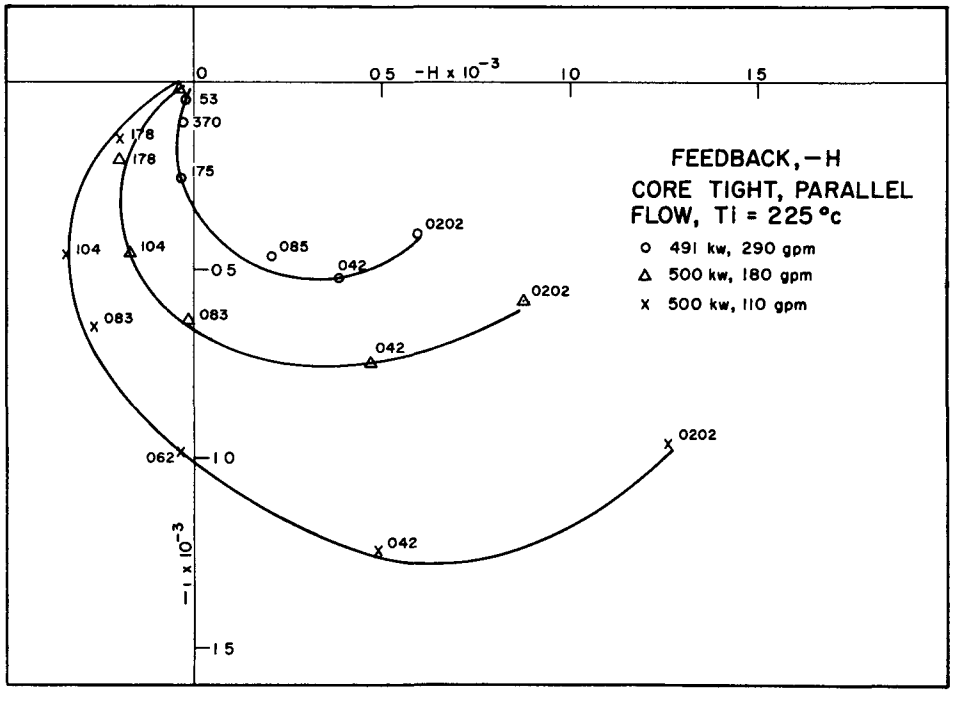

Fig. 15. Reduced Flow Feedbacks, Parallel Flow

Qualitatively, the results illustrated in Fig. 14 and 15 are subject to a simple interpretation. As the flow decreases at constant power, the temperature differential across the core increases. Under these conditions, a given power oscillation will effect larger oscillations in the temperature associated with fuel, coolant and structure. The larger temperature oscillations, in turn, result in larger changes of reactivity fed back to the reactor. The effect of reducing flow while maintaining power constant is reflected in the ideal case by inversely proportionate changes in the magnitude of the power coefficient X. In the absence of positive components, the feedback defined by one or more terms containing the product PX increases as the flow is reduced. The data illustrated in Fig. 14 and 15 are consistent with these concepts.

Quantitatively, as illustrated in Section VII-B, the data are satisfactorily explained in terms of an empirically deduced mathematical model described by the expression

$$-H = \frac{PX\, e^{-iwT}}{(1 + iwT_1)} \qquad (11)$$

where T_1 is the time constant associated with the expansion of fuel and T is an effective transport lag. Decreases in the coolant flow rate are reflected, not only by increases in X, but by increases in values for T_1 and T as well. One result of a flow decrease, therefore, is an increase in both the amplitude and phase of the feedback, a condition which effectively enhances the possibility of resonance.

In practice, the flow at significant levels of power cannot be reduced indefinitely, since the increasing temperature differential across the core may result in central fuel rod temperatures higher than those specified for safe operation. In the case under consideration, i.e., for 500 kw, the lowest permissible flow was limited in practice to the range from 100 to 110 gpm.

C. Stability of Mark III at Reduced Flow

From the complex plots of Fig. 14 and 15 it is clear that, if the power coefficient X is linear with power (at constant flow) increasing, the power will increase the magnitude of the feedback at all frequencies. For some value of power it is expected that the feedback will reach cancellation with the inverse zero power gain. For these special conditions $1/G$ approaches zero and resonance instability occurs. An estimate of the resonance power and flow rate for Mark III, accordingly, permits a direct comparison of the relative performances of the Mark II and Mark III cores. Obviously, such estimates are only approximate and serve only as relative figures of merit. Furthermore, the conditions under which Mark III will undergo resonance are purely hypothetical, since the power densities involved are impossibly high in view of extreme problems of heat removal.

From the Nyquist stability criterion, illustrated mathematically by the expression

$$G = \frac{G_0H}{1 - G_0H}, \tag{12}$$

it is clear that, when the magnitude of the product G_0H is equal to unity, the gain G approaches infinity. Assuming that the feedback is linear with power, a family of $-G_0H$ curves can be constructed for various values of power. The results of a Nyquist analysis based on empirical parameters (see Section VII-B) for the most rigorous operating conditions encountered in the Mark III tests (500 kw and 110 gpm) are illustrated in Fig. 16, from which it may be seen that $-G_0H$ approaches -1 in the vicinity of 10 megawatts at 100-gpm flow. The frequency at which resonance will occur is estimated from Fig. 16 to be of the order of 0.20 cps. Since the condition of resonance in Mark II occurred at 550 kw under similar conditions of flow, it follows that changes incorporated in the Mark III design have greatly extended the range of safe operation.

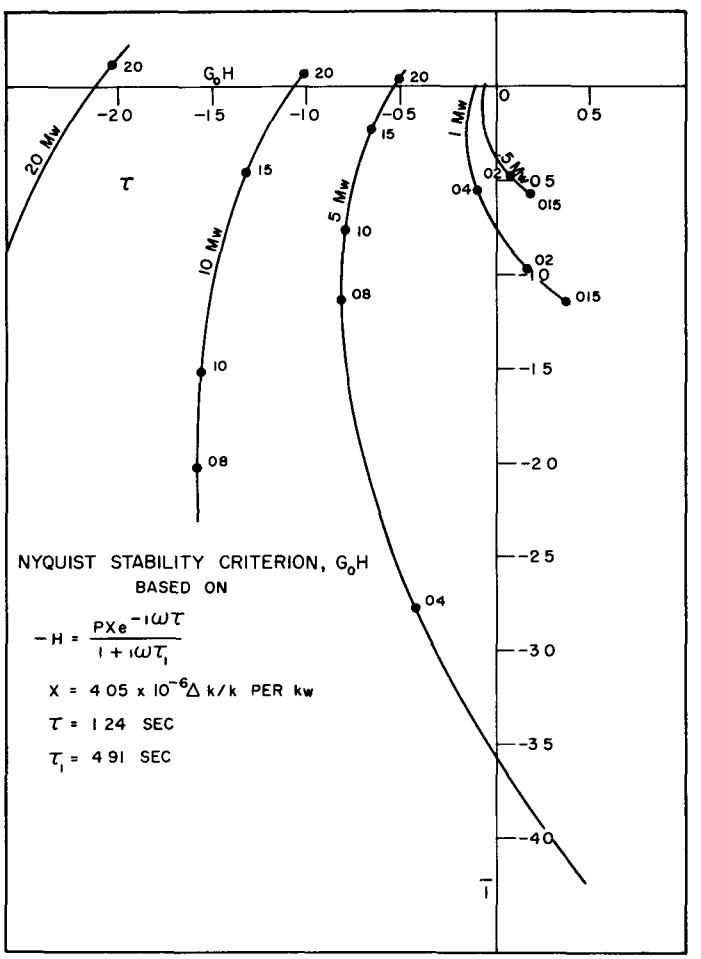

Fig. 16. Nyquist Stability Criterion for One-third Flow

A comparison of feedbacks measured for Mark II and Mark III under similar operating conditions is given in Fig. 17. The larger magnitudes and phases of the Mark II feedback (for a given frequency) in the III quadrant constitute a situation particularly conducive to resonance instability, since the possibility of feedback cancellation with the inverse zero power gain lying in the I quadrant is greatly enhanced. To produce comparable III quadrant feedbacks in Mark III would require drastic increases in power. As discussed in Section VIII, the unusually large III quadrant feedback in Mark II is the result of a combination between three power coefficient components arising from mechanical features peculiar to Mark II.

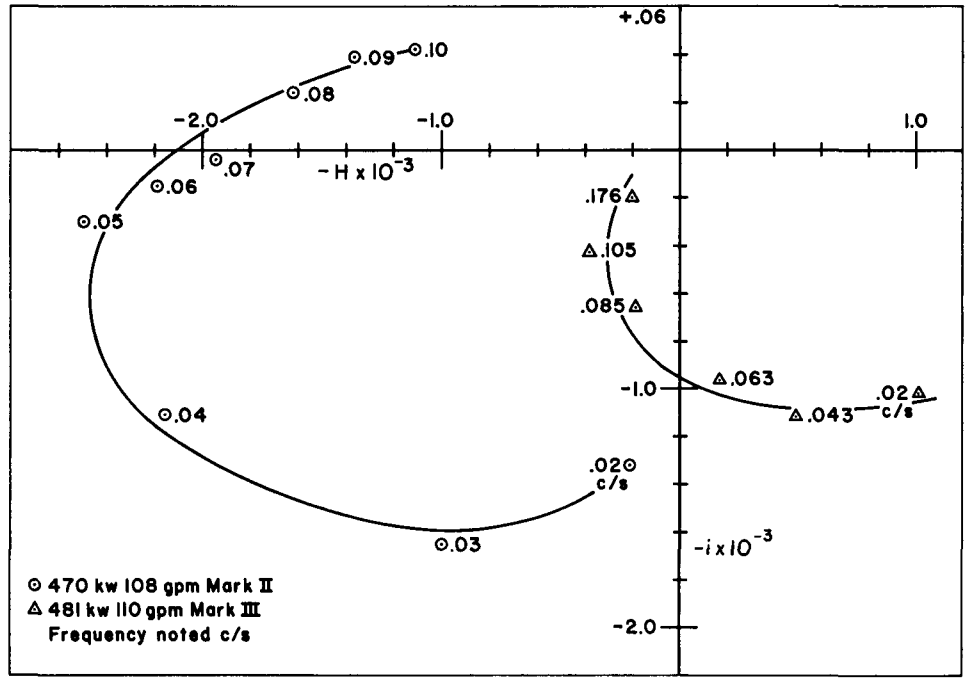

Fig. 17. Comparison of Mark II and Mark III Reduced Flow Feedbacks

D. Stability at Full Flow

One of the major and immediate benefits resulting from oscillator studies is the ability to predict the performance of the reactor at some higher level of power from the measured performance at some arbitrary lower level. In this way, if dangerous resonance effects do exist at full power in an "unproven" reactor, their presence will be revealed at power levels low enough to permit safe and detailed study. Depending on what low-power measurements indicate, the reactor power can be raised by some increment to a higher level indicated to be safe by extrapolation. The size of the incremental power increase depends, of course, on the stability situation indicated by the low-power results.

The results of oscillator studies conducted on Mark III provide a direct measure of the validity of these concepts. Between zero and full power (1200 kw), transfer function measurements were conducted at the following levels: 40, 80, 370, 500, 655, 875 and 950 kw. In retrospect it is clear that this approach to full power was extremely conservative.

The results of transfer function measurements at 489, 877, 952 and 1150 kw are summarized in Fig. 18.

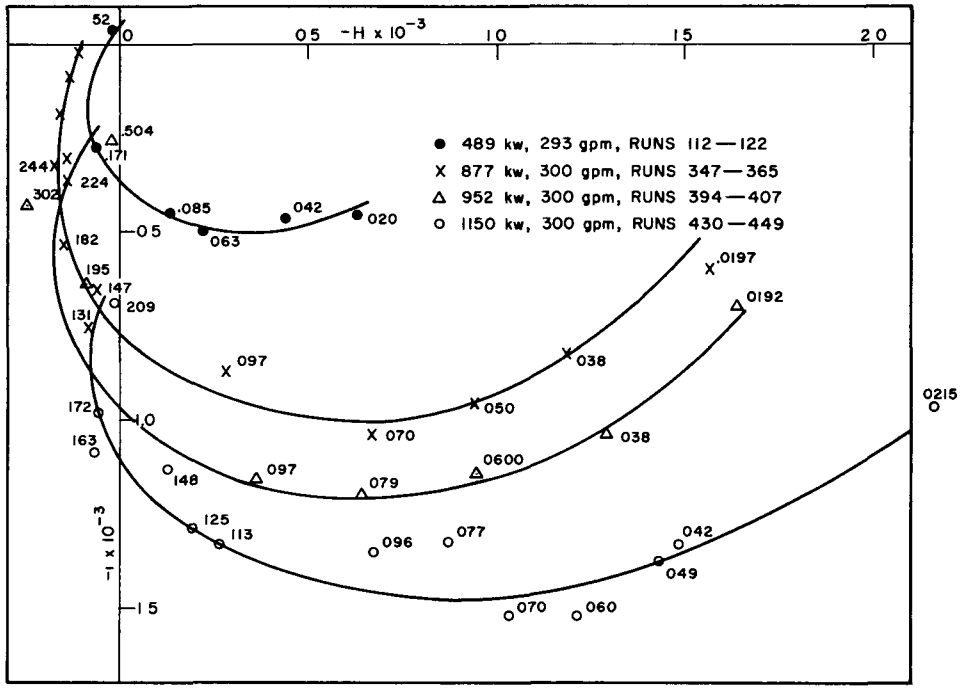

Fig. 18. Full-flow Feedback as a Function of Reactor Power

(The results of measurements at lower powers have been omitted for the purpose of clarity.) For the most part, the results are inconsistent with a feedback which varies linearly with power, since a linearly varying feedback would lead to a family of curves consistent in phase and differing in amplitude by amounts directly related to the incremental changes in power. From these results it is apparent that, as the power is increased above 877 kw, the phase of the feedback, particularly at the higher frequencies, tends definitely to decrease. Such behavior suggests that the time constants governing the frequency dependence are themselves sensitive to power. Although not obvious from Fig. 18, it has also been established that nonlinearities exist in the power coefficient. Nonlinearities in the time dependence and power coefficient can result in the essentially unanticipated feedbacks measured at 952 and 1150 kw.

The complexity of the power coefficient nonlinearity is illustrated in Fig. 19, which consists of data taken approximately at the time of the 877 and 1150-kw experiments. Three distinct regions are recognizable.

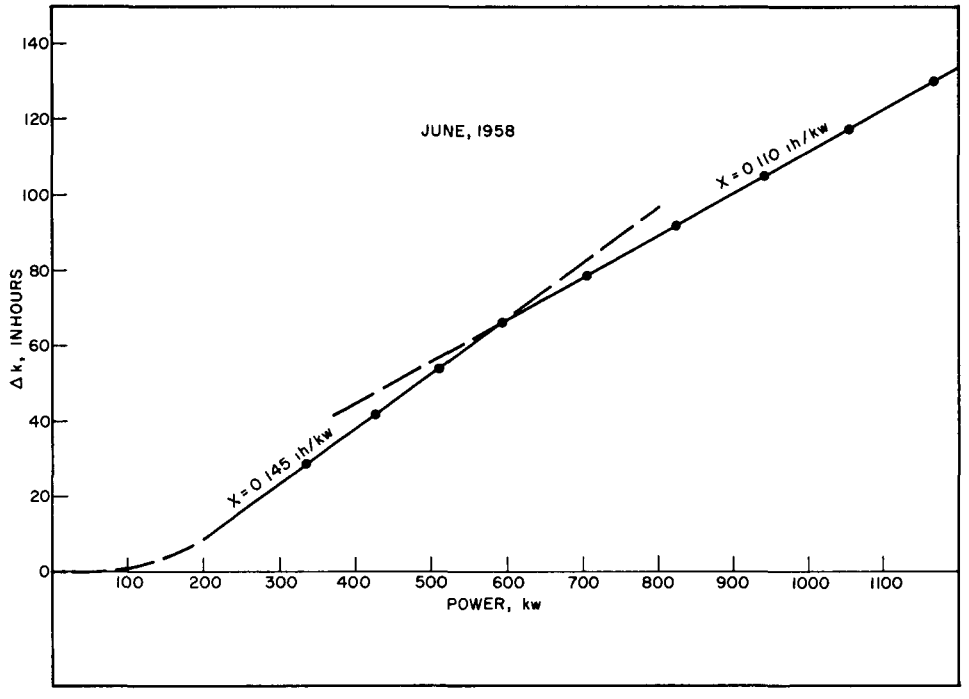

Fig. 19. Power Coefficient, Series Flow

In the region from 0 to 200 kw the reliability of measurements is seriously affected by relatively large errors associated with power measurements. Nevertheless, the results of several earlier measurements indicate rather definitely the general shape described by the dashed portion of the curve in this region. Each of the regions 200-600 and 600-1200 kw is characterized by a definite and significantly different slope. That such discontinuities are real is indicated by similar observations on a large number of power coefficient determinations carried out over a considerable period of time. As an additional complication it has also been observed that the power level at which the discontinuity between the two high-power regions occurs has varied, not only over a long term basis (months), but on a day-to-day basis as well.

The physical explanation for the origin of the discontinuities most likely involves a power and temperature-sensitive system of clearances. Because the linear expansion coefficient of stainless steel ($18 \times 10^{-6} \Delta L/L$ per °C) is larger than that of the fuel (approximately $13 \times 10^{-6} \Delta L/L$ per °C at 200°C), the core, which is tightened at a relatively low temperature (approximately 50°C), actually loosens as the primary coolant is brought to operating temperature, usually around 230°C. According to McVean,[26]

an isothermal temperature rise of 300°C causes the hexes to expand 0.004 in. more than the contained fuel, blanket and tightening rods. The preferential expansion results in opening or increasing already existing clearances between fuel rods. Clearances between hexes are, however, unaffected by isothermal temperature increases, since the hexes and the stainless steel structure rings restraining the hexes expand by similar amounts. The situation at elevated inlet temperatures for zero power, then, is characterized by the existence of significant clearances between fuel rods and between fuel rods and hexes. As the reactor power increases, the structure rings, maintained at the temperature of the inlet coolant, effectively restrain the hexes from further expansion. As McVean has shown, the temperature differential across the core at nominal full power is sufficient to cause the hexes to expand relative to the structure rings by 0.0075 in. After nominal clearances between cans are closed, further radial expansion of the cans is restricted. The fuel rods, on the other hand, continue to expand until clearances between rods and between rods and hexes are closed.

For the region 0-200 kw, the degree of coupling between fuel rods is best described as partial. Because of mechanical imperfections it is certain that the additional clearance afforded by the differential expansion associated with the rise from room to operating temperature will not be distributed equally to all fuel rods. Some rods will be in rib-to-cladding contact with neighboring rods; others will not. As the reactor power increases, the hexes expand radially more or less freely until the clearances between are eventually closed. The effect of such action on the power coefficient is strongly negative, since the radial expansion of the hexes effectively increases the core radius through the movement of fuel rods contiguous with the inner surfaces.

At low power, i.e., 0-200 kw, the fraction of rods contiguous with the inner hex surfaces is small and the resulting power coefficient is weak. Above 200 kw, the clearances between hexes decrease to an extent that the radial expansion of hexes is no longer unrestricted. In this region of power, radial fuel expansion tends to "catch up" with hex expansion. The degree of coupling between rods and the fraction of rods contiguous with the surfaces increase, and the resulting power coefficient is strong. As the power is raised to approximately 600 kw, the clearances between hexes become closed and further radial expansion is denied. As a consequence, the contribution to power coefficient at this point suffers a sharp reduction and consists chiefly of contributions from axial expansion and from the radial expansion of fuel rods within the no longer unrestrained hexes.

The effect of nonlinearities in the power coefficient and time constants on the ability to predict full-power performance from low-power data is illustrated in Fig. 20. Clearly the reactor is seen to be more stable than the low-power extrapolations indicate.

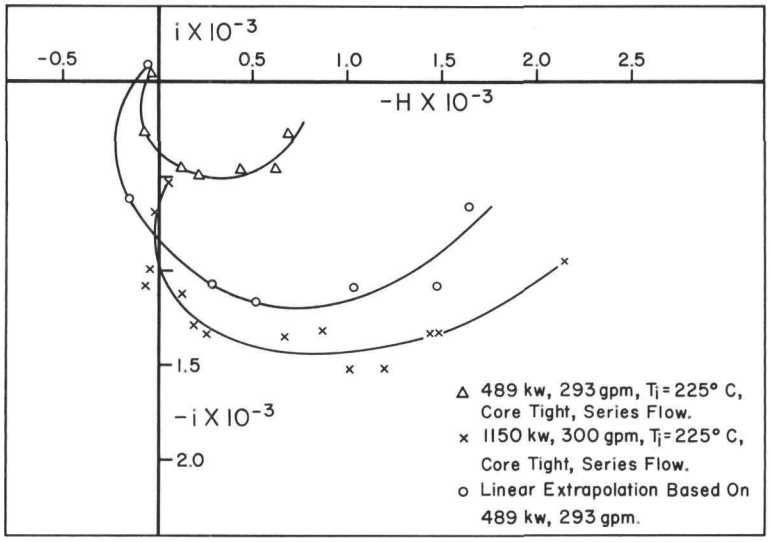

Fig. 20. Prediction of Full-power Feedback from Low-power Data

Although discrepancies between experimental and extrapolated feedback do exist, the magnitudes of the discrepancies in the important III quadrant are so small relative to the magnitudes of the corresponding $1/G_0$ vectors that conclusions based on low-power results regarding the stability at full power remain essentially unchanged. Even for a feedback system known to be nonlinear the extrapolation method suggested by Bethe[14] appears to retain a high degree of usefulness. However, although the nonlinearities in the Mark III feedback caused extrapolations to be conservative, it does not follow that such will always be true for any given unproved fast reactor. Such possibilities must be anticipated, particularly if extrapolations are carried out for large power increments.

E. Prediction of Resonance at Full Flow

Application of the Nyquist stability criterion to the full-power, full-flow data given in Fig. 18 results in the conclusion that instability would never occur regardless of how high the power of the reactor is raised. Such a conclusion is the direct consequence of the low values, i.e., in the vicinity of 90°, measured for the phase of the feedback at higher frequencies. Later in the tests, full-power, full-flow feedbacks slightly different from those illustrated in Fig. 18 were noted, with the sense of the difference such that larger phase values were measured at the higher frequencies. A feedback typical of those measured later in the tests is illustrated in Fig. 21. The difference between the earlier and later full-power full-flow feedbacks is apparently the result of clearance changes effected in the core through the continual accumulation of power.

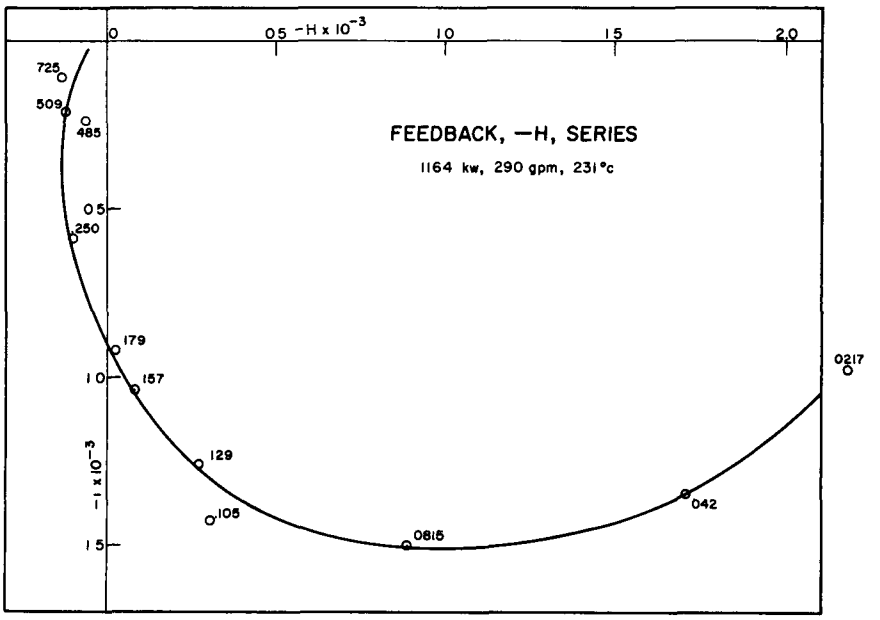

Fig. 21. Typical Full-power, Full-flow Feedback

A Nyquist stability analysis based on a mathematical model with associated empirical parameters (see Section VII-C) for full-flow conditions results in essentially the same conclusions reached with the earlier data, that the reactor would be hypothetically stable at extremely unrealistic values of power. From Fig. 22 the resonance power is seen to be in excess of 1000 megawatts, a power level absurdly high in view of the problems of heat removal.

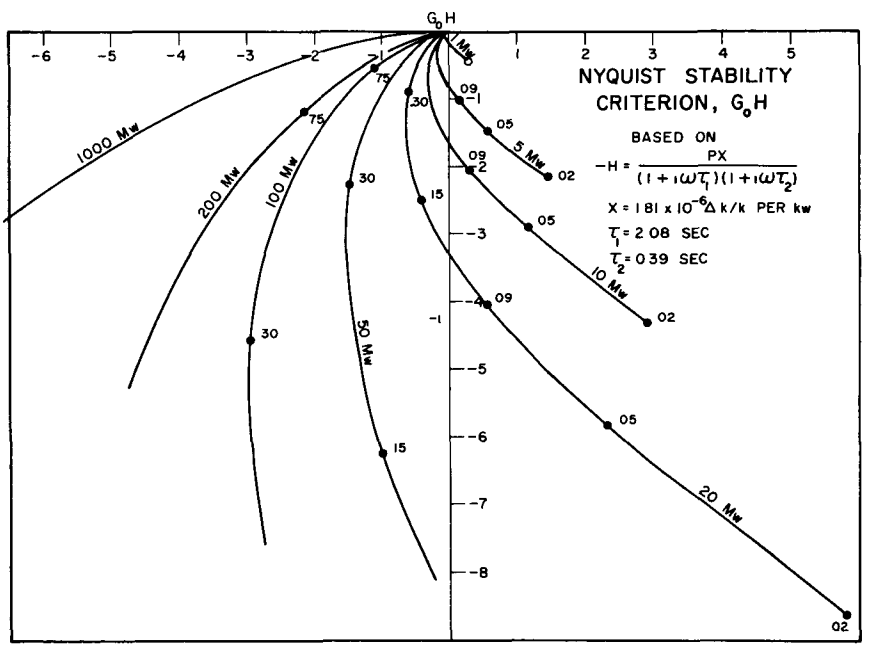

Fig. 22. Nyquist Stability Criterion for Full Flow

F. The Effect of Inlet Temperature

The results of a large number of transfer function and power coefficient measurements have established unambiguously the existence of a strong dependence of feedback on inlet temperature. The magnitude of this effect is illustrated in Fig. 23, which compares the feedbacks for series and parallel flow at two significantly different inlet temperatures.

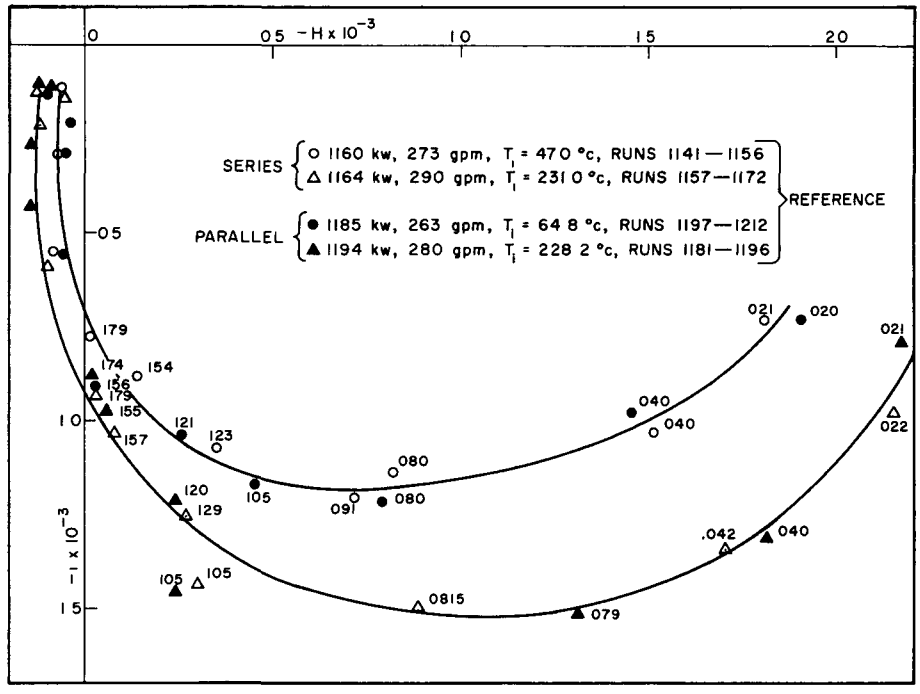

Fig. 23. Full-power, Full-flow Feedback for Series and Parallel Flow, High and Low Inlet Temperatures

For both series and parallel flow, increasing the inlet temperature from approximately 75 to 230°C results in an approximate increase of 22 percent in the amplitude of the feedback at all frequencies. The fact that the phase of the feedback remains essentially unchanged suggests that the processes responsible for the feedback are essentially the same at both high and low inlet temperatures and that the change in feedback magnitude simply reflects proportionate changes in the magnitude of the power coefficient. The results of independent measurements of the power coefficient carried out in conjunction with these studies substantiate this conclusion. The strong dependence of feedback on inlet temperature has been attributed to temperature-sensitive changes in the expansion coefficient for the Mark III fuel. A discussion of the effect is given in Section VII-C.

G. The Effect of Flow Path on Feedback

The importance of heat transfer across the flow separator from core outlet to blanket inlet as a feedback mechanism can be assessed in various ways, among which are (a) measurements of temperature fluctuations at the bottom of the blanket with the reactor oscillating at a fixed frequency, (b) measurements of temperature fluctuations in an inner blanket channel as a function of elevation with the reactor oscillating, and (c) measurements of feedback under series and parallel flow conditions.

The results of transient temperature measurements carried out at three different radial positions at the bottom of blanket hex R with the reactor oscillating at 0.04 cps and under the rigorous conditions of 500 kw and 100-gpm flow did reveal the existence of small oscillations in temperature ranging from 0.70 to 1.10°C. Oscillations of this magnitude, however, can be satisfactorily explained in terms of the blanket flow, the amplitude of the power oscillation, and the fraction of total power generated in the blanket. Attempts to detect oscillations in the temperature of coolant entering hexes A and F under the same conditions were unsuccessful, indicating that if such oscillations did exist their amplitudes were smaller than 0.5°C, the lower limit of measurement.

Additional temperature measurements carried out as a function of elevation in a blanket channel bordering the flow divider demonstrated that temperature oscillations were not observable for elevations higher than sixteen inches above the lower support plate, precisely the region where heat transfer across the separator should be important. These results also proved that the temperature oscillations observed at the bottom of the blanket were the result of sinusoidal variations in blanket power.

Another measure of the importance of feedback effects originating in the radial blanket may be obtained from a comparison of the feedbacks measured under similar conditions for series and parallel flow. Feedback effects arising from a transfer of heat across the flow separator into the blanket would almost certainly involve a dependence of transport lag peculiar to series flow. Differences between series and parallel flow feedbacks should accordingly reflect the existence of such a dependence. The results of measurements carried out for both high and low inlet temperatures and for series and parallel flow are summarized in Fig. 23. Within the limits of experimental accuracy it is clear that the series and parallel flow feedbacks are essentially identical. From these results it may be concluded that feedback effects originating in the blanket are inconsequential.

Vigorous attempts to promote additional heat transfer across the flow separator by shifting fuel elements substantiated this conclusion. Since the seven inner assemblies included a total of 47 blanket rods arranged along the outer edges the temperature gradient across the flow separator was

abnormally depressed. To promote a higher degree of heat flow, blanket rods along the outer edges of hexes D and E were exchanged for fuel rods in other assemblies until both hexes were filled completely with fuel. Under these conditions approximately one-third of the core-blanket interface consisted of fuel and blanket rods immediately separated by the flow divider. The results of transfer function measurements carried out under series flow at high and low inlet temperatures are compared with reference values in Fig. 24.

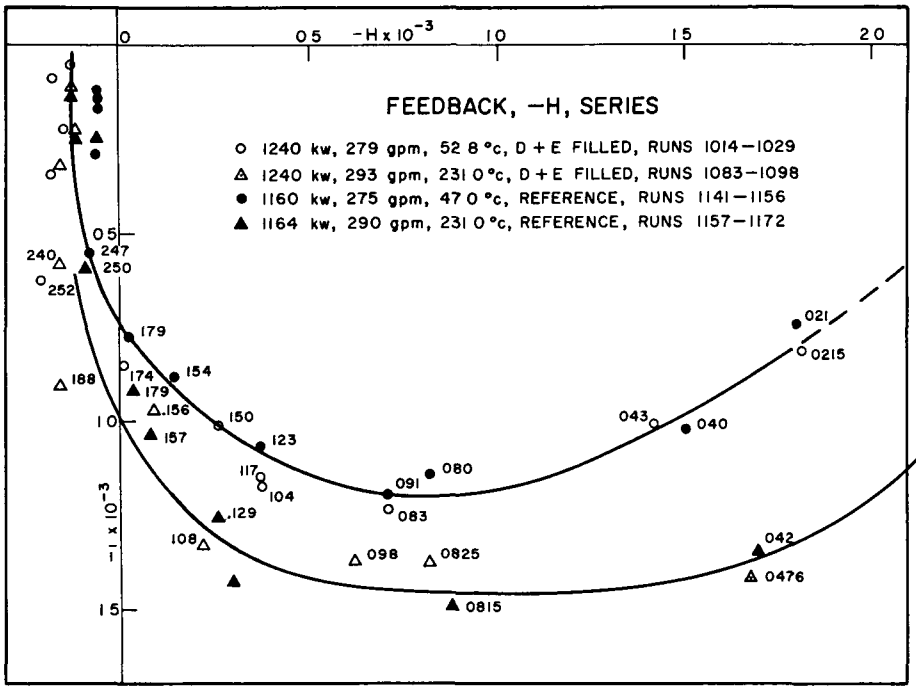

Fig. 24. Comparison of Reference and Distended Core Feedbacks; Full Series Flow, High and Low Inlet Temperatures

A similar comparison for parallel flow is given in Fig. 25. From these results it is clear that increasing the heat flow across the flow divider results in little or no change in feedback. Similar conclusions resulted from power coefficient measurements carried out in conjunction with these measurements.

Since the considerations of heat flow across the flow separator in series flow are similar for Mark II and Mark III, it follows that arguments basing the delayed negative power coefficient of Mark II on preheating mechanisms are considerably weakened.

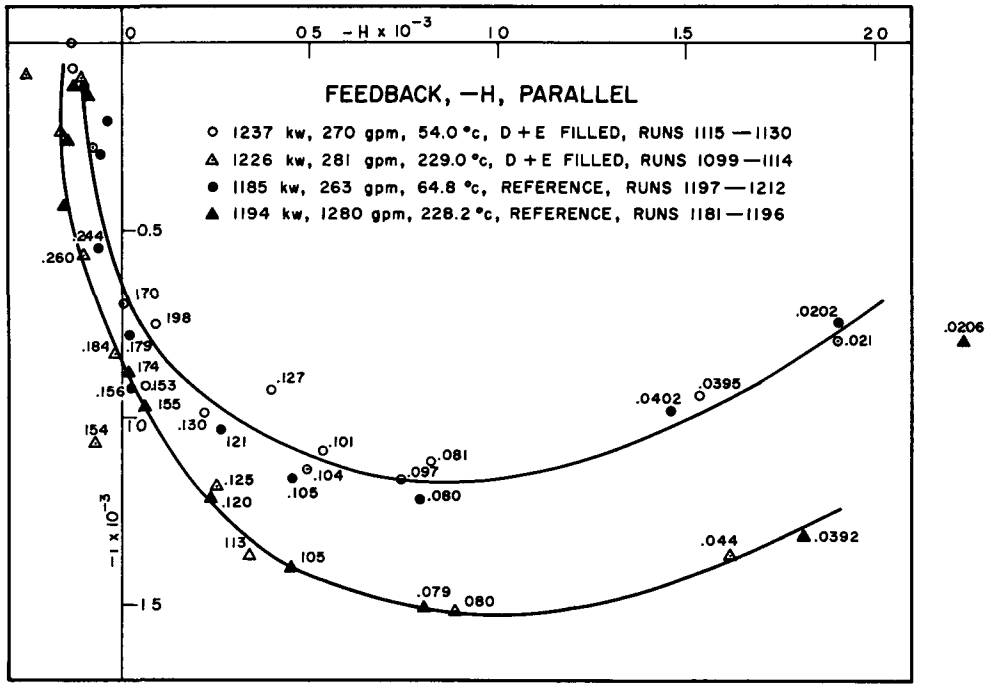

Fig. 25. Comparison of Reference and Distended Core Feedbacks; Full Parallel Flow, High and Low Inlet Temperatures

H. The Effect of Core Tightness on Feedback

A comparison of feedbacks measured under rigid and loosened core conditions provides further information on the effects of fuel rod coupling and illustrates the importance of radial restraint for fuel rod bowing.

A comparison of feedbacks measured at high and low inlet temperatures with the central tightening rods loosened in all core and blanket assemblies is given in Fig. 26. In qualitative agreement with the results obtained for the rigid core, larger feedback amplitudes occur at the higher inlet temperature. The difference between high and low-temperature feedback amplitudes is, however, less marked than for the case of rigid core conditions. Whereas a 22 percent difference was noted for the rigid core, the difference for the loosened core, after correcting for flow difference, amounted to only seven percent. A further difference, which may or may not be significant, is found for frequencies greater than 0.12 cps. While the high-temperature feedback amplitudes appear to be consistently higher than corresponding low-temperature values, the high-temperature phase lag seems to be consistently lower than those measured at low inlet temperature. Finally, another difference, not immediately apparent from Fig. 26, consists of marked decreases in the values measured for the static power coefficient at both high and low inlet temperatures for the loose core

condition. At the high inlet temperature, the static power coefficient decreased from 0.113 to 0.085 ih/kw, whereas at the low inlet temperature a decrease from 0.0825 to 0.0733 ih/kw was noted. Although the smaller difference existing between the high and low-temperature feedback amplitudes is not susceptible to simple interpretation, it seems plausible that the decrease in coupling between rods through a relaxation of tightening rod tension effectively decreases the radial contribution to power coefficient at both high and low inlet temperatures.

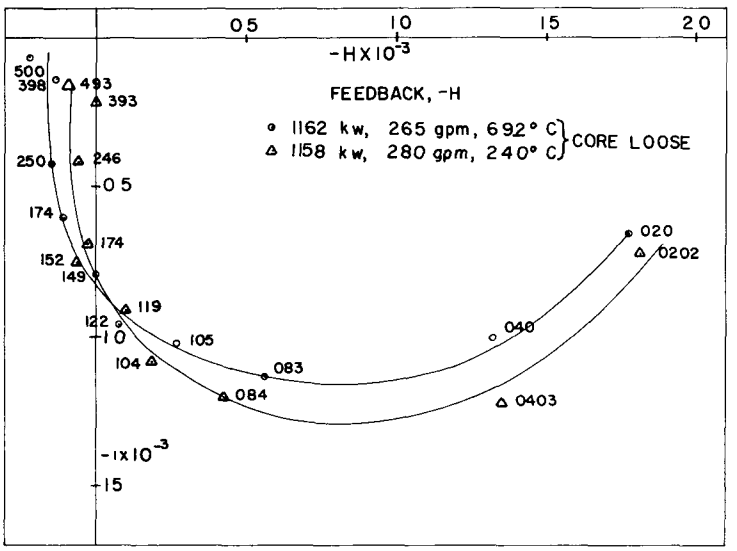

Fig. 26. Loose Core Feedback; Full-power, Full-flow, High and Low Inlet Temperatures

A comparison of loose and tight core data at high inlet temperature is given in Fig. 27. The effect of loosening the tightening rods is manifested by a decrease in the feedback amplitude at all frequencies. Such results are completely consistent with the concept of a decrease in power coefficient through a loss of coupling between fuel rods. On the other hand, the significant increases effected in the phase of the feedback through loosening are also consistent with the introduction of a positive power coefficient component which conceivably could be the result of rod bowing. The presence of such a component would also explain the decrease noted in the feedback amplitude. It is quite possible that both effects, i.e., rod bowing and decreased coupling, resulted from the relaxation of tightening rod action.

In some respects it is surprising that so little evidence of rod bowing was found, since loosening of the tightening rods effectively increases the rod clearances to the extent that rod bowing would no longer be prohibited. On the other hand, as will be discussed in Section VI-I, rod bowing is a consequence of rather special conditions of end restraint not realized in the loose core tests.

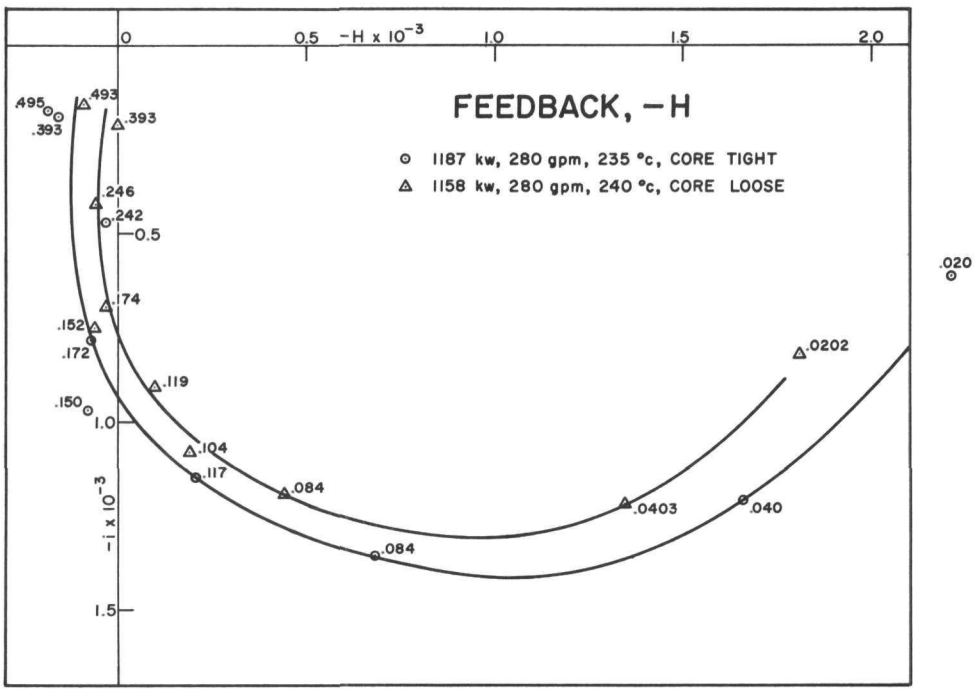

Fig. 27. Comparison of Tight and Loose Core Feedbacks: Full-power, Full-flow, High and Low Inlet Temperatures

I. Stripped Rib Experiments

The temperature differential across a given fuel rod under steady-state conditions depends on a variety of factors, among them being the reactor power, the shape of the neutron flux distribution, the velocity of coolant, and the heat transfer properties of the fuel, coolant and cladding material. Under equilibrium conditions the temperature differential across a given fuel rod will remain invariant with time. If, however, the power is increased, the flux profile across the core will change in such a manner that the gradient of the flux will increase. As a consequence, the temperature differential across a fuel rod, located in any position other than central, will increase. The inner surface of the rod is heated relative to the outer and, because of differences in thermal expansion between the surfaces, the rod will tend to deform. Although it is clear that the inner surface will undergo a preferential expansion, it does not follow that the deformation will necessarily be manifested by an inward bowing of the rod. The exact form that the deformation will assume and the subsequent effect of fuel displacement on reactivity will depend on the kind and the degree of radial restraint above and below the fuel section. If the rod is perfectly restrained from radial motion above and below the fuel, the deformation will result in an inward bow, an effect that is clearly positive. If, however, the rod is restrained above the core and is free to move radially at the bottom, it

does not follow that the reactivity will be positive, since under these circumstances deformation may effect an outward radial movement of the rod at the bottom. In the practical case where the rod tips are positioned in holes in a perforated plate, some rod tips will bear on the outer edges of their locating holes. In these cases the rods cannot move outward at the bottom, and the deformation will again assume the form of an inward bow. The reactivity effect under these conditions will be the sum of positive and negative components both of which result from conditions too obscure to define in the practical case.

For a system of rods fixed at the bottom and free to move radially at the top, it seems likely that deformation accompanying differential expansion will result in an outward movement at the top and a consequent reactivity loss. For a system of rods free to move radially at both top, bottom, and center, the exact form of deformation will depend on the bearing positions of the rod tips in the positioning holes. For rod tips bearing on the inner edges a negative effect will most likely result; for those bearing on the outer edges the effect will more likely be positive. Again, the net reactivity change may be either positive, negative, or even zero, depending on the magnitude of the positive and negative components.

For the ideal case in which the rods are restrained from radial motion at both top and bottom, the extent of inward bowing will depend on additional factors: whether or not the restraining point is a simple pivot, whether or not the rod is clamped in a cantilever arrangement, or whether or not the restraint is sufficient to permit compressional bowing. In regard to the first two cases, if the restraining point is better described by a simple pivot, some adjustment of the deformation can occur above the pivot. If, however, the rod is tightly clamped at the restraining point, no such adjustment is possible and a given deformation will lead to a smaller bow. Finally, if the rods are so tightly clamped that axial expansion is denied, the result may be a compressional bowing or "buckling" which, if inward, will accentuate the thermal bowing.

From these considerations it is clear that, although rod deformation is a logical consequence of a change in temperature differential across a rod, it does not follow that the net associated reactivity effect will be positive. To promote as large a bowing effect as possible, care must be taken to eliminate radial movement at restraining points while still permitting radial movement in the vicinity of the fuel. The importance of this requirement was demonstrated conclusively in the stripped-rib experiments.

J. Blanket Rod Bowing

To establish the importance of blanket rod bowing, attempts were made to detect small changes caused in the feedback through the removal of stabilizing ribs from all blanket rods in hex M. One-inch rib sections

were left intact at the upper and lower ends of the blanket pieces to provide proper tightening action for the centrally located tightening rod. In principle this arrangement provided a system of rods restricted from radial motion at upper and lower ends yet still free to move radially at intermediate points. The results of transfer function measurements carried out for full series flow and at high and low inlet temperatures are illustrated in Fig. 28. Within the limits of experimental accuracy it may be concluded that the effects of shearing ribs from blanket rods are insignificantly small. Similar conclusions follow from the results of high and low inlet temperature transfer function measurements conducted under parallel flow conditions (see Fig. 29). The results of power coefficient measurements carried out in conjunction with these measurements also substantiated this conclusion.

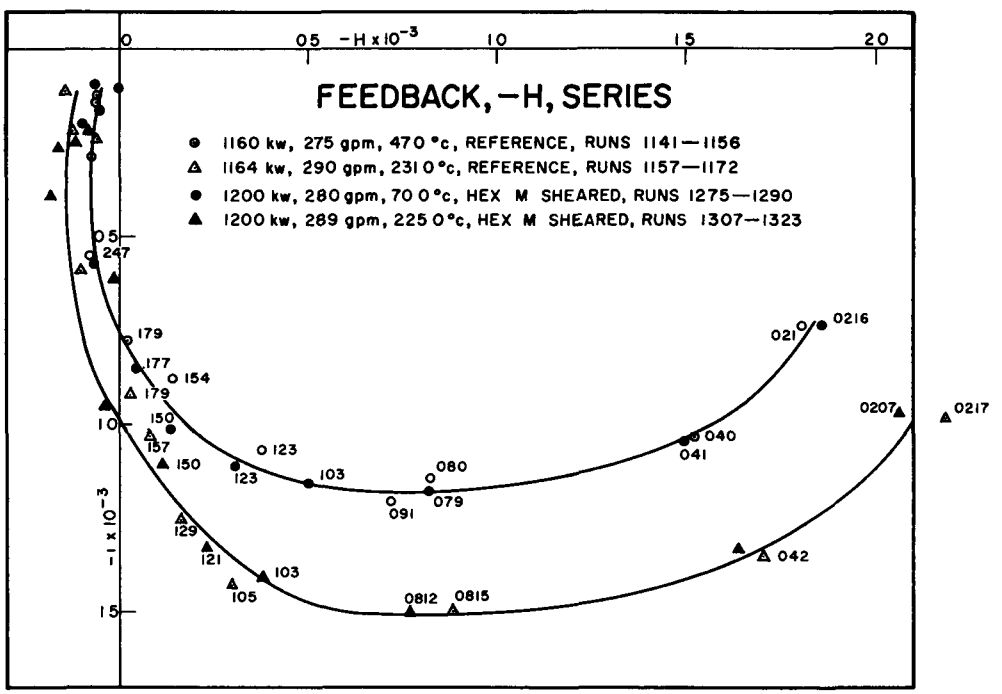

Fig. 28. Comparison of Reference with Partially Sheared Blanket Feedback: Full-power, Full-series Flow, High and Low Inlet Temperatures

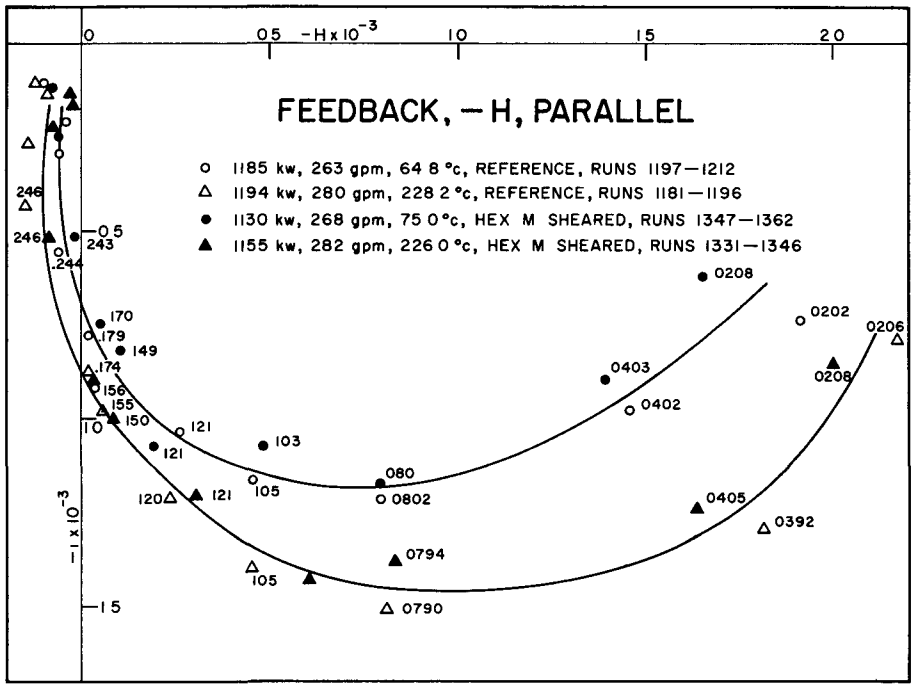

Fig. 29. Comparison of Reference with Partially Sheared Blanket Feedback: Full-power, Full-parallel Flow, High and Low Inlet Temperatures

K. Fuel Rod Bowing

One of the major problems associated with the stripped-rib experiments was the difficulty encountered in realizing a rigid arrangement of the sheared rods. From the results of early experiments in this series it was apparent that changes in feedback arising from the shearing were sensitive to the degree of radial restraint. On one occasion, tension from the existing tightening rod was purposely relaxed, with the result that the positive component existing at that time vanished. Such results illustrate the necessity for minimizing radial motion at restraining points in experiments of this nature. Accordingly, a considerable effort was devoted in subsequent experiments to the development of practical and reliable tightening systems. During the course of the measurements a total of four different systems was used. Of these the most successful consisted of two conical-action tightening rods per assembly: one operating at the upper restraining point, and the other at the lower. Pertinent details and dimensions are given in Fig. 30. Complete details of other less successful systems, along with corresponding results, are summarized in Progress Report 9.[25]

For the most part the earlier experiments were limited to successive attempts to enhance rod bowing through the shearing of additional increments of rods, through refinements intended to promote a more

normal temperature profile across the assembly, and through the achievement of a greater degree of tightness. Almost without exception as changes more conducive to rod bowing were initiated, the feedback changed in a manner consistent with the introduction of a positive component to the power coefficient.

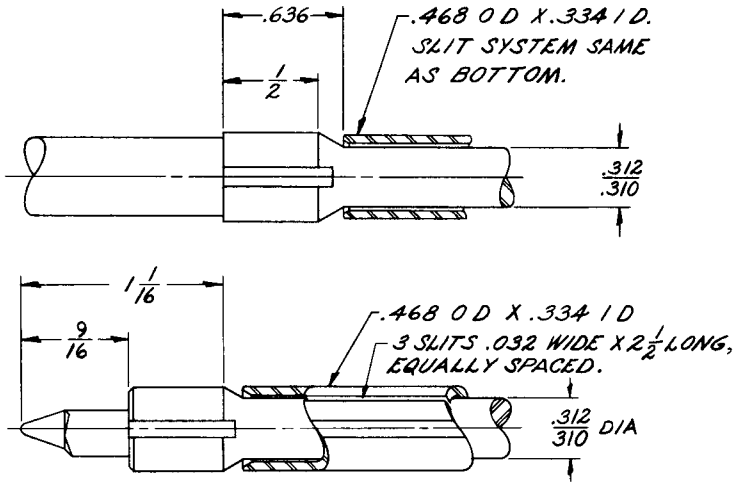

Fig. 30. Dimensions of Cone-action Tightening Rods

The results for conditions under which the maximum change in feedback was noted, i.e., for two completely sheared assemblies and for the most effective tightening system, are summarized in Fig. 31.

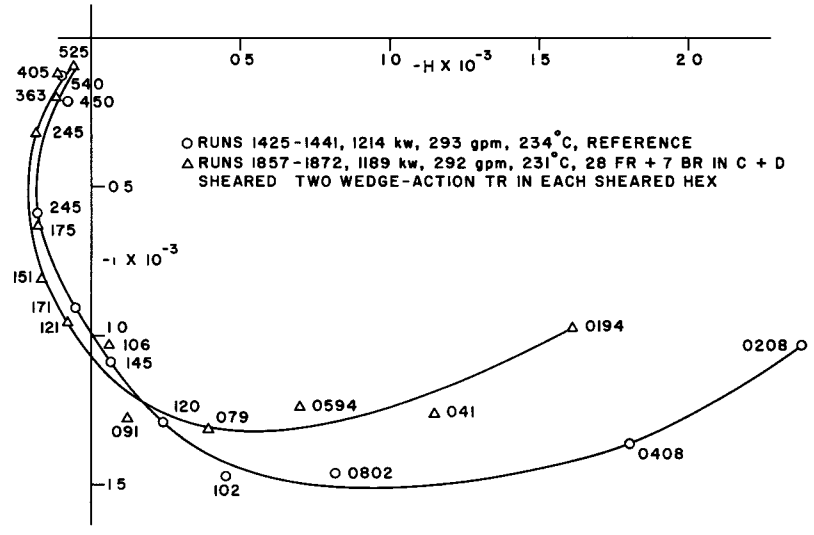

Fig. 31. Comparison of Reference and Partially Sheared Core Feedbacks: Full-power, Full-series Flow, High Inlet Temperature

Two features are immediately apparent. One of these consists of a marked decrease in the amplitude of the feedback and the other of an equally marked tendency for the phase of the feedback to increase as a result of the shearing. Both features are consistent with the introduction of a positive power coefficient component. Similar results obtained from studies carried out at low inlet temperature are illustrated in Fig. 32.

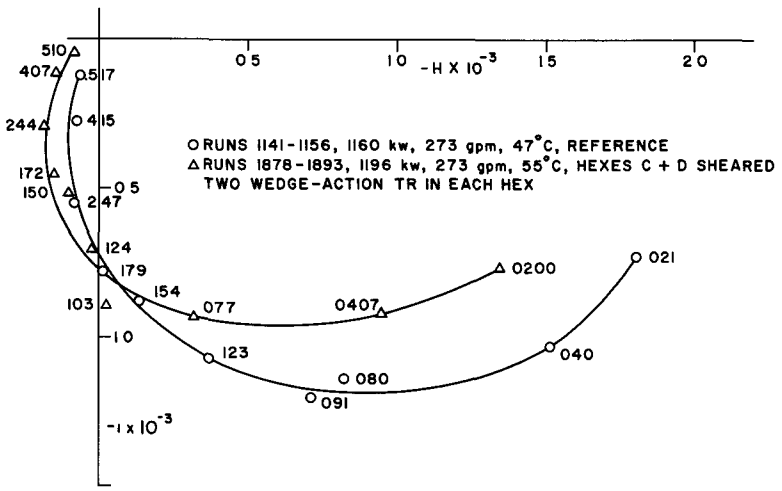

Fig. 32. Comparison of Reference and Partially Sheared Core Feedbacks: Full-power, Full-series Flow, Low Inlet Temperature

By smoothing the reference and partially sheared feedbacks and by applying first-order corrections for power and flow differences, it is possible to isolate the component responsible for the feedback change by subtracting the reference from the partially sheared feedback. The result of such a subtraction is given in Fig. 33.

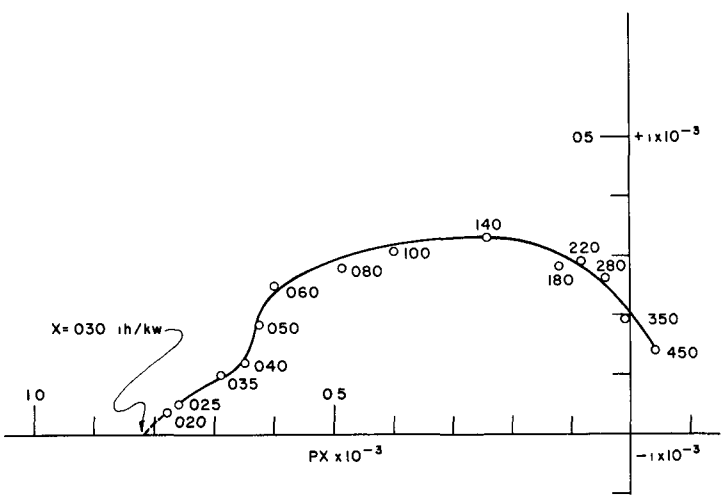

Fig. 33. Positive Feedback Resulting from Rib Shearing in Hexes C and D

Consistent with the concept of a positive component, the separated feedback lies almost entirely in the II quadrant of the complex plane. While no claim can be made for accuracy, because of a lack of information at low frequencies, a crude extrapolation to zero frequency results in a value of 0.030 ih/kw or 0.686×10^{-6} $\Delta k/k$ per kw. If it is assumed that bowing of the fuel rods in the central assembly may be neglected, the extrapolated rod bowing coefficient for the fully sheared core becomes 0.090 ih/kw or $2.06 \times 10^{-6} \Delta k/k$ per kw. The results of a Bode analysis of the feedback indicate a dependence upon frequency governed by a single time constant of 1.87 sec.

Although the separated feedback lies for all practical purposes entirely in the II quadrant, it does not necessarily follow that the power coefficient component initiated through rib shearing is positive. In fact, there is nothing in the experimental results which permits a differentiation between the effects of introducing a positive component and the effects of decreasing the magnitude of an already existing negative. It might be argued that rib shearing leads to a decrease in radial coupling between rods and that this decrease is reflected by a reduction in the net power coefficient. Such a reduction would be indistinguishable from the effects of a superimposed positive component resulting from bowing. Such arguments are, however, invalid. Although the radial coupling in the vicinity of the core is certainly affected by the shearing, the rods still remain strongly coupled as a consequence of the tightening action at upper and lower ends. Radial expansion of the rods and hexes in this region would still be manifested by a strong negative power coefficient component. Most likely, the time constant associated with the normal fuel expansion would be affected by the shearing, since the contribution of rod and hex expansion to the power coefficient would be delayed. Such effects would appear through feedback phase changes such as those actually observed experimentally. On the other hand, such a criterion cannot be applied to distinguish a superimposed positive from a lessened negative effect, since there is no assurance that the time constant for rod bowing will not differ from that normally associated with fuel expansion. The only definitive test which may be applied to differentiate between a lessened negative or an added positive component is to increase the magnitude of the effect until the power coefficient either decreases to zero (or to some minimum negative value) or changes sign. If the power coefficient cannot be made positive regardless of the amount by which the effect is increased, it follows that the effect is clearly one of a lessened negative nature. If the power coefficient changes sign and becomes positive, the effect is certainly one characterized by the addition of a positive component. In the ultimate analysis any difference between a superimposed positive and a lessened negative component is purely academic, since the effects of both, especially when pertaining to stability considerations, are identical. In subsequent discussions the component responsible for the feedback change will be referred to as positive since circumstantial evidence points to this conclusion.

The successful separation of the positive effect may be used as a basis for the extrapolated performance of the reactor under fully sheared conditions. Assuming a value of 0.090 ih/kw for the rod bowing coefficient and that all components, both positve and negative, vary linearly with power, the Nyquist stability criterion may be applied. Values for $-G_0H$ for various frequencies and power levels are plotted in Fig. 34, from which it may be seen that the resonance power is close to nine times nominal full power (1200 kw) or about 11 megawatts. The frequency at which resonance will occur is seen to be in the vicinity of 0.14 cps.

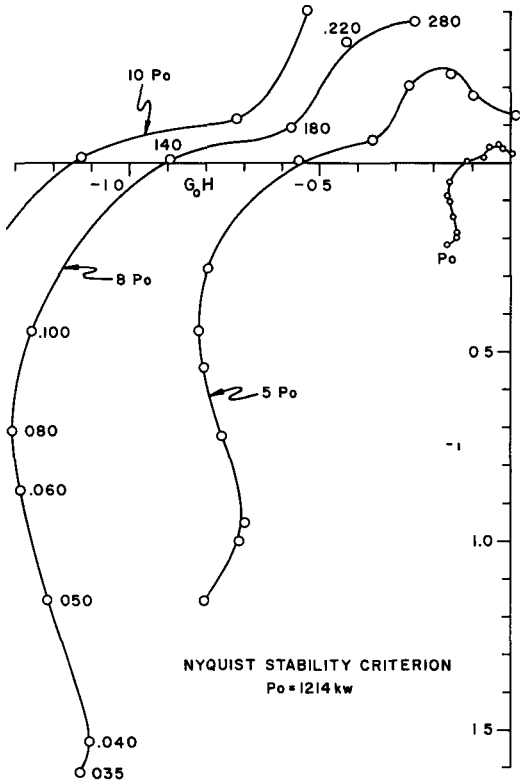

Fig. 34. Nyquist Stability Criterion for Fully Sheared Core

The predicted performances of the fully sheared core at nominal full power and at resonance are compared in Fig. 35. Although the effects of a complete removal of stabilizing ribs tends to make the reactor less stable, the effects are, nevertheless, so small that operation under full-power, fully sheared conditions would still be possible. For successively higher levels of power the reactor would become increasingly more unstable, until open resonance would be reached at 11 megawatts, a power level far beyond practical capabilities of heat removal.

One very important conclusion resulting from these studies concerns the fact that, even for a fully sheared core under conditions particularly conducive to rod bowing, the net prompt power coefficient would still be negative. This, of course, was not true for Mark II. The reason for this difference is discussed in Section VIII. The results of flow-change tests carried out on the partially sheared core demonstrated conclusively the absence of a prompt positive power coefficient component.

Another measure of the importance of the positive effect on the stability of the reactor may be inferred from the results illustrated in Fig. 36 for the transfer functions at nominal full power and at nine times full power for the fully ribbed and rigid core. At low frequencies and at nine times full power the reactor would still be extremely stable. No evidence of the resonance at 0.14 cps can be seen. For frequencies higher than 0.3 cps a small amount of reactivity amplification is indicated.

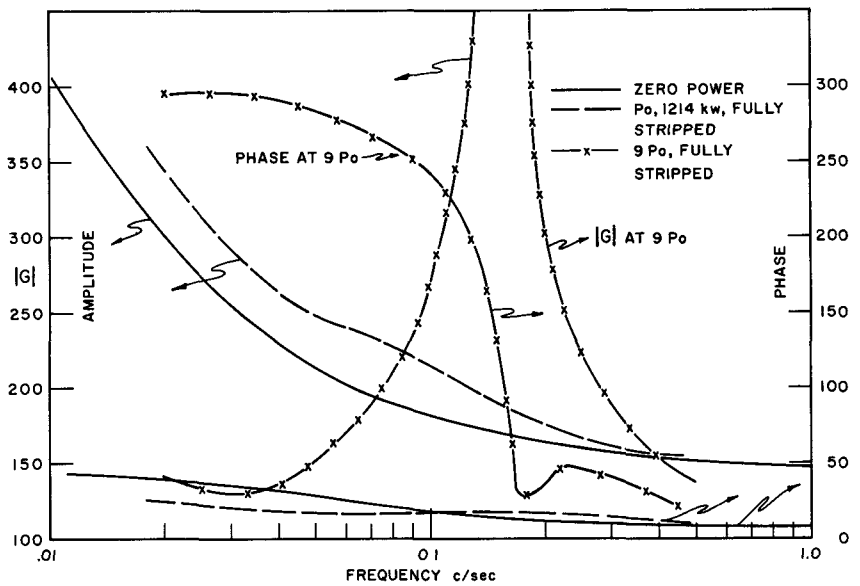

Fig. 35. Transfer Function for Fully Sheared Core at Full Power and at Nine Times Full Power

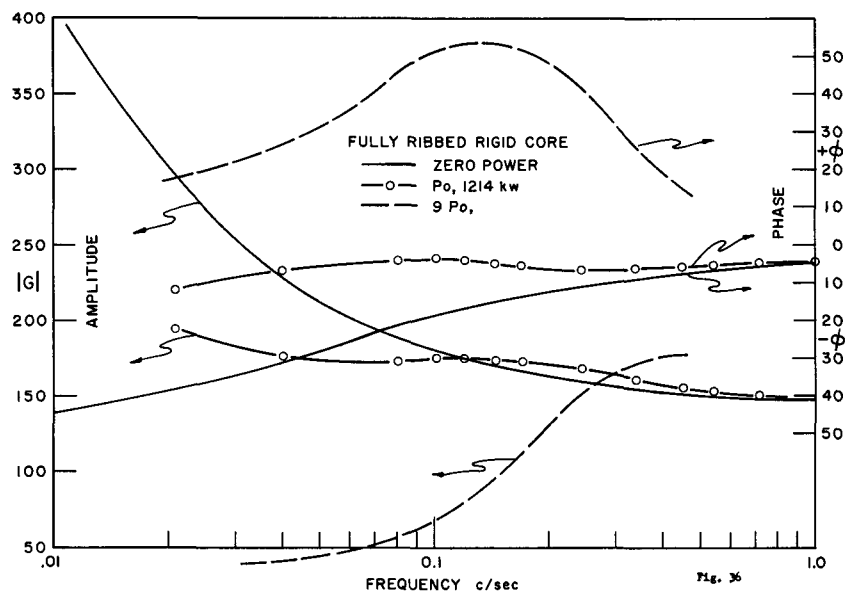

Fig. 36. Transfer Function for Fully Ribbed Core at Full Power and at Nine Times Full Power

Nevertheless, operation would still be possible, hypothetically, even under these conditions. In essence, then, the effect of the positive component is, as Bethe[14] has pointed out, manifested by a drastic reduction in the resonance power level.

L. Power Coefficient

The results cited above clearly indicate that the removal of stabilizing ribs leads to the introduction of a positive power coefficient component which logically must be associated with an inward bowing of fuel rods. With the exception of a few experiments dealing with an intentionally or unintentionally loosened configuration, the trend of the data indicates beyond reasonable doubt that the effects measured are real. This conclusion is strongly supported through the results of frequent zero power calibrations and the practice of duplicating data with a second ion chamber. There seems to be no valid reason to question the reliability of the results.

On the other hand, independent measurements of the static power coefficient carried out in conjunction with these studies resulted in values clearly inconsistent with those expected from logical extrapolations of the feedback to zero frequency. Although the results of transfer function measurements clearly indicated a reduction of 24 percent in the dynamic power coefficient, the static power coefficient remained essentially unchanged throughout the tests.

To explain this discrepancy it is necessary to postulate the existence of some physical process initiated through rib shearing, which acts to produce an extremely delayed negative reactivity effect with a time constant of the order of five minutes. The fact that a similar, but not necessarily related, component exists for the fully ribbed and rigid core has already been pointed out by Smith[27] and Storrer.[28] From a study of earlier Mark III data, both observers concluded that the measured static power coefficient is larger in magnitude than logical extrapolations of low-frequency feedback amplitudes indicate. Additional evidence of the existence of such an effect is indicated through the results of empirical analyses, discussed in Section VII. Thus, static power coefficient measurements which take place over a period of 10-20 minutes come under the influence of the delayed component. On the other hand, the process is so delayed in time that the reactor oscillating at frequencies as low as 0.02 cps cannot sense the feedback.

The origin of the postulated delayed feedback is unknown. Attempts to associate the action with the delayed expansion of the seal plate were unsuccessful. Thermocouple measurements carried out at three different elevations in the seal plate failed to reflect temperature decreases initiated by strong step decreases in reactor power. Actually, both sides of the seal plate (see Fig. 5) are maintained at inlet temperature.

Although the origin of this effect cannot be identified, there seems little doubt of its existence. In view of the extremely long time constant associated with this effect, it follows that some massive structural member located downstream from the core must be involved.

This effect, regardless of its origin, cannot explain the discrepancy between the static and dynamic power coefficients for the partially sheared core. Since the positive component introduced through rib shearing is known to be characterized by a short time constant, its effect must be reflected in the magnitude of the statically measured power coefficient. Since the positive component did not affect the magnitude of the static power coefficient, it follows that the positive effect was cancelled by an apparently equal, but much more slowly acting, negative component. It also follows that the delayed negative component in this case must be a consequence of rib shearing and is not necessarily related to the delayed component noted in the fully ribbed rigid-core tests.

To explain the experimental observations the following mechanism is postulated. As the remaining fuel rods in hex D, and later in C, were sheared the walls common with hex A (the central assembly) acquired a degree of flexibility previously denied through the influence of the stabilizing ribs. Pressures generated by the diametral growth of fuel rods in hex A could then be partially relieved through a deformation of the common walls. Without a physical examination of the walls it is meaningless to speculate about the exact form the deformation might have taken. It seems plausible, however, that the normal clearance, if any, existing between common walls would be seriously affected. Under normal conditions, i.e., for the fully ribbed rigid core, the action of the central core clamps and the pressures exerted by diametral growth would tend to reduce clearances between walls at fuel elevation to a minimum. Under these conditions the magnitude of the delayed negative effect arising from the expansion of the upper structure might well be limited to reactivity effects in the upper blanket where clearances between cans would be less affected by rod growth. If clearances are opened between hexes A and D and between A and C, or if pressures between hexes are relieved through wall deformation, it is possible that the structural expansion would be felt not only in the upper blanket but in the core as well. Such an effect would be negative and would have the same time behavior as the normal delayed negative effect arising through structural expansion. The two effects, one normal and one the consequence of rib shearing, would simply add. The presence of neither would be apparent from an analysis of the oscillator data alone.

The results of fuel rod growth measurements carried out for 1.14 and 1.63×10^6 kwh of operation have shown that the maximum diametral growth occurs in the upper one-fourth of the fuel section and that the average diametral growth of fuel in hex A at the time the discrepancy became apparent (1.63×10^6 kwh) was about 0.010 in. Such growths integrated across the flats of hex A would lead to pressures which, if relieved by rib shearing in neighboring assemblies, would almost certainly affect the normal clearances between common hex walls.

The results of attempts to demonstrate the existence of a delayed negative component sufficiently large in magnitude to explain the discrepancy through a time analysis of the power following a rod drop have substantiated the validity of the delayed negative postulate. A typical power-time trace following the essentially instantaneous loss of 11.35 ih is given in Fig. 37.

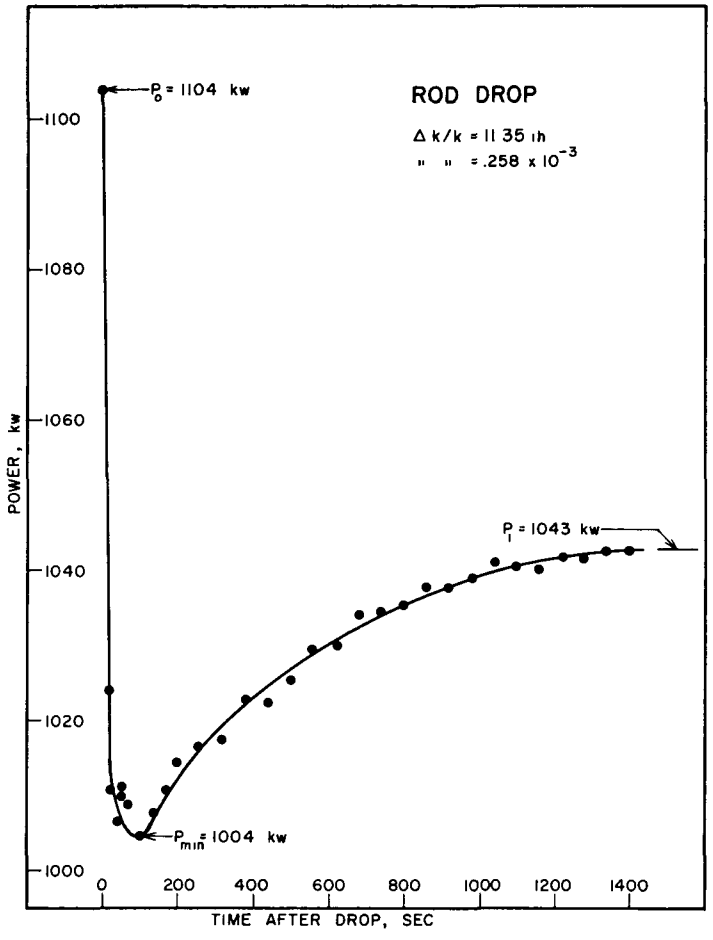

Fig. 37. Rod Drop Measurement of the Delayed Negative Power Coefficient Component

Approximately 41% of the static power coefficient consists of the delayed structural component. This is in excellent agreement with the value of 40% established through an empirical analysis of partially sheared feedback results (see Section VII-E). Presumably the 40% accounts for the 13% contribution normally associated with the fully ribbed core (see Section VII-C), and an additional contribution of 25% resulting from the rib shearing (see Section VII-E).

VII. EMPIRICAL MODELS

In principle, it should be possible to calculate the feedback arising from a sinusoidal forcing function from a complete knowledge of the reactor system (dimensions, physical properties of fuel, coolant, etc) and a solution of the transient heat transfer and heat conduction equations. However, the necessity for making simplifying assumptions limits the application of such mathematical approaches to special cases not usually encountered in practice. Since the solution of transient heat transfer and heat conduction equations even for idealized cases is in itself formidable, it is inconceivable at this time that any one mathematical model can satisfactorily explain the dynamic behavior of the Mark III loading under all conditions of power, temperature, and flow, particularly in view of the evidence pointing to strong temperature and power-sensitive processes which act nonlinearly. Furthermore, the development of a truly successful unified model applicable over the normal range of operating conditions would presume detailed knowledge of very poorly defined clearance systems. In the practical case, where nonlinearities do exist, the concepts of a single unified model must be abandoned in favor of slightly differing individual models, each of which finds immediate application over small ranges of power, temperature and frequency.

In the face of obvious difficulties an elegant and highly promising approach to the problem for linear systems has been made by Storrer.[30] From exact solutions of the transient heat transfer and heat conduction equations Storrer arrived at an expression for the amplitude and phase of fuel and coolant temperature oscillations as a function of spatial coordinates. By the substitution of physical parameters into Storrer's expressions, Long[31] has been able to show that calculated values for the phase and amplitude of temperature oscillations (with respect to power) at specific core locations are in reasonable agreement with values obtained experimentally in the Mark III transient temperature measurements. A comparison of experimentally measured feedbacks with values calculated from oscillating temperature data has revealed discrepancies which have not yet been resolved.

A somewhat different approach to the problem has been made by Carter,[32] who introduced the concept of nonlinearities arising from a frictional restriction of axial expansion. Through a combination of analytic and empirical techniques Carter was able to fit experimentally measured values of the transfer function to a truly nonlinear model.

A. The Empirical Approach

Attempts to fit the Mark III data to mathematical models through purely empirical methods have been reasonably successful. Whereas such an approach suffers from the disadvantage that less insight is provided

into the physical aspects of feedback, mathematical models deduced in this manner serve as reasonably reliable bases for performance extrapolations over limited ranges of operating conditions.

The following two models describe with acceptable accuracy most of the feedback phenomena observed in the Mark III loading:

$$-H = \frac{PX\, e^{-iwT}}{(1 + iwT_1)} \quad ; \tag{13}$$

$$-H = \frac{PX}{(1 + iwT_1)(1 + iwT_2)} \quad . \tag{14}$$

The first of these, the single-pole transport lag model, has been found useful in describing the feedback observed under conditions of reduced flow. For measurements at full flow, the second (double-pole) model has been found to be more applicable.

B. Empirical Solutions for Reduced Flow

The first step in the solution of Equation 13 for the unknowns X, T and T_1 consists of a Bode analysis of the feedback amplitude. This procedure results in a value for T_1 from which the feedback phase lag arising through the denominator of Equation 13 can be evaluated for any given frequency. The difference between experimentally measured phase values and the phase values associated with the time constant T_1 are then attributed to the influence of the parameter wT. This procedure results in an evaluation of T at each experimental frequency point. By means of an averaged value for T, the empirically established value of T_1, and the experimental values of -H, Equation 13 may be solved for the power coefficient X. A summary of values for T, T_1 and X deduced in this manner for series and parallel flow and at three different flow rates at approximately 500 kw is given in Table II.

Table II

EMPIRICAL PARAMETERS, SINGLE-POLE TRANSPORT LAG MODEL

Runs	Power, kw	Metered Flow, gpm	Core Flow, gpm	T_1, sec	T, sec	PX, $\Delta k/k \times 10^{-3}$	X, $\Delta k/k/kw \times 10^{-6}$
			Series Flow				
112-122	489	293	246	2.79	0.70	-0.837	-1.71
127-138	481	180	151	3.31	1.03	-1.13	-2.35
162-167	481	110	93	4.91	1.24	-1.95	-4.05
			Parallel Flow				
193-203	491	290	244	2.70	0.46	-0.881	-1.80
212-223	500	180	151	3.06	1.08	-1.14	-2.28
224-235	500	110	93	4.81	1.17	-2.03	-4.05

As discussed in Section III-E, the actual flow through the core, both in series and in parallel, is less than the flow metered at the primary inlet. Actual flow values given in Table II have been modified to account for bypass leakage in series flow and for the partition of flow between core and blanket in parallel flow.

A comparison of the feedbacks calculated from Equation 13 and based on the parameters of Table II with experimentally measured values is given in Figs. 38 and 39, respectively. Considering the uncertainties associated with experimental feedback values (see Appendix A) and parametric values of Table II, the fit may be regarded as satisfactory. The fact that values established for T, T_1 and X are essentially the same for both series and parallel flow supports the conclusion that feedback effects originating in the radial blanket in series flow are insignificant.

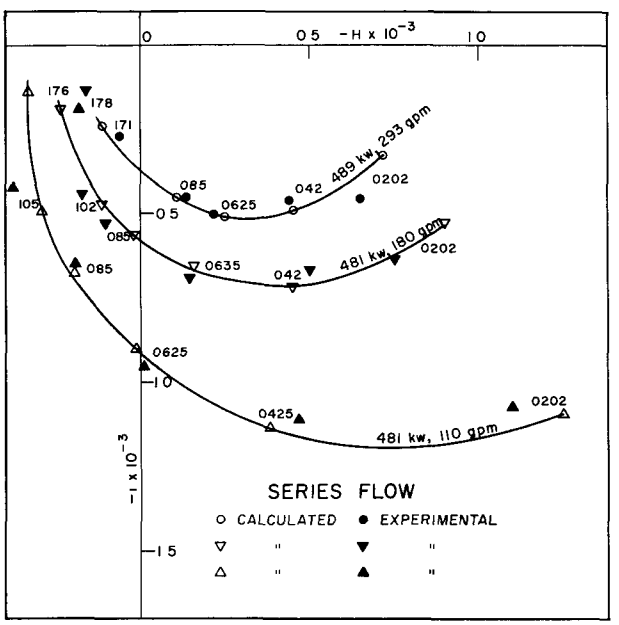

Fig. 38. Comparison of Experimental and Calculated Results for Single-pole Transport Lag Model, Reduced Series Flow

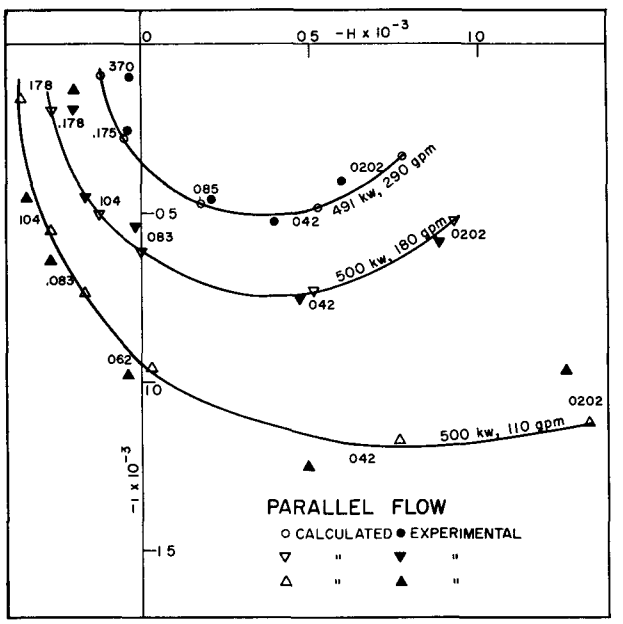

Fig. 39. Comparison of Experimental and Calculated Results for Single-pole Transport Lag Model, Reduced Parallel Flow

Actually, as Storrer has shown, the value determined for T is related to the physical transit time T_t through the relation

$$T = T_t \left[1 + (T_f/T_c)\right] \quad , \tag{15}$$

where T_f and T_c are the time constants associated with the fuel and coolant, respectively. In effect, the factor $[1 + (T_f/T_c)]$ is the ratio of the total heat capacity to the heat capacity of the coolant. The significance of this effect is essentially this: at low frequencies a temperature signal

transported by the coolant travels slower than the coolant by the factor $[1 + (T_f/T_c)]$. The effect arises through the exchange of heat between fuel and coolant and between coolant and nonheat-producing components such as blanket rods and rod extensions.

The location of the region coming under the influence of the transit time dependence may be inferred from a consideration of the empirical values for T, the actual velocity of the coolant, v, and an evaluation of the factor $[1 + (T_f/T_c)]$. The distance associated with the convective effect is given by

$$d = \frac{Tv}{1 + (T_f/T_c)} \tag{16}$$

where T is the empirical (effective) transport lag and the factor $[1 + (T_f/T_c)]$ has been evaluated for Mark III by Storrer as 9.5. A summary of values for the effective transport distance d for different series and parallel flow rates is given in Table III.

Table III

EFFECTIVE TRANSPORT DISTANCE

Core Flow, gpm	Velocity of Coolant, in./sec	T, sec	d, in.
	Series Flow		
245	74.5	0.70	5.5
151	45.8	1.03	5.0
93	28.2	1.24	3.7
	Parallel Flow		
244	74.4	0.46	3.6
151	45.8	1.08	5.2
93	28.2	1.17	3.5

The fact that the effective transport distance is of the order of 4-5 inches indicates that feedback effects described by a transport lag dependence are limited to the core and the lower portion of the upper blanket.

C. Empirical Analyses of Full-flow, Full-power Data

Without exception, feedback data under full-flow conditions were found to be more adequately described by the double-pole model described mathematically by Equation 14. An empirical evaluation of the parameters T_1, T_2 and X from experimentally measured feedbacks was carried out in the following manner. By inverting and rearranging Equation 14, it can be shown that the reciprocals of the real and imaginary components of the feedback are given by

$$(-1/H)_{Re} = \frac{1 - W^2 T_1 T_2}{PX} \tag{17}$$

and

$$(-1/H)_{Im} = \frac{W(T_1 + T_2)}{PX} \quad . \tag{18}$$

By plotting the real components of the inverse feedback as a function of W^2, it is possible to establish a value for $1/PX$ through an extrapolation to zero frequency. The slope, in turn, yields a value for T_1T_2/PX. If the imaginary component of the inverse feedback, $(-1/H)_{Im}$, is plotted as a function of w, an evaluation of the slope gives $(T_1 + T_2)/PX$. This procedure results in two independent equations with two unknowns (PX being known) which may be solved simultaneously for T_1 and T_2. The results of such a treatment for typical high and low-temperature series-flow runs are summarized in Table IV. An analysis of data taken approximately one year earlier under essentially identical conditions has been included for comparison. In this case X_{dy} is dynamic power coefficient evaluated empirically and X_s is the static power coefficient evaluated from rod drop measurements.

Table IV

EMPIRICAL PARAMETERS FOR THE DOUBLE-POLE MODEL; FULL FLOW (SERIES)

Runs	T_{in}, °C	Power, kw	T_1, sec	T_2, sec	PX_{dy}, $\Delta k/k \times 10^{-3}$	X_{dy}, $\Delta k/k/kw \times 10^{-6}$	X_s, $\Delta k/k/kw \times 10^{-6}$
1141-1156	47.0	1160	2.16	0.32	-2.12	-1.83	-1.84
1497-1512	75.4	1225	2.00	0.46	-2.17	-1.78	-1.87
1157-1172	231	1164	2.14	0.37	-2.56	-2.20	-2.50
1425-1441	234	1214	2.30	0.43	-2.69	-2.21	-2.57

Averaging the results at low inlet temperature gives values of 2.08 sec, 0.39 sec, and -1.81×10^{-6} $\Delta k/k/kw$ for T_1, T_2, and X_{dy}, respectively. A similar average for the high-temperature parameters are 2.22 sec, 0.40 sec, and -2.21×10^{-6} $\Delta k/k/kw$. A comparison of experimental

results with those calculated at high and low inlet temperatures from the parameters given in Table IV is given in Figs. 40 and 41, respectively. Within the limits of experimental accuracy (see Appendix A) the fit may be regarded as satisfactory. It is also significant that an equally satisfactory fit is obtained if the values used for T_1 and T_2 represent averages without regard to temperature.

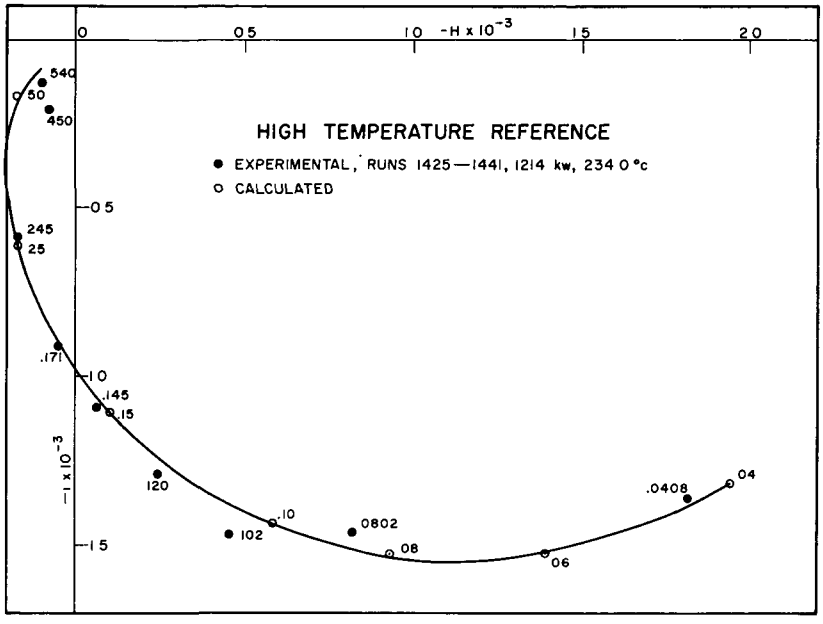

Fig. 40. Comparison of Experimental and Calculated Results for Double-pole Model, Fully Ribbed Core, Full-power Full-series Flow, High Inlet Temperature

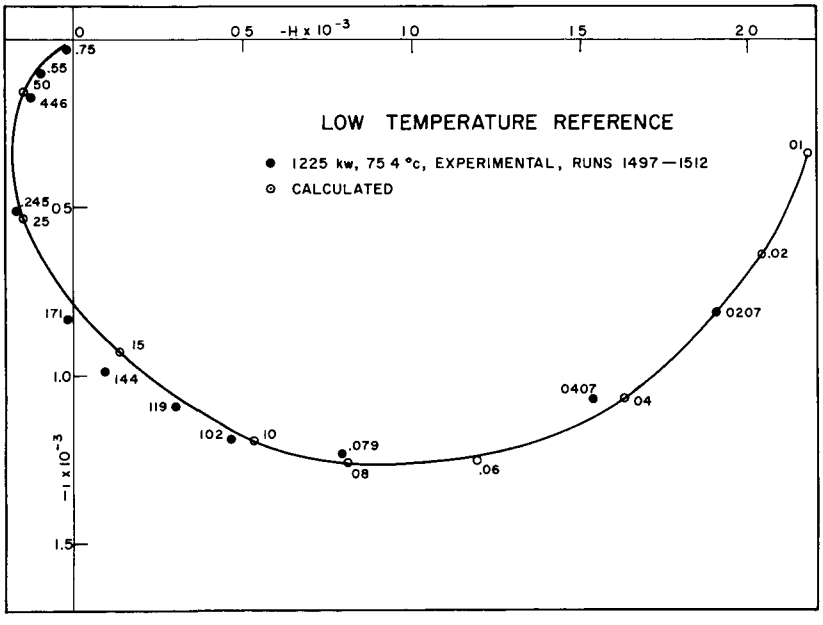

Fig. 41. Comparison of Experimental and Calculated Results for Double-pole Model, Fully Ribbed Core, Full-power Full-series Flow, Low Inlet Temperature

From the data given in Table IV it is clear that one significant difference distinguishing the high and low-temperature parameters appears in values obtained for the dynamic and static power coefficients. The differences effected in X_{dy} and X_s through an inlet temperature increase of 175°C, say from 60 to 235°C, amounts to approximately 22% and 41%, respectively. A similar dependence, although not as pronounced, has been noted for the isothermal temperature coefficient. Values measured for the incremental and integral isothermal temperature coefficients are summarized in Fig. 42. From 60 to 235°C, approximately the range of comparison for feedbacks, the incremental isothermal temperature coefficient increases from 1.16 to 1.32 ih/°C, an increase of approximately 14%. Such changes effected by temperature in the isothermal temperature coefficient are certain to be reflected in the power coefficient. The explanation of the isothermal temperature coefficient dependence on temperature lies in the temperature-sensitive dependence of the linear expansion coefficient for the 98% uranium-2% zirconium alloy fuel used in Mark III. From Fig. 43, which illustrates the expansion coefficient dependence on temperature, it may be seen that increase of the temperature from 60 to 235°C causes the expansion coefficient to increase from 11.0 to 13.5 $\times 10^{-6} \Delta L/L/°C$, an increase of 23%. Thus, if the isothermal temperature coefficient is considered to be the result of expansion effects in fuel, only a corresponding increase of 23% would be expected in the magnitude of the isothermal temperature coefficient. The fact that a smaller increase was noted is probably not significant since the full increase would be realized only for the special case of complete radial coupling of fuel rods. The comparison of the 23% increase in the linear expansion coefficient of the fuel with the 22% increase in the dynamic power coefficient is not significant since the two coefficients are not linearly related. Detailed calculations based on fuel and coolant temperature distributions throughout the core and blanket are needed to test the validity of these concepts.

Perhaps the most significant result of the empirical treatment is the 13% discrepancy existing between values established for the dynamic and static power coefficients at the higher inlet temperatures. A smaller 2.7% discrepancy in the same direction is noted for the low-temperature results, but, in view of an approximate ± 3% uncertainty associated with static power coefficient measurements, this discrepancy may or may not be significant.

Since the dynamic and static power coefficients become identical in the limit of zero frequency, it must be concluded that 13% of the net power coefficient (statically measured) at high inlet temperatures consists of a component so delayed in time that the reactor oscillating at frequencies as low as 0.02 cps cannot sense the feedback. Confirmatory evidence of the existence of the delayed negative effect, particularly for the partially sheared core, has been discussed in Section VI. The origin of this effect is obscure, but in view of the extremely long time constant (of the order of 400 seconds), some portion of the upper structure must be involved. Why the effect is more marked at higher inlet temperatures is not understood.

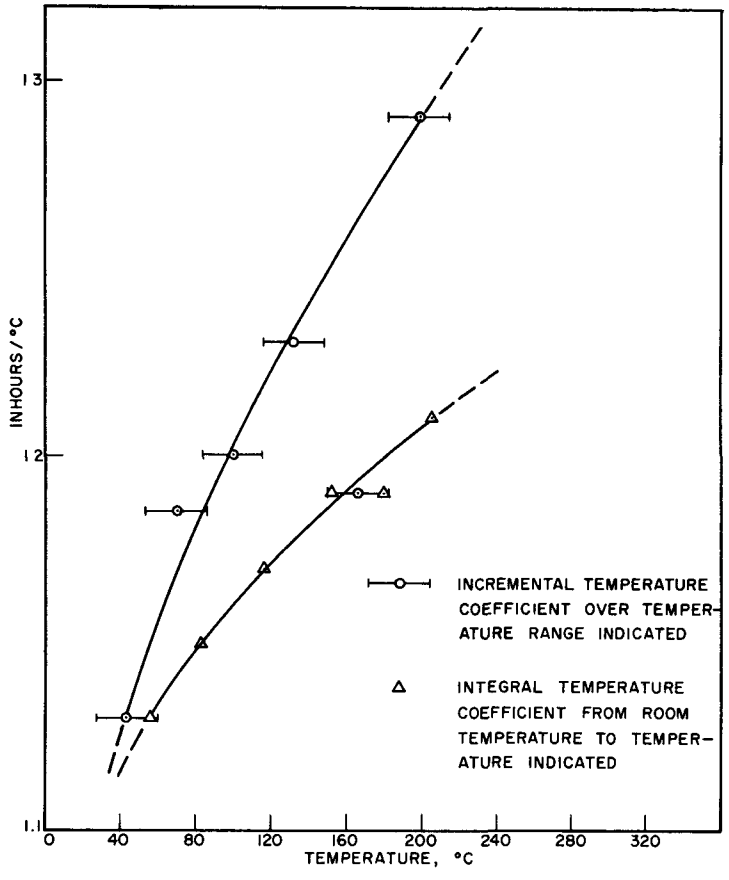

Fig. 42. Isothermal Temperature Coefficient for EBR-I, Mark III

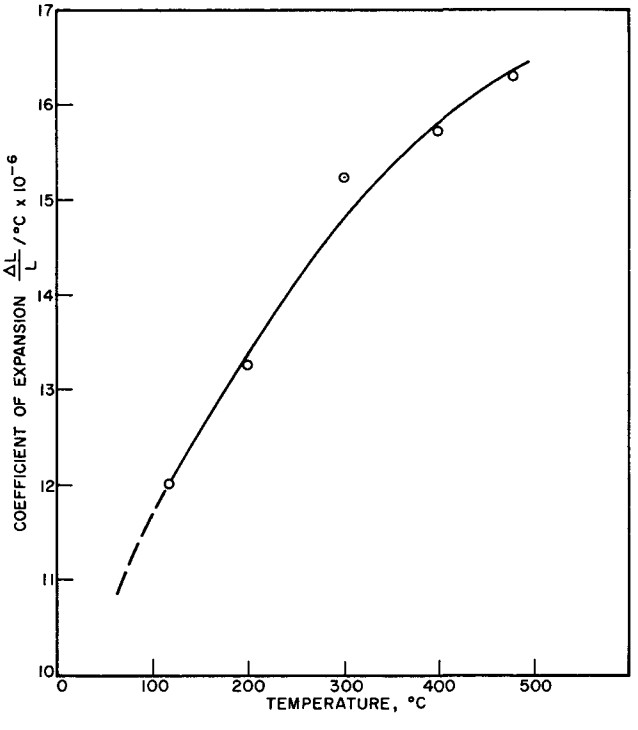

Fig. 43. Fuel Expansion Coefficient for EBR-I, Mark III

D. Model, Including Delayed Feedback, for the Rigid Fully Ribbed Core

The effects of the delayed structural contribution to the reactivity feedback for the rigid fully ribbed core at high inlet temperatures are described by the expression

$$-H = \frac{PX_1}{(1 + iwT_1)(1 + iwT_2)} + \frac{PX_2}{(1 + iwT_3)} \qquad (19)$$

where the first term on the right describes the feedback arising from core and blanket heating, and the second term describes the delayed structural feedback. Empirically deduced values for the various parameters are given in Table V. Values for X_1, T_1, and T_2 are average values established from an empirical analysis of experimentally measured feedbacks. The power coefficient X_2 is simply the difference between the static and dynamic power coefficients, and the value for the time constant T_3 is an estimate based on rod-drop data typically illustrated in Fig. 37. From Fig. 44, which compares calculated and experimental results, it is clear that Equation 19 adequately describes the feedback over the frequency range 0.02 to 0.54 cps and leads to a satisfactory extrapolation of the low frequency feedback to a value consistent with the measured static power coefficient.

Table V

PARAMETERS FOR DELAYED FEEDBACK MODEL OF THE RIGID FULLY RIBBED CORE

$P = 1214$ kw

$X_1 = -2.21 \times 10^{-6}\ \Delta k/k/kw$

$X_2 = -0.33 \times 10^{-6}\ \Delta k/k/kw$

$T_1 = 2.22$ sec

$T_2 = 0.40$ sec

$T_3 = 400$ sec

E. Model, Including Delayed Feedback, for the Partially Sheared Core

Mathematically the following model describes the behavior of the partially sheared core:

$$-H = \frac{PX_1}{(1 + iwT_1)(1 + iwT_2)} + \frac{PX_2}{(1 + iwT_3)} + \frac{PX_3}{(1 + iwT_4)} \quad , \qquad (20)$$

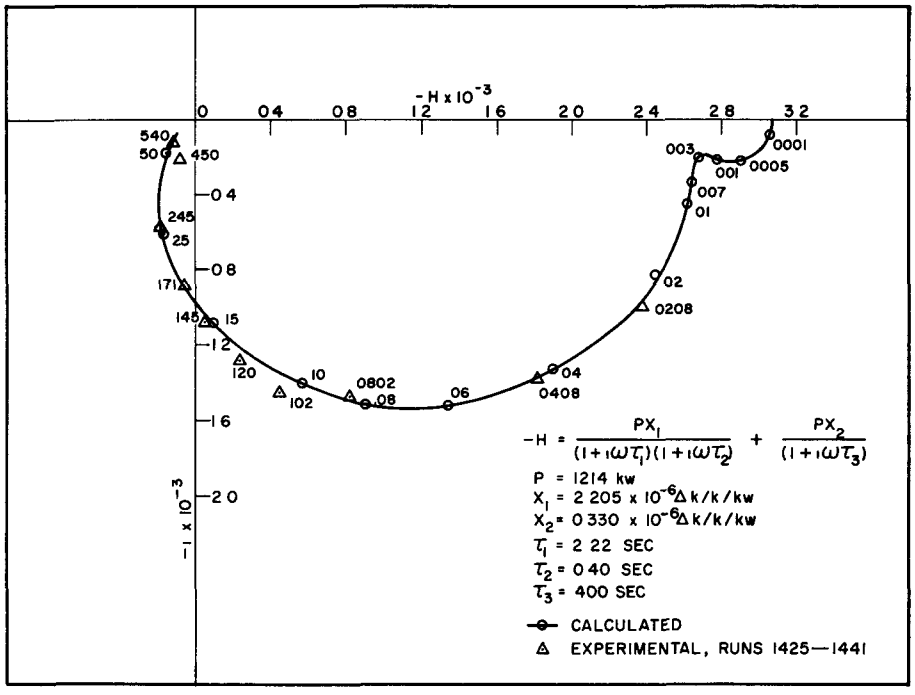

Fig. 44. Comparison of Experimental with Calculated Results for Fully Ribbed Core, Full Power, Full Flow, High Inlet Temperature

where the terms on the right describe, respectively, the feedback associated with the reference core (rigid fully ribbed), rod bowing, and delayed structural expansion. A summary of the various parameters and their respective empirical values is given in Table VI.

Table VI

PARAMETERS FOR DELAYED FEEDBACK MODEL OF THE PARTIALLY SHEARED CORE

P = 1189 kw	T_1 = 2.22 sec
X_1 = -2.21 x 10^{-6} Δk/k/kw	T_2 = 0.40 sec
X_2 = +0.543 x 10^{-6} Δk/k/kw	T_3 = 1.20 sec
X_3 = -0.873 x 10^{-6} Δk/k/kw	T_4 = 400 sec

Values for T_1, T_2, and X_1 are those deduced for the fully ribbed rigid core, as described in Section VI-C. Values for the rod bowing parameters X_2 and T_3 were obtained empirically from a solution of the equation

$$-H = \frac{PX_1}{(1 + iwT_1)(1 + iwT_2)} + \frac{PX_2}{(1 + iwT_3)} \quad , \tag{21}$$

where -H is the dynamic feedback associated with the partially sheared core and the first-term parameters X_1, T_1, and T_2 are those associated with the rigid, fully ribbed core. The power coefficient associated with delayed structural expansion X_3 was established through the relation

$$X_{static} = X_1 + X_2 + X_3 \quad . \tag{22}$$

Finally, the time constant T_4 was assumed to be 400 sec, the value estimated from rod-drop measurements.

A comparison of experimentally measured feedbacks with those calculated from Equation 20 and the parameters of Table VI is given in Fig. 45. Again, the fit may be regarded as satisfactory. Assuming that the values used for the various power coefficients are realistic, it is clear from this model that the effects resulting from shearing ribs from the remaining fuel assemblies will not be sufficiently large to cause $|X_2| > |X_1|$, i.e., that the prompt behavior of the reactor will still be governed by a negative but smaller power coefficient.

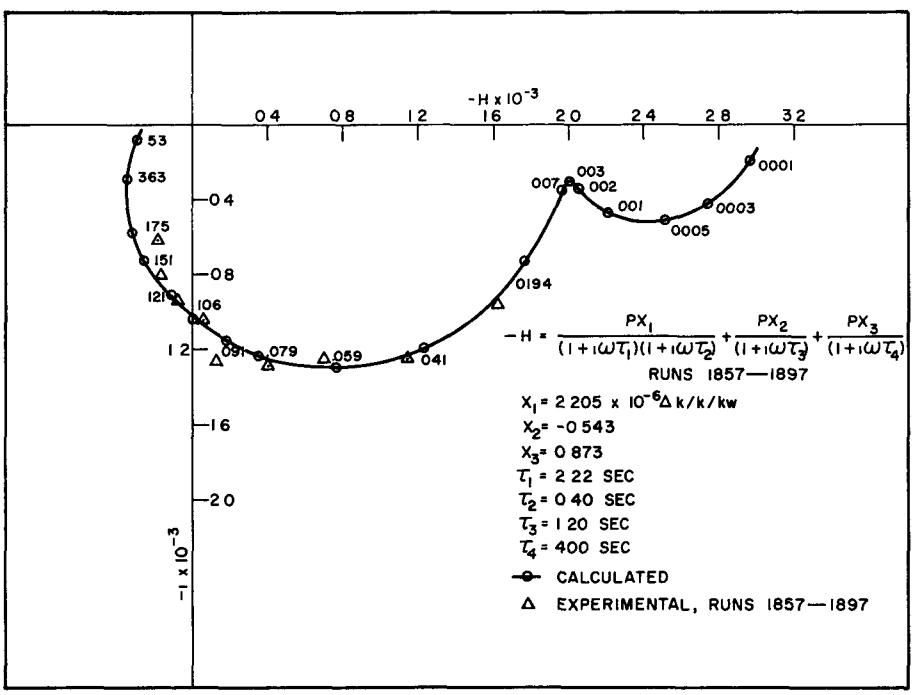

Fig. 45. Comparison of Experimental with Calculated Results for Partially Sheared Core, Full Power, Full Flow, High Inlet Temperature

VIII. CORRELATION OF MARK III RESULTS WITH MARK II BEHAVIOR

The following important conclusions pertinent to an understanding of the Mark II behavior have resulted from the Mark III test results: (1) the delayed negative power coefficient component contributing to the instability of Mark II was eliminated in Mark III through changes in mechanical design, (2) the addition of stabilizing ribs to the fuel rods eliminated, or at least greatly reduced, positive reactivity effects arising through rod bowing, and (3) positive reactivity effects associated with rod bowing are the consequence of special, not easily realized, mechanical conditions.

Empirical analyses of Mark III feedback data taken under full and reduced flow conditions have failed to reveal any evidence of a delayed negative power coefficient component similar to the one associated with Mark II. Although it is certain that a delayed structural effect does exist in Mark III, the fact that its time constant is exceedingly long, i.e., approximately 400 sec, indicates rather definitely that the processes responsible for the delayed negative component in Mark II and Mark III cannot be the same.

The results of empirical analyses do indicate the existence of a transport lag dependence for reduced flow conditions in Mark III. The transport lag dependence in Mark III differs considerably from that directly responsible for the instability of Mark II. As discussed in Section VII-B, the feedback process associated with the transport lag in Mark III operates over a distance of only 4-5 inches, a distance which effectively limits the process to one involving the expansion of fuel and, possibly, of upper blanket material.

Since the effective transport lag of the Mark II negative feedback was much larger (10 sec according to Bethe[14] for one-third flow), the effect must have operated between the core and some structural region considerably removed from the core. The fact that no comparable feedback component was observed in Mark III after the elimination of all downstream Mark II structure strongly supports this conclusion.

As the result of recent studies, discussed in Appendix B, it now seems quite likely that the mechanism responsible for the delayed Mark II feedback involved thermally induced motions in rod-positioning ligaments of the Mark II lower shield plate. To appreciate the intricacy of this mechanism it is necessary to review pertinent details of the Mark II construction. A cutaway view of the reactor proper and a cross-sectional view taken through the core center are given in Fig. 46 and 47, respectively. The fuel portion consists of a hexagonal assembly of 217 fuel rods, each of which consists of a stainless steel tube, 0.448 in O.D. with a 0.020-in. wall thickness, containing concentrically spaced fuel and blanket slugs, 0.384 in. in diameter. The fuel rods are positioned at the bottom on 0.494-in. centers

by a tube plate perforated with triangular holes which, in the case of Mark II, engaged conical-shaped rod tips. Dimensions and tolerances were such that the following clearances between rod tips and holes were afforded: minimum, 0.004 in; maximum, 0.008 in. Surrounding each positioning hole are six coolant passages, each $\frac{3}{16}$ in. in diameter, and three, each $\frac{1}{16}$ in. in diameter. Approximately 16 inches above the center of the fuel region is the four-inch thick lower shield plate illustrated in Fig. 48. (The photograph shown is actually one of a dummy two-inch plate similar in design and all other dimensions to the four-inch plate actually present in Mark II.)

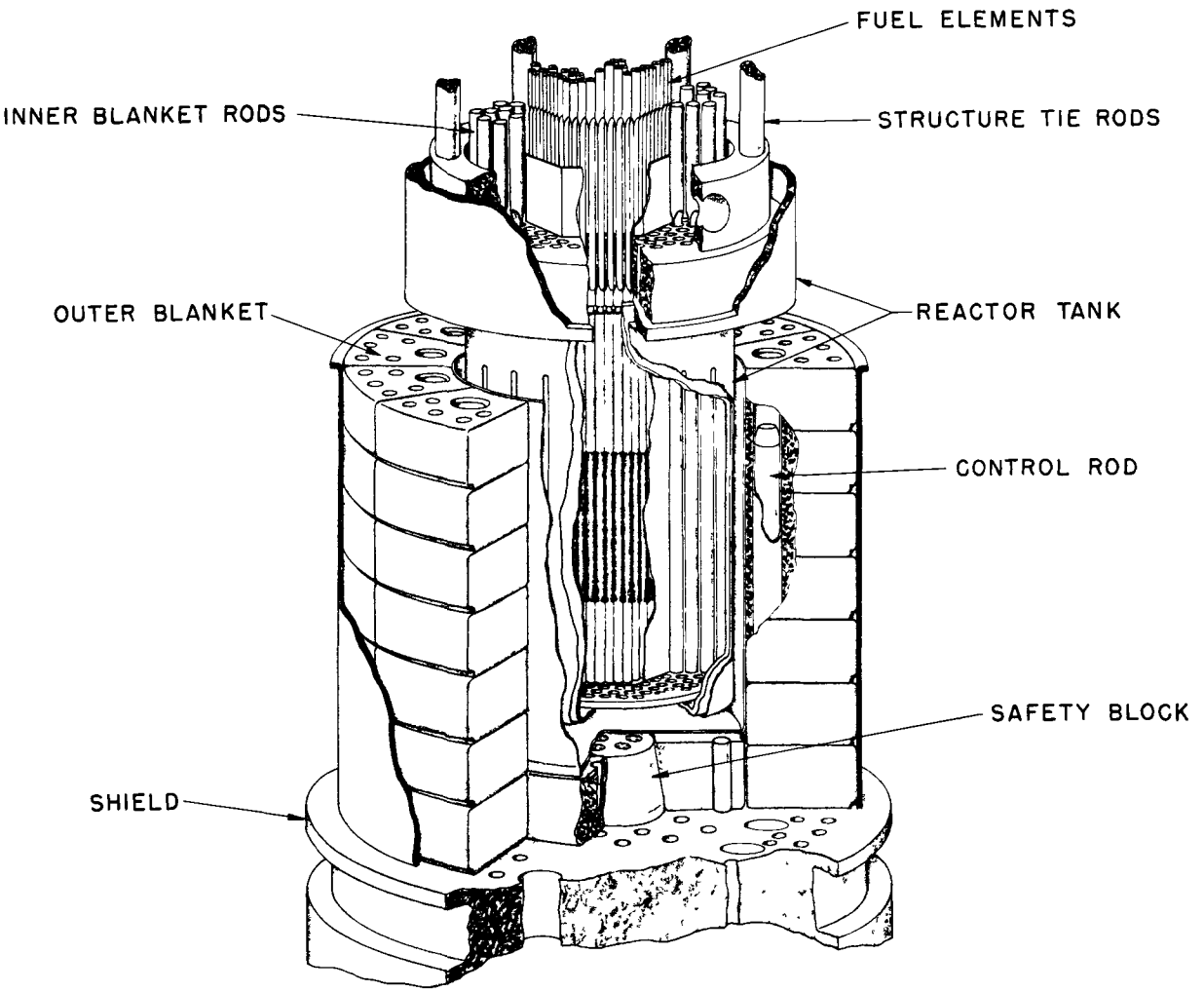

Fig. 46. Cutaway View of EBR-I, Mark II Reactor

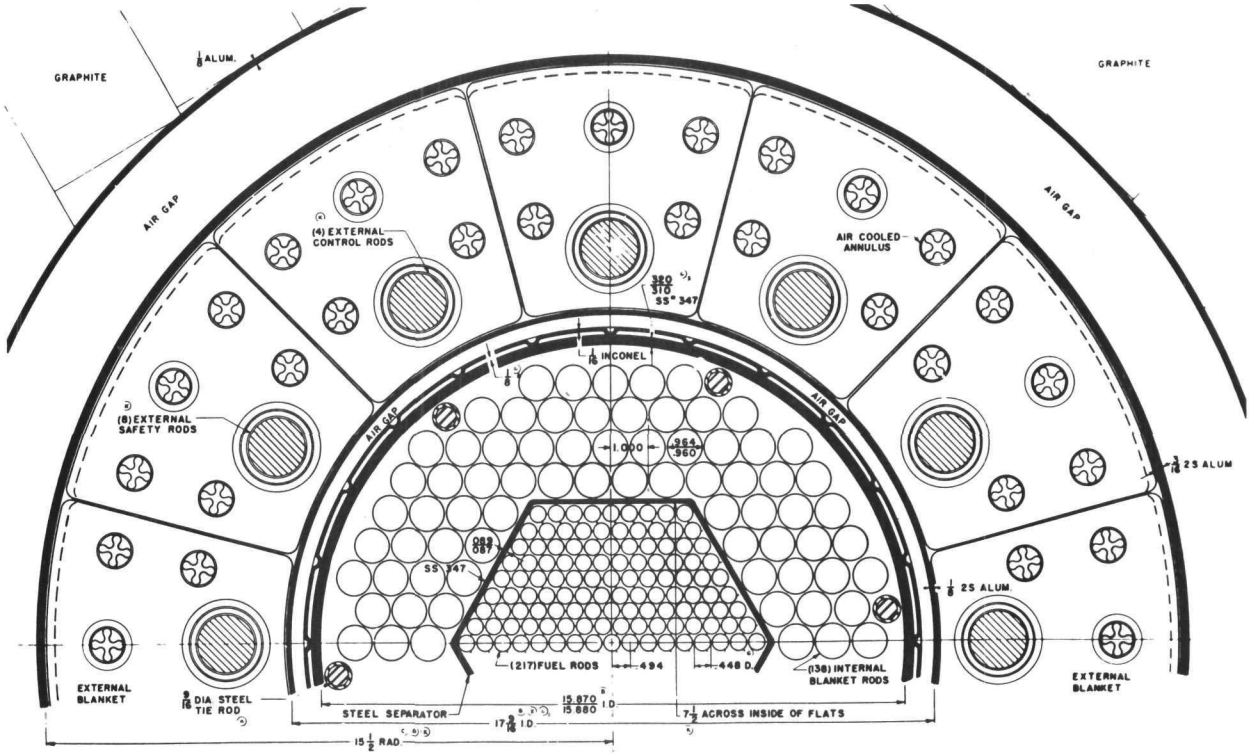

Fig. 47. Cross Section through EBR-I, Mark II Core

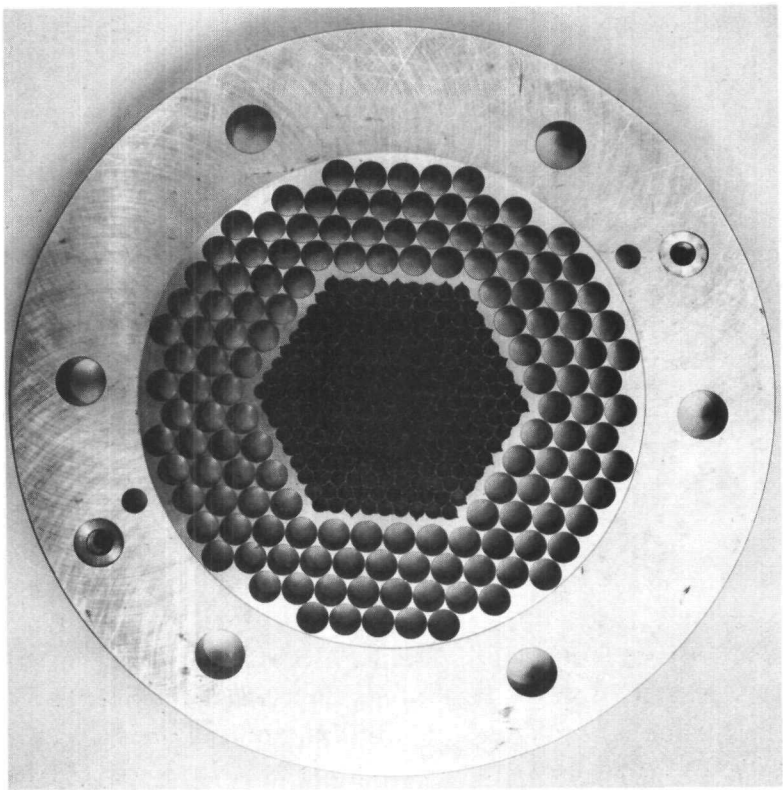

Fig. 48. Lower Shield Plate, EBR-I, Mark II

The plate consists of two regions: an inner hexagonal section containing 217 fuel rod holes, each nominally 0.460 in. in diameter, and an outer arrangement of 138 holes for blanket rods, each 0.964 in. in diameter. Separating the two regions is a hexagonally shaped annulus, approximately 0.200 in. wide with grooves milled to a depth of 0.125 in., in the upper and lower surfaces. Two hexagonal flow dividers of 347 stainless steel, 0.088 in. in thickness, fitted into the grooves serve to separate inlet and outlet coolant. The 24-in. lower flow separator extends between the tube sheet and the lower surface of the lower shield plate, whereas the 4-in. upper separator extends from the upper surface of the lower shield plate to the lower surface of the seal plate.

To permit the passage of coolant, blanket rod extensions are fluted in the vicinity of the lower shield plate and fuel rod extensions are fluted over the length extending from the bottom of the lower shield plate to the top of the seal plate. The nominal dimensions of the fuel rod extensions (at maximum diameter) and shield plate perforations are 0.449 and 0.460 in., respectively, giving a nominal diametral clearance of 0.011 in. In series flow, the only arrangement possible, the coolant flows downward around the blanket rod fluting into the lower plenum chamber, where the flow reverses and passes upward through the core, through the fluted portion of the fuel rod extensions, and into the outlet plenum.

Above the two-inch seal plate is a series of two and four-inch shield plates alternating with four-inch spacer rings running to an elevation of 86 inches above the bottom of the lower shield plate. Six $1\frac{1}{2}$-in. tie rods penetrating the outer portion of the various shield plates and structure rings tighten the entire collection.

As discussed in Appendix B, the results of experiments conducted on a dummy two-inch Mark II shield plate have demonstrated that rods penetrating the perforations are subject to radial motions initiated by expansive and contractive actions of ligaments in the inner fuel rod region following temperature perturbations. It now seems plausible that such motions were responsible, not only for the delayed negative component of Mark II, but indirectly for the prompt positive rod-bowing power coefficient as well. In the following discussion, a mechanism based on temperature-induced ligamental motions is postulated.

As the Mark III test results have shown, positive reactivity effects from rod deformation require that the fuel rods be rigidly restrained from radial motion immediately above and below the core. In view of the substantial clearances at upper and lower restraining points, i.e., the lower shield plate and tube sheet, respectively, these conditions were not realized. The fact that rod bowing was important in Mark II under conditions apparently nonconducive to rod bowing has long constituted a source of considerable speculation. For similar reasons it has also been difficult

to associate the strong delayed negative power coefficient component with the expansive action of shield plate ligaments, since statistically only those rods accidently bearing on the inner surfaces of holes would be affected by expansive motions. To explain these apparent inconsistencies it is necessary to consider the effects of an elevated inlet temperature and of power generation on these critical clearance systems.

As the inlet temperature increases, for example during a normal startup, both the tube sheet and the lower shield plate expand more or less freely, since the outer portions of the inner tank assembly expand by essentially similar amounts. The effect of isothermally increasing the inlet temperature, with electric heaters for example, would tend to move perforations in the lower shield plate and tube sheet outward. Rod extensions and rod tips more or less randomly oriented at room temperature would eventually be gathered in an orderly arrangement along the inner edges of the perforations. In principle, for a system of rods so oriented deformation accompanying power increases would be manifested by an outward movement of rod tips at the bottom, an effect that is clearly negative. In practice, the temperature differential existing across the core as the result of power generated results in an additional radial movement of shield plate ligaments, which effectively moves the fuel rods outward until the tips bear against the outer edges of the positioning holes. Under these highly ordered conditions the most logical manifestation of rod bowing will be an inward bow.

It is particularly interesting to note that the structural member indirectly responsible for the positive rod-bowing component appears to be directly responsible for the delayed negative component. Outward radial motions of shield plate ligaments effected through a power increase carry the already gathered rod extensions and effectively increase the size of the reactor core. Conversely, the recovery of ligaments following a power decrease allows rod extensions to drift inward and to decrease the core radius.

Before the Mark II results can be interpreted in terms of a physical feedback model, it is necessary to understand why the prompt power coefficient of Mark II was positive and why an extrapolation of Mark III data to fully sheared conditions indicates a prompt negative. The explanation of this important difference lies in the degree of radial coupling between fuel rods. Whereas the fuel rods in Mark III are strongly coupled, even when stripped of their ribs (one-inch sections remain at upper and lower ends), essentially no coupling existed in Mark II. In Mark III the effective core radius following a power change is influenced by the number of fuel rods contiguous with the hexes and with each other. In Mark II, on the other hand, the effect of radial expansion on core radius was limited by expansion effects in individual rods. From these considerations it follows

that the prompt radial power coefficient should be large in Mark III and should have been small in Mark II. As the results of extrapolation show, the Mark III prompt radial and axial power coefficient is sufficiently large to override the entire prompt positive rod-bowing component. In Mark II the prompt negative component, which consisted chiefly of axial effects, was insufficiently large and the net prompt power coefficient was positive.

Based on these concepts, the following mathematical model describing the Mark II behavior at full flow is postulated:

$$-H = \frac{PX_{ax}}{(1 + iwT_1)(1 + iwT_2)} + \frac{PX_{rb}}{(1 + iwT_3)} + \frac{PX_d e^{-iwT}}{(1 + iwT_4)} \quad , \qquad (23)$$

where X_{ax}, X_{rb}, and X_d are the power coefficients for axial expansion, rod bowing, and shield plate expansion, respectively. The coefficients X_{ax} and X_d are, of course, negative, and X_{rb} is positive. The first two terms on the right-hand side of Equation 23 describe the feedback arising from axial fuel expansion and rod bowing, and are, in fact, related, at least qualitatively, to the corresponding terms in Equation 20, which describes the feedback for the partially sheared Mark III core. The third term, which describes the delayed feedback from ligamental expansions in the lower shield plate, is peculiar to Mark II, since such structural members were eliminated in the Mark III design.

Reasonable estimates of the parameters X_{ax}, X_{rb}, T_1, T_2, and T_3 may be obtained from the results of empirical analysis of Mark III data. As a first approximation, values for T_1, T_2, and T_3 can be assumed equal to the corresponding values quoted in Table VI for the full-power, full-flow, partially sheared core. The value of X_{ax} may be approximated as one-third that given for the prompt negative power coefficient in Table VI and the value of X_{rb} may be approximated by three times the value given for the corresponding rod-bowing coefficient. From physical considerations, values of 2.0 and 2.1 sec may be estimated for the time constant T_4 and the effective transport lag T_1, respectively. The parameter least capable of evaluation is the delayed power coefficient X_d. An estimate of the magnitude of this coefficient may be obtained from a solution of Equation 23 where -H is given by actual Mark II data and where all other parameters are defined by the values cited above. The value of Xd resulting from such a treatment amounts to 2.73×10^{-6} $\Delta k/k/kw$. In terms of the effect on core radius, this value requires a 0.020-in. increase in core radius for a nominal 100°C temperature differential across the core, an increase inconsistent with the value of 0.007 in. which would be expected for an unrestrained radial expansion of the shield plate ligaments. In effect, then, to explain the experimental Mark II results at full power and full flow based on the above assumptions, radial movements approximately threefold larger than those predicted on the basis of unrestrained expansion are required. Some

mechanism which mechanically amplifies ligamental motions is required to explain this apparent anomaly. As discussed in Appendix B, such a mechanism has indeed been found in a pronounced dishing action of the lower shield plate.

Attention must also be called to the possibility of amplification mechanisms operating in the shield plate region. If the alignment of the lower shield plate and seal plate (four inches above) happened to be such that ligaments in the seal plate acted as pivots, a given radial displacement of fuel rods at shield plate level would lead to an approximate three- or fourfold mechanical amplification at core elevation. Deposits of sodium and potassium oxides in the 0.0055-in. radial clearance existing between rod extensions and ligaments of the seal plate could, of course, enhance the possibility of leverage action.

IX. SUMMARY

From the results of instability studies it may be concluded that the operational characteristics of the fully ribbed and rigid Mark III loading are governed by feedback processes which guarantee safe and stable operation under normal operating conditions. The influence of the stabilizing ribs is felt in two ways, both of which are in the direction of increased stability. The ribs provide strong radial coupling between fuel rods and between fuel rods and hex cans, with the consequence that a large radial contribution to power coefficient is realized. The ribs have also eliminated, for all practical purposes, positive feedback effects arising from the inward bowing of fuel rods during power increases. Absolutely no evidence of positive reactivity effects was noted for the fully ribbed and rigid core.

The results of logical extrapolations of full-power, full-flow test data indicate that the reactor could be brought into a resonant condition for power levels exceeding 1000 megawatts. Since nominal full-power operation is limited by design to 1.2 megawatts, the hypothetical instability power is one of mere academic interest. The limit to which power may be increased is dictated, not by matters of instability, but by matters of heat removal. In a practical sense, then, the fully ribbed Mark III loading could never be made unstable.

The strong nonlinearities observed in the power coefficient pose no serious operational problems, at least over the range of power associated with the tests. Except for the region between zero and 200 kw, in which the power coefficient is small but still negative, the power coefficient is everywhere very strongly negative. The nonlinearities are, in fact, relatively unimportant from the stability viewpoint. They are, however, bothersome, since they greatly complicate the interpretation of test data in terms of a single unified model which may be applied over wide ranges of power, flow and temperature conditions. The origin of the nonlinearities appears to be a consequence of power and temperature-sensitive clearance systems existing between rods, between rods and hexes, and between hexes. Attempts to define such systems mathematically are further frustrated by differences existing in the expansion coefficients of fuel and structural materials. Obviously, the association of such extremely tenuous clearance systems with power coefficient nonlinearities cannot be placed on an analytical basis. The descriptive interpretation of the effects of such clearance systems is nevertheless important, not only for an understanding of Mark III behavior, but to serve as a guide in the prediction of power coefficient nonlinearities in other conceptual designs of fast reactors.

As an additional complication, the power coefficient has also been shown to be sensitive to the temperature of the inlet coolant. The effects of increases in inlet temperature are reflected by significant increases in

the magnitudes of both static and dynamic power coefficients. The time dependence of feedback has been found to be insensitive to such changes. The explanation of this effect lies unquestionably in the strong temperature dependence of the expansion coefficient for the uranium-zirconium alloy fuel material. The effects of more feedback at higher temperatures, while real are relatively minor At higher inlet temperatures the reactor would be more stable at the lower frequencies but would be less stable for frequencies above 0.12 cps. The effect is nevertheless small and in no way invalidates general stability conclusions based on data obtained at lower temperatures.

The influence of structural feedback has also been observed in Mark III, fortunately to a degree much less serious than in the earlier, Mark II design. At the higher inlet temperatures approximately 13% of the static power coefficient is associated with a feedback process operating with a time constant of the order of 400 sec. In view of the extreme slowness of action the physical process responsible for the feedback must certainly be one associated with some massive portion of the structure at some downstream location. The existence of this delayed component has little effect on stability conclusions since its effect cannot be sensed for frequencies greater than 0.003 cps. For frequencies less than this its presence actually causes the reactor to be more stable

Attempts to enhance and to measure possible feedback effects arising in the radial breeding blanket were unsuccessful As a consequence it must be concluded that feedback mechanisms based on the preheating of inlet coolant by the transfer of heat between core outlet and blanket inlet in series flow are unimportant. Since preheating possibilities are very nearly the same for both Mark II and Mark III it may also be concluded that strong blanket feedback mechanisms postulated as the source of the Mark II delayed negative component are considerably discredited.

As the coolant flow is reduced (at constant power), three basic changes occur in the feedback The power coefficient increases by an amount roughly inversely proportional to the change in flow rate. The time constants for the expansion of fuel and the effective transport lag also increase. All of these changes are in the direction of increasing instability, since the result of such changes is manifested by strong increases in the phase and amplitude of feedback vectors in the important III quadrant.

Logical extrapolations of test data for approximately one-third flow result in the conclusion that the reactor would reach resonance instability in the vicinity of 10 megawatts, a power level approximately twenty times that of the designed value for one-third flow. Further reductions of flow at constant power would result in an accelerated lowering of the resonance power. Further reductions would be inadvisable not only because of the lowered resonance power level, but because of the possibility of fuel rod temperatures exceeding limits set by design.

The results of removing the stabilizing ribs from fuel rods have demonstrated conclusively the existence of a strong positive effect which must logically be associated with the inward bowing of fuel rods. An extrapolation of the results obtained from shearing the ribs from approximately one-third of the fuel rods results in a value of $+2.06 \times 10^{-6} \Delta k/k/kw$ for the fully sheared core. Since the prompt negative component associated with fuel, coolant and blanket expansion is $-2.205 \times 10^{-6} \Delta k/k/kw$, the response of the reactor, even when fully sheared, would still be governed by a smaller, but still negative, prompt power coefficient. Under these conditions, runaway excursions, such as that which damaged the Mark II core, would be impossible.

An application of the Nyquist stability criterion to the extrapolated fully sheared data results in the conclusion that the reactor would attain resonance instability at full flow at approximately 11 megawatts. The frequency at which resonance will occur is in the vicinity of 0.14 cps. The net result of the positive component associated with rod bowing is a drastic lowering of the resonance power.

It has also been shown that rib shearing results in an unexpected and unexplained increase in the magnitude of the delayed structural power coefficient component. An empirical fit of feedback data to a model describing the dynamic and static behaviors of the partially sheared core resulted in the following values for the respective prompt negative, rod-bowing, and delayed structural power coefficient components: -2.21×10^{-6}, $+0.543 \times 10^{-6}$, and $-0.873 \times 10^{-6} \Delta k/k/kw$. These values correlate in a curious manner with those empirically deduced for the prompt negative and delayed structural power coefficient component for the fully ribbed core, namely, -2.21×10^{-6} and -0.330×10^{-6} $\Delta k/k/kw$. The magnitude of the positive power coefficient component is equal to the increase in the magnitude of the structural component. Apparently, rib shearing introduces two feedback processes: rod bowing, which is prompt and positive, and one of an unspecified nature that is negative and extremely delayed in time. A postulate has been formulated to explain the origin of the increased delayed negative effect; this considers wall deformation in those assemblies containing sheared fuel rods. Regardless of the exact nature of the process, it is clear that the strong increase in the negative structure term does not affect conclusions regarding the resonance stability of the partially or fully sheared cores since the process acts so slowly that the reactor oscillating at frequencies as low as 0.02 cps cannot sense the feedback.

The overall behavior of the Mark III core, whether fully ribbed and rigid, fully ribbed and loose, and even partially or fully sheared, is one of extreme stability, a behavior in striking contrast with that of Mark II. To appreciate the reasons for this significant difference it is instructive to show how those features responsible for the instability of Mark II have been eliminated in Mark III through changes of design.

The most important and disturbing feature of Mark II was the existence of the prompt positive rod-bowing component. The inclusion of stabilizing ribs and a system of tightening rods in the Mark III design has eliminated, or at least reduced to a point beyond detection, similar effects in Mark III. It is equally significant from the viewpoint of understanding Mark II results that the Mark III tests have shown that rod bowing is the consequence of special, not easily obtained, conditions of fuel rod restraint.

The explanation of why rod bowing existed in Mark II in which conditions were superficially nonconducive to rod bowing is based on an ordered arrangement of rod tips brought about by expansive action of the lower shield plate. Expansion based solely on the temperature differential across the core was evidently sufficient to force the fuel rods outward until the tips were bearing against the outer edges of the locating holes. Under these conditions, inward rod bowing is the most likely consequence of deformations accompanying power increases.

The explanation of why the prompt power coefficient of Mark II was positive and is indicated to be negative in Mark III, even for the fully sheared case, is found, not so much in the magnitudes of the positive components, as it is in the magnitudes of the prompt negative components. Because of the lack of radial coupling between fuel rods in Mark II, the effects of radial expansion contributed little to the prompt power coefficient. The net prompt power coefficient was associated with axial fuel expansion and coolant expulsion, and was insufficiently large to cancel the prompt positive component from rod bowing. In Mark III, on the other hand, which represents a strongly coupled rod system, the prompt negative power coefficient includes contributions from both axial and radial expansions. The combined prompt negative effects are sufficiently large to override the positive component from rod bowing, and the net power coefficient is negative. The inclusion of stabilizing ribs in the Mark III design is therefore beneficial in two respects: rod bowing is eliminated, and the prompt negative power coefficient is strengthened.

The second disturbing feature noted in Mark II was the presence of a delayed negative power coefficient component, which now appears to have been the result of delayed expansions in the ligamental structure of the lower shield plate. As discussed in Appendix B, the results of experiments carried out on a dummy shield plate have established the existence of radial movements of the shield plate ligaments which, because of their contiguity with the fuel rod extensions, effectively modify the core size following power changes. Such an effect is clearly negative and operates with a time dependence reasonably consistent with that deduced analytically from a consideration of Mark II test results. Structural features such as the shield plate system of Mark II have been eliminated in Mark III. This fact, coupled with the observation that no similar component has been observed in Mark III, supports the validity of this explanation.

In summary, those features responsible for the instability of Mark II, namely, the prompt positive and delayed negative power coefficient components, were unquestionably the result of design peculiarities. The elimination of the perforated shield plate system coupled with the addition of stabilizing ribs to the Mark III fuel rods has resulted in a reactor whose performance is unquestionably stable under all credible operating conditions.

REFERENCES

1. H. V. Lichtenberger et al., Operating Experience and Experimental Results Obtained from a NaK Cooled Fast Reactor, Proceedings of the International Conference on the Peaceful Uses of Atomic Energy, Geneva, 1955, P/813, Vol. 3, p. 345, United Nations, NY (1956).
2. W. H. Zinn, Basic Problems in Central Station Nuclear Power, Nucleonics, 10 (9), 8-14 (September 1952).
3. M. Levenson, Determination of the Conversion Ratio of the Experimental Breeder Reactor by Radiochemical Methods, ANL-5095 (December 23, 1953).
4. C. D. Curtis et al., A Physical Determination of the Conversion Ratio of the Experimental Breeder Reactor, ANL-5222 (August 1954).
5. W. Y. Kato, F. S. Kirn, and W. C. Redman, Conversion Ratio for a Fast Breeder Reactor, Symposium on Reactor Operating Problems, Nuclear Engineering and Science Congress, Cleveland, Ohio, December 12-16, 1955. Vol. II, Pergamon Press, 1957.
6. Progress Report on the Experimental Breeder Reactor, April 1, 1951 to January 31, 1953, ANL-5023 (February 20, 1953).
7. W. H. Jens and R. W. Klecker, EBR Transfer Function Experiment, unpublished.
8. R. O. Brittan, Analysis of the EBR-I Core Meltdown, Proceedings of the Second United Nations International Conference on the Peaceful Uses of Atomic Energy, Geneva, 1958, United Nations, NY (1958) Vol. 12, p. 267.
9. J. H. Kittel, M. Novick, and R. F. Buchanan, The EBR-I Meltdown, Physical and Metallurgical Changes in the Core, Nuclear Science and Engineering, Vol. 4, No. 2 (August 1958).
10. R. Mela and R. Dana, Progress Report on EBR Work, NDA-14-104 (September 1955).
11. R. Siegel and H. Hurwitz, Jr., The Effect of Positive Temperature Coefficients on Reactor Stability and Reactor Transfer Function, KAPL-1138 (March 1956).
12. F. W. Thalgott, unpublished.
13. G. H. Kinchin, The Instability of Fast Reactors, RP/M83, AERE, Harwell (June 1956).
14. H. A. Bethe, Reactor Safety and Oscillator Tests, APDA-117 (October 1956).

15. R. T. Frost, W. Y. Kato and J. Butler, Measurement of Doppler Temperature Coefficients in Intermediate and Fast Assemblies, Proceedings of the Second United Nations International Conference on the Peaceful Uses of Atomic Energy, Geneva, 1958, United Nations, NY (1958), Vol. 12, p. 79.

16. J. E. Mann, A Note on EBR-I Oscillations, IGR-TM/R, 114 FRDC/P226 (March 1957).

17. R. A. Wilson and H. R. Moore, Analysis of EBR-I Dynamic Performance, BA C/RL-991 (May 29, 1958).

18. R. E. Rice et al., EBR-I Mark III Design, ANL-5836 (March 1958).

19. J. M. Harrer, R. E. Boyar and Darwin Krucoff, Measurement of the CP-2 Reactor Transfer Function, ANL-4373 (June 1952).

20. D. Okrent, Effective Delayed Neutrons and Zero Power Transfer Function for EBR-I, Private Communication.

21. G. R. Keepin et al., Delayed Neutrons from Fission. Isotopes of U, Pu, and Th, LA-2118 (July 23, 1957).

22. W. G. L. Brownigg and P. J. Littler, Pile Modulation and Statistical Fluctuations in Piles, AERE N/R 476.

23. R. T. Frost and R. J. Schemel, Private Communication.

24. J. F. Boland, R. R. Smith and R. E. Rice, A Measurement of the Transfer Function of a Fast Critical Facility, ANL-5782 (September 1957).

25. R. R. Smith, F. W. Thalgott and J. F. Boland, EBR-I, Mark III Oscillator Studies, Progress Reports 1-9, ANL, Idaho Division.

26. R. L. McVean, Private Communication.

27. D. C. G. Smith, Private Communication.

28. F. Storrer, Analysis of the Power Feedback Relations on the Enrico Fermi Fast Reactor, Conference on Transfer Function Analysis and Reactor Stability Analysis, ANL, May 2-3, 1960.

29. F. D. McGinnis, Internal Memorandum, ANL, Idaho Division, (June 6, 1960).

30. F. Storrer, Temperature Response of Power, Inlet Coolant Temperature and Flow Transients in Solid Fuel Reactors, APDA-132 (June 5, 1959).

31. J. K. Long, Analysis of EBR-I Power Temperature Relations, Winter Meeting, American Nuclear Society, Washington, D.C. (November 4-6, 1959).

32. J. C. Carter, D. W. Sparks, and J. H. Tessier, The Internal Feedback of EBR-I, Mark III, ANL-6124 (February 1960).

APPENDIX A

Accuracy of Feedback Measurements

The effect of errors inherent in measurements of the transfer function on the separated feedback is particularly important at the higher frequencies, since the feedback in this region constitutes a difference between two numbers of almost equal magnitude. From the results of a large number of zero power calibrations it may be concluded that systematic, i.e., nonrandom, errors were negligibly small, since the calculated zero power curve was reproduced repeatedly within the limits of small obviously random errors.

The major source of random errors and the only source warranting consideration was the inability to determine precisely the null points for phase and amplitude measurements. A measure of the standard error associated with these measurements may be obtained from a statistical consideration of phase and amplitude values determined at discrete frequencies at zero power. The standard error associated with a single measurement may be defined by the expression

$$\sigma_i = \sqrt{\frac{\sum_{j}^{n-1} (x_j - \bar{x})^2}{n-1}} \quad , \tag{A-1}$$

where $\bar{x}$ is the mean value, x_j is the j^{th} measurement, and n is the total number of observations. By grouping zero power phase and amplitude values according to frequency, σ_i may be conveniently evaluated at several discrete frequencies from Equation A-1 for the zero power case. Although values for σ_i determined in this manner apply strictly to measurements at zero power, they may be applied with little loss of significance to measurements carried out at other levels of power.

The results of an evaluation of σ_i from zero power calibrations for both phase and amplitude are summarized in Fig. 49. To simplify error analysis the standard error is given in percentage units. A smooth curve has been drawn through the data to facilitate the extrapolation of σ_i for intermediate frequencies.

The effects of statistical errors inherent in phase and amplitude measurements on the feedback may then be found from the following considerations. The feedback is defined by

$$-H = \frac{1}{G} - \frac{1}{G_0} = \frac{1}{G\cos\phi - i\,G\sin\phi} - \frac{1}{G_0\cos\theta - i\,G_0\sin\theta} \quad , \tag{A-2}$$

where ϕ and θ are the phase angles of the measured and zero power transfer functions, respectively.

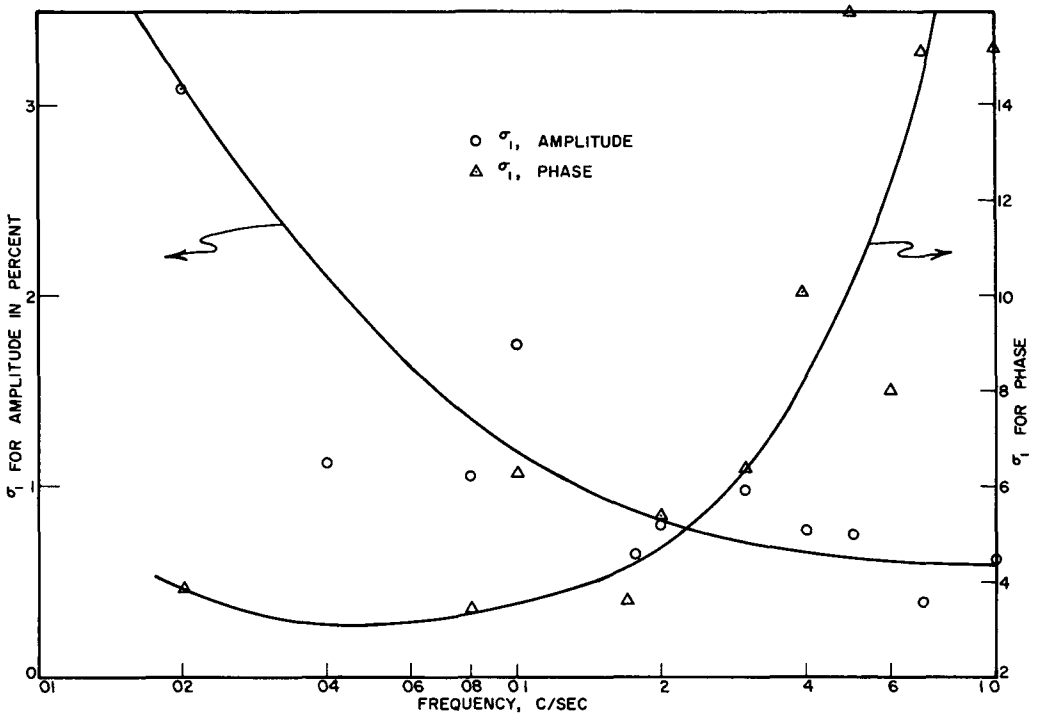

Fig 49 Standard Errors Associated with Phase and Amplitude Measurements

Rearranging Equation A-2, there is obtained

$$-H = \frac{\cos\phi + i\sin\phi}{G} - \frac{\cos\theta + i\sin\theta}{G_0} \quad . \tag{A-3}$$

The real and imaginary components are given by

$$-H_{Re} = \frac{\cos\phi}{G} - \frac{\cos\theta}{G_0} \tag{A-4}$$

and

$$-H_{Im} = \frac{\sin\phi}{G} - \frac{\sin\theta}{G_0} \quad . \tag{A-5}$$

The error in the real portion of -H caused by statistical errors associated with the phase and amplitude of the measured transfer function is given by

$$\Delta(-H_{Re}) = \sqrt{\left[\frac{\partial(-H_{Re})\,\Delta G}{\partial G}\right]^2 + \left[\frac{\partial(-H_{Re})\,\Delta\phi}{\partial\phi}\right]^2} \quad . \tag{A-6}$$

Similarly, the error incurred in the imaginary portion is given by

$$\Delta(-H_{Im}) = \sqrt{\left[\frac{\partial(-H_{Im})\ \Delta G}{\partial G}\right]^2 + \left[\frac{\partial(-H_{Im})\ \Delta\phi}{\partial\phi}\right]^2}\ , \qquad \text{(A-7)}$$

where ΔG is the standard error associated with measuring the amplitude G and $\Delta\phi$ is the standard error expressed in radians associated with measurements of the phase ϕ. Upon carrying out the differentiations indicated in Equations A-6 and A-7, the results are

$$\Delta(-H_{Re}) = \sqrt{\left(\frac{\cos\phi\ \Delta G}{G^2}\right)^2 + \left(\frac{\sin\phi\ \Delta\phi}{G}\right)^2} \qquad \text{(A-8)}$$

and

$$\Delta(-H_{Im}) = \sqrt{\left(\frac{\sin\phi\ \Delta G}{G^2}\right)^2 + \left(\frac{\cos\phi\ \Delta\phi}{G}\right)^2}\ . \qquad \text{(A-9)}$$

A measure of the effect of statistical errors on the accuracy of separated feedback values is given for a typical case in Fig. 50. Vertical and horizontal bars drawn through the data points indicate the amounts of statistical inaccuracy associated with the imaginary and real components, respectively.

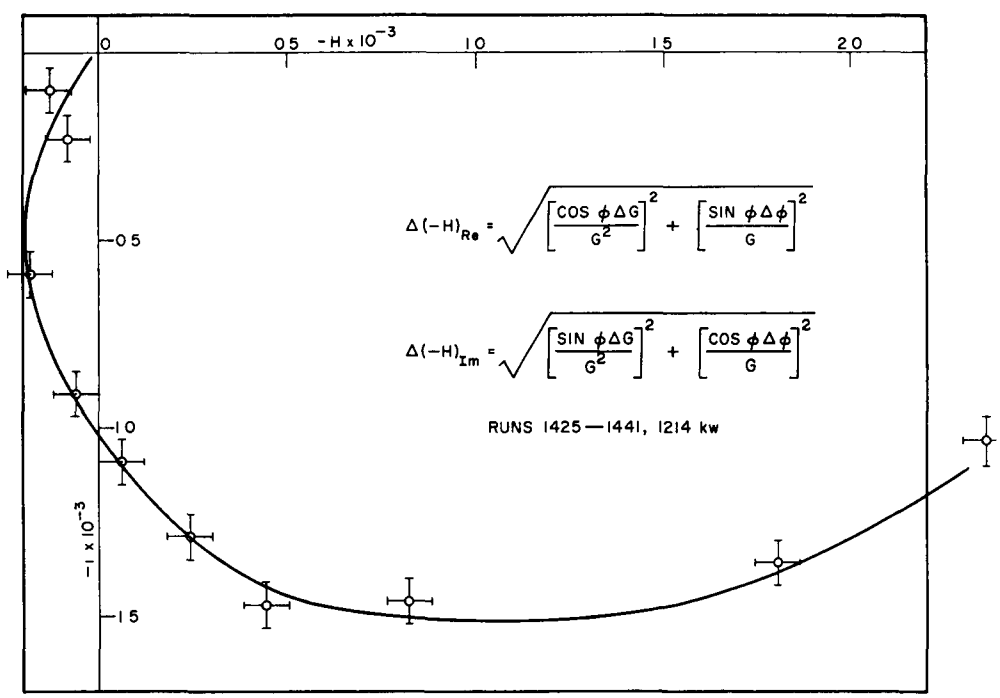

Fig. 50. Statistical Errors for Full-power, Full-flow Feedback

In one respect the illustration of real and imaginary statistical uncertainties given in Fig. 50 is misleading, since superficially it seems that the high-frequency feedback values are more precisely defined. On a more realistic basis, in which the amplitude of the feedback is considered, it is clear that in spite of larger absolute errors the amplitude of the feedback is more precisely defined at the lower frequencies. For this reason the evaluation of values for the dynamic power coefficient by the empirical methods discussed in Section VII from the feedback amplitude is considerably more reliable at the lower frequencies.

APPENDIX B

The Effect of Temperature Transients on Shield Plate Ligamental Motions

The results of attempts to detect motions induced by temperature variations in the ligaments of a dummy two-inch shield plate have demonstrated conclusively that such motions do exist.

The first attempts to observe motions involved heating the ligaments with the exhaust from a hydrogen blast lamp. To prevent the heating of the outer portion of the shield plate (which remained at constant temperature in the reactor), a pyramidal shroud was installed beneath the plate in such a manner that the shroud effectively channeled the heated air through the central section and left unaffected areas outside the hexagonal annulus (see Fig. 48). To limit the extent of heating, the blast was interrupted after approximately four seconds. Temperatures in the central portion of the plate rose rapidly to about 200°C. Measurements of expansive motions were carried out with a dial indicator butted against a quartz rod which, in turn, was sealed into a stainless steel insert machined to provide a flush fit with the fuel rod perforations. Asbestos shielding was installed around the measuring equipment to prevent extraneous heating effects. The responses of approximately 20 holes were tested. Although no two responded exactly alike, a general pattern of behavior was clear. With the indicator butted against the outside of the quartz rod (approximately 4 in. above the plate), heating the ligaments was followed immediately, i.e., within 2-3 sec, by a movement of the rod inward. After approximately 5-6 sec, the inward motion ceased and the rod began to move outward at a much slower rate, coming to rest eventually at a position approximately 4-5 mils outward from its initial position. With the indicator bearing on top of the rod, i.e., in a position measuring vertical deflections, the initial movement was 3-4 mils downward over a period of approximately 2-3 sec, followed by a much slower return to a position approximately 4-5 mils above its initial elevation.

The explanation of this behavior is clear. Immediately following the 4-sec heat blast the first motion consists of a warping or a dishing of the plate. A dial indicator butting against the outside of the rod senses the motion as an inward motion. An indicator mounted on top of a rod senses the motion as a decrease in elevation. The dishing is apparently the result of preferential expansion in the lower portion of the ligaments. As the entire collection of ligaments reaches a more or less equilibrium temperature, the dishing effect disappears, i.e., the axes of the perforations return to vertical. Such actions are consistent with the recoveries noted. The overshoot in elevation is the result of an overall vertical expansion which essentially raises the rod and bearing point of the indicator. The overshoot in radial displacement is a consequence of a much slower expansion of the hexagonal annulus which allows ligamental stresses to be

at least partially relieved. Observations carried out on a $\frac{1}{8}$-in. stainless steel pin positioned in the annulus substantiated this conclusion. Indicator measurements carried out as a function of elevation along the outside of the rod verified the existence of the dishing effect, i.e., significantly larger inward displacements were measured at the upper portions of the rod. Other measurements carried out on the right and left-hand sides of the rod demonstrated that lateral motion also occurred.

In another series of experiments, hot water was used as a heat transfer medium. In these experiments, water at approximately 50°C was stored in a tank contiguous with the lower broached portion of the shield plate. An overflow chamber fitting around the periphery of the hexagonal annulus was mounted on the upper side. If mating surfaces were gasketed, hot water could be forced upward through the rod perforations into the overflow chamber without sensibly affecting the temperature of the outer portion of the plate. Again dial indicators were used to measure displacements by expansive motions.

The results of measurements conducted on approximately 25 rod locations confirmed the results obtained in the heated air experiments. With an indicator butting against the outside of the quartz rod at an elevation approximately four inches above the plate, the initial motion was consistently inward. In general, the initial motion consisted of about 0.5 to 1.0 mil over a period of 2-3 sec, followed by a somewhat slower recovery to the initial position. In nearly all cases an overshoot, i.e., an outward motion, of approximately 0.5 mil taking place over a period of 5-10 sec was observed. Upon reducing the flow of water through the plate, the initial tilting could be exaggerated and the time required for tilting, recovery, and overshooting could be increased. It was also observed, consistently, that the tilting effect was more pronounced in the outer two or three rows of rod perforations.

The results of experiments in which the bearing point of the indicator was placed on top of the rod, i.e., in a position measuring vertical movement, were consistent with the results of similar experiments conducted with heated air. The initial motion consisted of a 0.2 to 0.3-mil dip over a period of 2 to 3 sec, followed by a slower recovery to initial elevation. In most cases a small overshoot of approximately 0.3 mil was observed.

The results of experiments conducted with two dial indicators, both bearing against the inside of the rod but with one at four-inch elevation above the plate and the other at eight inches, demonstrated conclusively that the initial action consisted of a tilt. In nearly all experiments of this nature the upper indicator registered significantly larger radial displacements than was the case for the lower indicator.

From these results it is clear that the immediate consequence of a sudden increase in the temperature of coolant flowing through the ligaments is a rapid dishing action which tilts the axes of contiguous fuel rods towards the normal. Since the tilting is more pronounced along the periphery of the perforations, it seems likely that the thin (approximately 0.20 in.) hexagonal annulus is also involved in the dishing action. Apparently the temperature gradient established across the plate effects a preferential expansion, not only of the ligaments, but of the annulus as well. Such action would be manifested by an inward tilting of fuel rod extensions contiguous with the ligaments. The recovery and overshoot are consistent with the behavior expected for a system which eventually comes to a higher (and uniform) equilibrium temperature.

Based on these observations, the following mechanism may be postulated as the source of the delayed negative power coefficient of Mark II. As the temperature wave resulting from a power increase reaches the shield plate, dishing begins. The effect of the dishing on fuel rod movement depends to a very large extent on the exact physical relationship of the rod extensions with respect to the perforations. Two cases are recognized: one in which the rod extensions bear against the inner edges of the perforations, leaving the entire diametral clearance between the outer edges of the rod extensions and the outer edges of the perforations, and the other in which the rod extensions are tightly bound by the ligaments. A third possibility, in which the rod extensions penetrate the perforations without touching the ligaments, is not recognized, since the expansive action associated with reaching an outlet temperature of 300-400°C should be easily sufficient to gather all rod extensions along the inner edges of the perforations. In the first case, i.e., with the rod extensions bearing along the inner edges, the dishing action will result in an outward movement of the rod by an amount dictated by the displacement of the bottom inner edges of the perforations. In the second case, dishing results in a torque which effectively amplifies the movement of fuel at core elevation.

Of the two motions, the latter is far more effective in modifying the core radius following a power change. In fact, as will be shown, the radial movement of fuel rods resulting from unrestrained radial expansions of the ligaments is too small by a factor of two or three to explain the instability of Mark II at 550 kw and one-third flow. Since the expansion of the ligaments is restrained to a large degree, this factor is undoubtedly much larger. For this reason, mechanisms based on the simple radial movement of rod extensions through ligamental expansions are untenable. Some amplification of motion is necessary to explain the large amount of delayed reactivity controlled by thermal induced motions of the plate.

In his analysis of Mark II data, Bethe arrived at values of +1.45 and -6.9×10^{-6} $\Delta k/k/kw$ for the magnitudes of the power coefficient components for rod bowing and delayed structural expansion, respectively, for the

operating conditions of 550-kw power and 100-gpm flow. Assuming that the entire negative component consists of delayed radial expansion, it can be shown that the amount of radial movement at the core center necessary to explain the negative power coefficient for a temperature differential across the core of 128°C is approximately 24 mils. Actually, a small fraction of the net negative power coefficient arises through prompt axial expansion, and the value of 24 mils becomes an upper limit. Since the upper limit for the amount of radial movement associated with the unrestricted radial expansion of the ligaments for the same operating conditions (550 kw, 100-gpm flow, and 128°C temperature differential across the core) is only 9 mils, the necessity for amplification is clear.

The explanation of the amplification necessary to explain the experimental Mark II results may well lie in the dishing and tilting actions noted, since such effects effectively provide a certain amount of mechanical amplification. Unfortunately, the results of the water and air simulations do not constitute a reliable basis for the extrapolation of the dishing action expected for Mark II. Several important points of difference prevent such extrapolations. In the first place, heated air and water were used in the simulations in place of NaK. In view of the superior heat transfer properties of NaK, it is likely that dishing action would be more pronounced in a NaK system. Secondly, the flow rate, which exerts a strong influence on dishing, was considerably lower in the simulations than was the case for Mark II. Thirdly, the simulations neglected the effects of rod extensions which, through their combined heat capacities, undoubtedly attenuated the effects of temperature changes in the reactor. It must also be emphasized that the simulations were conducted on a much thinner shield plate, two inches in thickness contrasted with four inches for the one installed in Mark II. A greater degree of dishing and hence amplification would, of course, be expected for the thicker plate. Finally, it must be recognized that the extent of dishing is undoubtedly dependent on the manner in which the temperature gradient across the plate is imposed. In the simulation the plate was subjected to a step change of temperature with the result that the temperature gradient across the plate existed for a relatively short period of time, i.e., for a period of time of the order of seconds. For this reason it is conceivable that the maximum dishing effect was never observed. With the reactor oscillating at low frequencies, as in the Mark II instability studies, more prolonged temperature gradients were imposed. For example, at low frequencies a sinusoidal increase in temperature would be manifested by a reasonably prolonged (but varying) negative temperature gradient across the plate, i.e., the bottom would always be at a higher temperature than the top. For an oscillation frequency of 0.02 cps a temperature gradient of the same sign could exist for as long as 25 sec, a time duration which would permit a greater degree of expansion in the more slowly responding hexagonal annulus and presumably a greater degree of dishing. As an additional point of difference during the other half of the cycle, i.e.,

during the decreasing portion of the sinusoidal variation, the upper surface of the plate would be at a higher temperature than the lower and a dishing effect in the opposite direction would be expected.

It must also be emphasized that the effectiveness of the dishing mechanism relies on strong modifications in the nominal 0.0055-in. radial clearances existing between rods and the edges of the perforations, i.e., that the rods are reasonably contiguous with the perforations under operating conditions. If they are not contiguous, dishing action will not lead to amplification and the resulting effect on core size will be insufficient to explain the Mark II experimental results. In view of the massive, continuously cooled outer portion of the shield plate, it is likely that expansion effects in the ligaments brought about by the temperature differential across the core will be manifested by a partial compression of the rod perforations. Such a compression could conceivably reduce the clearances between the rods and their perforations such that torque action and mechanical amplification become possible.

Because of the conditions under which the simulations were conducted, it is not possible to conclude positively that the dishing action noted is the mechanism responsible for the Mark II delayed negative power coefficient component. The simulations do indicate, however, that the major effect resulting from temperature transients is a dishing effect which is in the proper direction to explain the Mark II experimental results. Much more elaborate experiments are needed before an unequivocal answer is given. Before the above-postulated mechanism can be accepted with assurance, it will be necessary to measure fuel rod deflections (at core center) initiated through temperature changes in a faithful simulation of the Mark II core For this purpose the simulation must include a rod tip-locating plate, a lower four-inch shield plate, and a seal plate identical with those installed in the Mark I and Mark II cores. Care must be taken to maintain the outer portions of the structure under rigid and constant temperature conditions. All of the rod perforations should be occupied by reasonable simulations of the Mark II fuel rods. NaK must be used as a heat transfer medium and provision must be made to maintain the rod ligaments at a temperature approximately 100°C higher than the outer massive portions of the structure. Temperature transients could be initiated by valving heated NaK into the "core" inlet. Finally, to study the deflection of fuel rods at core elevation it will be necessary to develop unusual mechanical and electronic techniques since the core will not be easily accessible. Such an experiment will be costly but, if more definitive information on the effects of dishing is needed, there seems to be no reasonable alternative.

ACKNOWLEDGMENT

The authors express their appreciation to C. Doe, R. Haroldsen, and other members of the EBR-I operating crew for their assistance in these measurements.

The authors also express their appreciation to Mr. C. Miles who assisted in measurements conducted on the deformation of the M-2 shield plate and to Mrs. Norma Price for her part in the reduction of data.